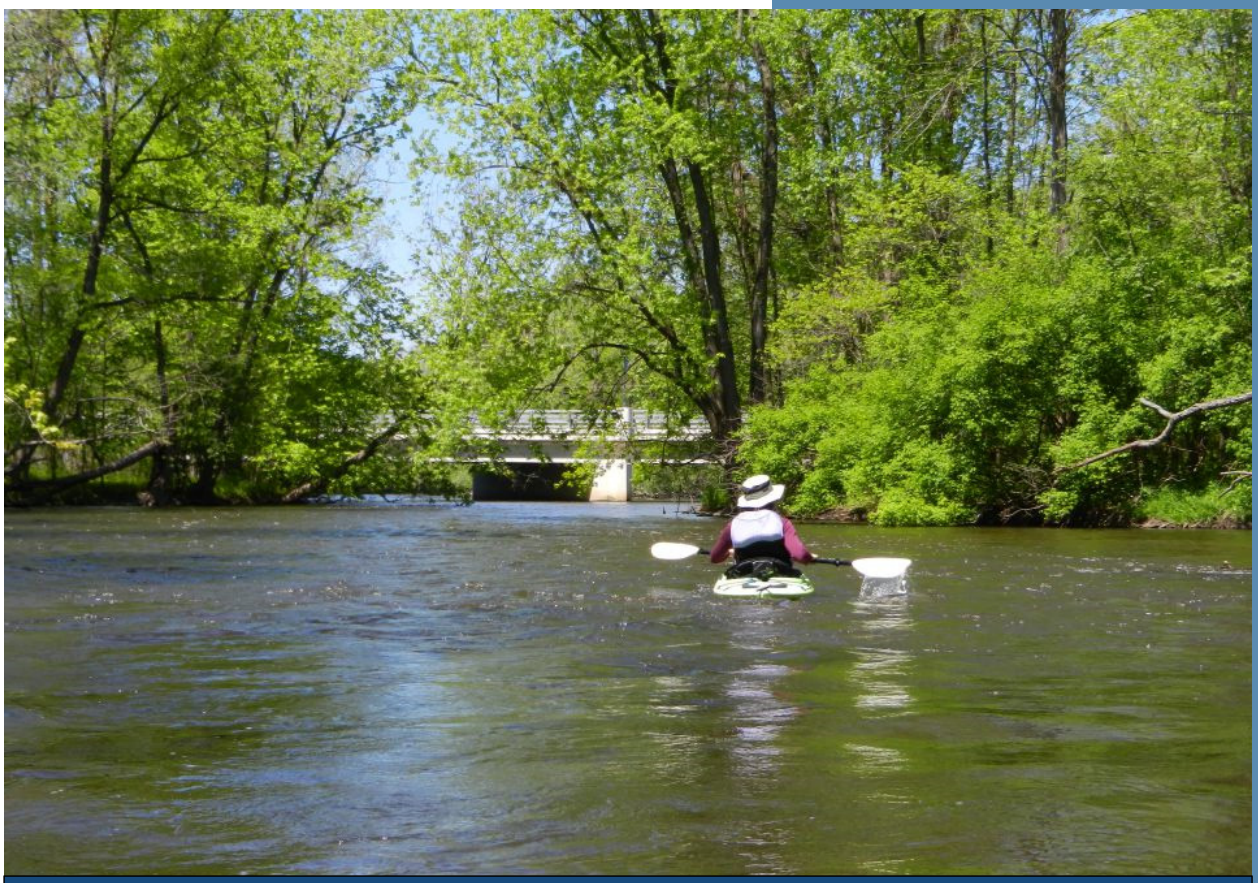

Kalamazoo River Hydrodynamic and Sediment Transport Model

Documentation

Prepared for: USEPA, Weston Solutions

Final

Date: January 26, 2015

LimnoTech
Water Environment | Scientists Engineers

Blank Page

LimnoTech
Water Environment | Scientists Engineers

501 Avis Drive
Ann Arbor, MI 48108
734.332.1200
www.limno.com

Kalamazoo River Hydrodynamic and Sediment Transport Model Documentation

Prepared for:
USEPA

Under Contract to:
Weston Solutions

January 26, 2015

Prepared by:
LimnoTech
501 Avis Drive
Ann Arbor, MI 48108

Blank page

TABLE OF CONTENTS

LIST OF FIGURES

LIST OF TABLES

1 Introduction

This report describes the 2013-2014 development of updates to models (riverine and floodplain) that were developed by Enbridge (Tetra Tech, 2012) to simulate Kalamazoo River hydrodynamics, sediment transport and submerged oil. The models were updated for and under the direction of United States Environmental Protection Agency (USEPA), with new information to support the following objectives:

- To characterize probable areas of sediment deposition and/or erosion which based on 2010 and 2011 field work relates to submerged oil occurrence. Areas of deposition/erosion were characterized for a range of flow conditions.
- To assess down river transport of submerged oil for a range of flow conditions.
- To assess sedimentation rates for selected locations as a function of flow and sediment particle size.
- To simulate scenarios of contaminant and recovery efforts on erosion, transport and deposition of submerged oil.
- To provide a modeling framework to simulate sediment transport and submerged oil migration for future scenarios following dredging.

The overall model domain included 38 miles of the Kalamazoo River between the location of the spill release at Talmadge Creek in Marshall, Michigan to Morrow Lake near Kalamazoo, Michigan. The Environmental Fluid Dynamics Code (EFDC), was used to model the hydrodynamics of the river and the Sandia National Labs version of EFDC (SNL-EFDC) incorporating the SEDZLJ sediment transport algorithms was used to simulate sediment and oiled sediment transport for a series of representative periods following Enbridge Energy Partners' (Enbridge) Line 6B Mile Post (MP) 608 crude oil release (Line 6B) on July 26, 2010. This report also describes model applications that were performed to simulate Kalamazoo River hydrodynamics and sediment transport over a range of flow conditions.

The modeling process included updates to two base models originally developed by Tetra Tech for Enbridge (Tetra Tech, 2012). The domain for one model represents only the river channel (riverine model). The domain for the other model represents both the river channel and the floodplain (floodplain model). Both models were developed in 2-dimensions (2-D). The model grids were developed for the base models to provide cells with spatial descriptive data and also to support model numerical finite difference calculations.

Updated model inputs were developed based on revised bathymetry information, floodplain topography, tributary flows, sediment rating curves, HEC-RAS models, channel roughness, dam configurations and rating curves, improved representation of the sediment bed characteristics, and the addition of an oiled particle algorithm. Discharge and sediment concentration boundary

conditions were established based on new data collected after the development of the 2012 Enbridge models. The updated models were calibrated to discharge, water surface elevation, and velocity using data from United States Geological Survey (USGS) Gaging Stations located on the Kalamazoo River, along with additional water surface elevation and velocity data collected in 2011 and 2013.

The following sections of this report include a description of the model, updates and sources of model input data, model to data comparisons, updated model to Enbridge model comparisons, and updated model applications.

2 Model Description

In 2013-14, the 2012 Enbridge models were updated by USEPA with new and expanded data sets. The goals of the USEPA modeling remained similar to Enbridge's, to simulate the potential migration and deposition of remaining submerged oil along a 38-mile stretch of the Kalamazoo River between Marshall and Kalamazoo affected by the Enbridge July 2010 pipeline release of diluted bitumen.

2.1 EFDC

The updates to the Kalamazoo River hydrodynamic model described in this report were developed in the EFDC model framework, an EPA-endorsed modeling framework that has been applied on many rivers throughout the United States. A 2-D EFDC hydrodynamic and sediment transport model was first developed by Tetra Tech for Enbridge in 2012.

EFDC is a general-purpose model for simulating three-dimensional (3-D) flow, transport, and biogeochemical processes in surface water systems including: rivers, lakes, estuaries, reservoirs, wetlands, and near-shore to shelf-scale coastal regions. The EFDC model was originally developed by John Hamrick at the Virginia Institute of Marine Science for estuarine and coastal applications and is public domain software (Hamrick, 1992). The USEPA has continued to support its development and now EFDC is part of a family of models recommended by EPA for TMDL development. Special enhancements to the hydrodynamics code, including vegetation resistance, drying and wetting, hydraulic structure representation, wave-current boundary layer interaction, and wave-induced currents, allow refined modeling of wetland and marsh systems, controlled-flow systems, and near-shore wave-induced currents and sediment transport (EPA EFDC website). The EFDC code has been extensively tested and peer reviewed. The code is currently used by university, government, and engineering and environmental consulting organizations.

The EFDC hydrodynamics algorithms were employed without modification to the EPA-supported version. The code used for this application employs the second moment vertical turbulence closure model of Mellor and Yamada (1982) as modified by Galperin et al. (1988). This model provides a calculation of vertical turbulent viscosity and diffusivity, making it possible to fully close the system of equations of fluid motion for a structured model domain.

The updated EFDC hydrodynamic model was run for four flow scenarios. High-flow periods in July – August 2010 and April – May 2013 were run using the floodplain model. The riverine model was used to simulate a more moderate high base flow period in October – November 2011, as well as a low flow period in July 2013. A more detailed description of the flow conditions for each period is provided in Section 3.2 of this report.

2.2 SNL-EFDC / SEDZLJ

The updated Kalamazoo River sediment transport model is based on the SEDZLJ model algorithms developed by Craig Jones and Wilbert Lick at the University of California – Santa Barbara (Jones and Lick, 2001). Sandia National Laboratory (James et al., 2005, Thanh et al., 2008) modified a version of the EFDC model to incorporate the SEDZLJ algorithms into a model known as SNL-EFDC. The SNL-EFDC sediment transport algorithms, as incorporated into LimnoTech's in-house version of the EFDC model, were used to simulate sediment transport behavior for the Kalamazoo River.

SEDZLJ is capable of simulating the resuspension, deposition, and transport of cohesive and noncohesive sediments. The model predicts temporal and spatial variations in suspended sediment concentration, sediment bed elevation, and bed composition (relative fractions of different particle size classes). The effects of wind and waves on resuspension can be included during simulations. The SEDZLJ model includes bedload transport of noncohesive sediment (coarse sand and gravel), but bedload was not simulated because field evidence and geomorphic mapping showed that submerged oil was associated with deposits of fine-grained sediment in the Kalamazoo River.

The use of SEDZLJ algorithms for the updated sediment transport model was a departure from the April 2012 Enbridge model, which applied native EFDC sediment transport (Tetra Tech, 2012). The switch to SEDZLJ provides an expanded capability to represent sediment transport using the latest and most widely accepted sediment transport algorithms. SEDZLJ also allows for direct incorporation of local measurements of sediment bed erodibility made using the SEDFLUME measurement technique. The use of the SEDZLJ algorithms also provided a framework that was convenient for incorporation of a new algorithm for description of oil-particle aggregate (OPA) transport.

The updated sediment transport model was run as part of the riverine model for the October – November 2011 and July 2013 time periods. These two scenarios were used to evaluate sediment transport behavior for in-bank flow conditions and to provide the framework for simulation of oiled sediments. No attempt was made to expand the sediment transport simulations to the floodplain model due to the lack of data to parameterize the model inputs and to evaluate the resulting transport behavior through the floodplain.

2.3 OPA Algorithm

Transport of oiled sediments was modeled using an OPA algorithm for the Kalamazoo River developed by the U.S. Army Corps of Engineers (ACOE). The algorithm is layered onto the updated hydrodynamic and sediment transport models. The OPA model represents oiling conditions in the riverbed in 2012, after formation of OPAs, and models the resuspension, transport, and deposition of OPAs. Three classes of OPAs are used to represent the multiple sizes and structures of oil globules and OPAs in the riverbed, with modeled OPA classes that range from a large 2 mm single oil globule with a 10 μm silt coating to more complex OPAs with multiple smaller globules and OPA diameters of 31 μm and 100 μm. The OPA algorithm development and application is document separately by the ACOE (Hayter et al., 2015).

2.4 Riverine and Floodplain Grids

The updated models use the same EFDC grids used in the 2012 Enbridge models for both the riverine and the floodplain models. The riverine and floodplain grids include the portion of the river from the I-69 Bridge near Marshall, Michigan to the Morrow Lake Dam near Comstock, Michigan (an approximately 40 mile portion of the river). Further description of the grids and their development is included in Section 3.1 of the 2012 Enbridge modeling report (Tetra Tech, 2012).

The riverine model uses a boundary fitted curvilinear-orthogonal horizontal grid which follows the sinuosity of the river. It has 26,077 cells. The horizontal grid cell dimensions are 10 to 80 meters long (longitudinally) and 5 to 40 meters wide (laterally). The variability in cell width is a result of the general representation of the channel by five cells across the lateral direction. As channel width varies along a reach, the cell width varies accordingly. The floodplain model is a Cartesian grid cell network which includes the river channel and the floodplain. The grid has 101,675 cells. The grid cells are square at approximately 15 meters long at each face.

In the riverine model the curvilinear grid allows for cells to be aligned with the river shoreline and conform to the shape of the river channel, allowing for the dominant direction of flow under most conditions to be aligned with the grid. Conversely, the rigidly configured rectangular floodplain grid is often not consistent with river orientation. Misalignment between the grid and primary direction of flow can in some cases lead to apparent momentum loss that is a numerical artifact of the grid configuration. Modifications to the model to compensate for the momentum loss included adjustments to the bathymetry and a decrease in roughness values (See sections 3.1, 3.3, and 4.2.1).

Blank Page

3 Data Inputs and Sources

In 2013-14, the 2012 Enbridge models were updated by USEPA with new and expanded data sets. These data sets were collected by Enbridge and USEPA over the course of the three years following the July 2010 oil spill. These data were used to set up and verify the updated models. Table 1 provides a listing of the types of data and how they were used for the updated model. This section describes the updated model inputs and their associated data sources, including bathymetry and floodplain topography, river and tributary flows, suspended sediment rating curves, stage discharge relationships at the dams, hydraulic parameters, and sediment transport inputs such sediment size classes, settling velocities, critical shear stresses, and streambed substrates. Data used to compare against hydrodynamic model output are discussed in Section 4, and data related to sediment transport model output are discussed in Section 5.

Table 1. Summary of available data and uses for updated model.

Data Type	Use in Updated Model
Bathymetry and topography	Model grid cell elevations in channel and floodplain (INPUT)
Discharge at USGS gages	Upstream and tributary flows (INPUT) Comparison to modeled discharge (OUTPUT)
Staff gages and USGS stage recorders	Adjustment of roughness height (INPUT) Comparison to modeled water surface elevations (OUTPUT)
Water velocities	Adjustment of roughness height (INPUT) Comparison to modeled velocities (OUTPUT)
Dam configurations and stage-discharge data	Stage-discharge relationships at Ceresco and Kalamazoo dams (INPUT)
Headwater elevations at Morrow Lake Dam	Downstream boundary condition (INPUT)
Suspended sediment concentrations and particle size distributions	Upstream and tributary sediment loads (INPUT) Comparison to modeled suspended sediments (OUTPUT)
Physical characterization of sediment cores	Sediment bed properties (INPUT)
Sediment erosion measurements	Sediment bed properties (INPUT)

3.1 Bathymetry and Floodplain Topography

The river bathymetry and floodplain topography data for the 2012 Enbridge model were derived from poling data, single beam sonar surveys, HEC-RAS cross-sections and Light Detection and Ranging (LiDAR) data. The river bathymetry and floodplain Digital Elevation Models (DEM) were updated by Weston. As described in the Weston bathymetry documentation (Weston Solutions, 2014), the bathymetry updates were based on the point bathymetry measurements used for the 2012 Enbridge model plus subsequent point measurements made during 2012 and 2013. The

updated bathymetry approximates waterway conditions at the time of the 2010 oil spill, although the updates incorporated a few post-spill bathymetry modifications that resulted from early oil spill response activities carried out in 2010 and 2011. The locations of known bathymetry changes relative to spill conditions that were incorporated in the updated bathymetry, and the corresponding response activities, were identified by Weston as follows: downstream end of the Ceresco impoundment (partial dredging at MP 5.50 to MP 5.75; Fall 2010), upstream end of Ceresco impoundment (removal of small in-channel islands and a tributary delta at MP 4.00 to MP 4.50; Summer 2011), and MP 21.50 oxbow channel (partial dredging; Summer 2011). Importantly, the updated bathymetry provided by Weston did not use any data collected after the 2013-2014 Ceresco large-scale channel dredging and dam removal, and other 2013-2014 major dredging of sediment traps, Mill Ponds and Morrow delta areas, and thus the bathymetry updates used for the updated model represent waterway conditions prior to those activities.

LimnoTech used the updated DEM to develop model grid cell elevations for both the riverine and floodplain models, using the zonal mean from the ArcGIS Zonal Statistics tool. Due to model grid alignment and resolution issues, the mean elevations resulting from this bathymetric update process were not always satisfactory, in some cases creating obstructions or constrictions to flow that were not representative of actual river geometry. In these cases, manual adjustments were made to key areas to improve the physical representativeness of the model and eliminate unrealistic flow conditions. The alignment was especially problematic in the floodplain model in places where the grid was poorly aligned with the river channel (See Sections 3.3 and 4.2). A list of significant elevation adjustments to grid cells is provided in Table 2.

Elevations were adjusted in the floodplain grid in the concrete channel just below the Mill Ponds area. In this area, some cells were located halfway in and halfway out of the channel, which caused the average elevation to be too high to allow for passage of flows under normal flow conditions. These elevations were adjusted to allow the water to pass through the channel at the proper elevation (Figure 1). Grid cell elevations were adjusted to the elevations represented by the Weston DEM along a channel centerline, allowing the adjusted channel to approximate the slope of the concrete channel.

Augusta Creek also required adjustment in the floodplain grid to account for a road represented in the topographic dataset between the tributary input and the river. The roadway topography limited the connectivity of the tributary to the river in the 2012 Enbridge model because the cells were left at the elevation of the road (Figure 2). The elevation of these cells was adjusted in the updated model to allow the tributary to flow directly to the river (Figure 3).

The floodplain model grid was also poorly aligned with the dams and abutments for the Kalamazoo River and Ceresco Dams. DEM-based elevations for grid cells intended to represent the abutments were understated due to this misalignment. Manual adjustments to the grid cell elevations were made to prevent passage of water around the dams in the floodplain model.

Elevation adjustments were also made at all of the tributaries in both grids to allow the water from the tributaries to freely flow to the river. The model grid resolution was often too coarse to represent the tributaries, with single grid cells overlapping the tributary channel and overbank area. The resulting average grid cell elevations overstated the bed elevations for the tributary

channels. For the floodplain grid, misalignment of the rectangular grid with the path of the tributaries also prevented flow from properly reaching the river. These grid resolution and alignment issues were resolved through manual adjustment of grid cell elevations to create a flow path for each tributary to reach the river. Tributary elevations along the flow path were specified by imposing a uniform slope from the bathymetry at the confluence with the river to the head of the modeled portion of the tributary.

Similar to the grid resolution issues for the tributaries, key geomorphic features such as oxbows, sediment traps, and islands had grid cells overlapping the river channel and overbank, resulting in average elevations that overstated the channel elevation. Adjustments were made in these areas to reflect the elevation of the in-channel bathymetry.

Additional changes were made to the upper river channel upstream of Talmadge Creek, where no bathymetry data were available. For this reach, the channel elevation was extended upstream by assuming a longitudinal slope equal to the slope of the top-of-bank elevations from the topography data. Side slopes of the channel were formed by extending the topography data from top-of-bank down to the channel invert elevation, which was assumed to be 50 feet in width. A list of significant elevation adjustments to grid cells is provided in Table 2.

Table 2. Areas of manual adjustments to bathymetry for the updated model.

Adjusted area	Explanation	Grid
Concrete Channel just below Mill Ponds	Floodplain cells were not well aligned with parts of the concrete channel.	Floodplain only
Tributaries	Overstatement of elevations due to grid resolution and alignment issues was resolved by imposing a uniform bed slope.	Riverine and floodplain
Bridges	Elevations were lowered under some bridges where grid resolution and alignment restricted flow passage.	Floodplain only
River channel upstream of Talmadge Creek	No bathymetry data were available for this part of the river. Topography data at the banks were used to create a channel based on assumed bank slope, and the elevation of the river channel at Talmadge Creek where the river bathymetry dataset began.	Riverine and floodplain
Oxbows, Sediment Traps, Islands	Overstatement of elevations due to grid resolution issues. Allow flow to pass realistically though these areas with manual adjustment to topography and bathymetry.	Riverine only
Kalamazoo River and Ceresco Dams	Floodplain cells adjacent to dam structures were not well aligned with the dam abutments. Grid cell elevations were increased from DEM-based mean values to prevent passage of water around the dams.	Floodplain only

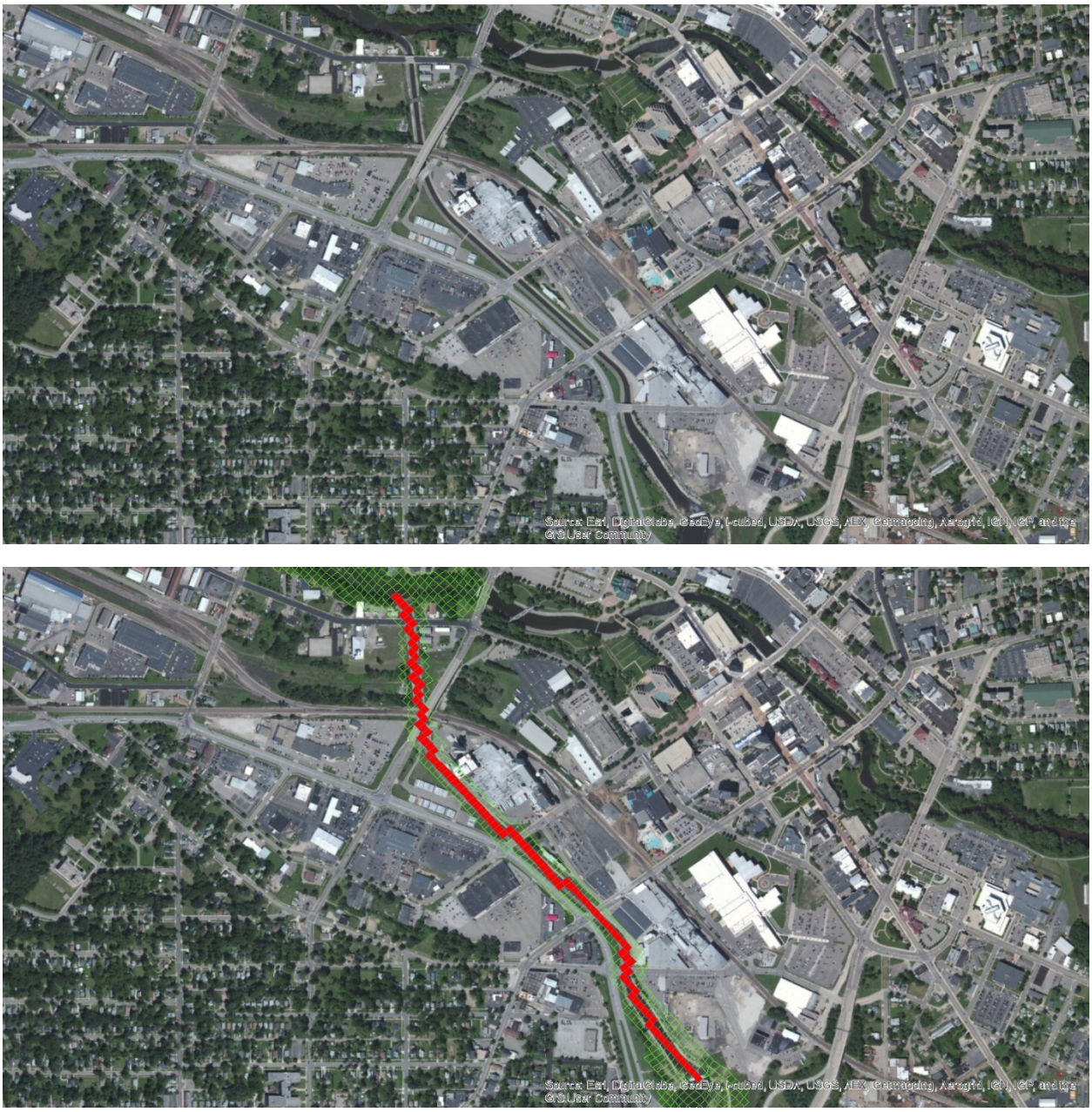

Figure 1. Top panel: Aerial photo of the concrete channel downstream of the Mill Ponds area. Bottom panel: Floodplain grid cells that had elevation adjustments are outlined in red (green cells represent the floodplain grid).

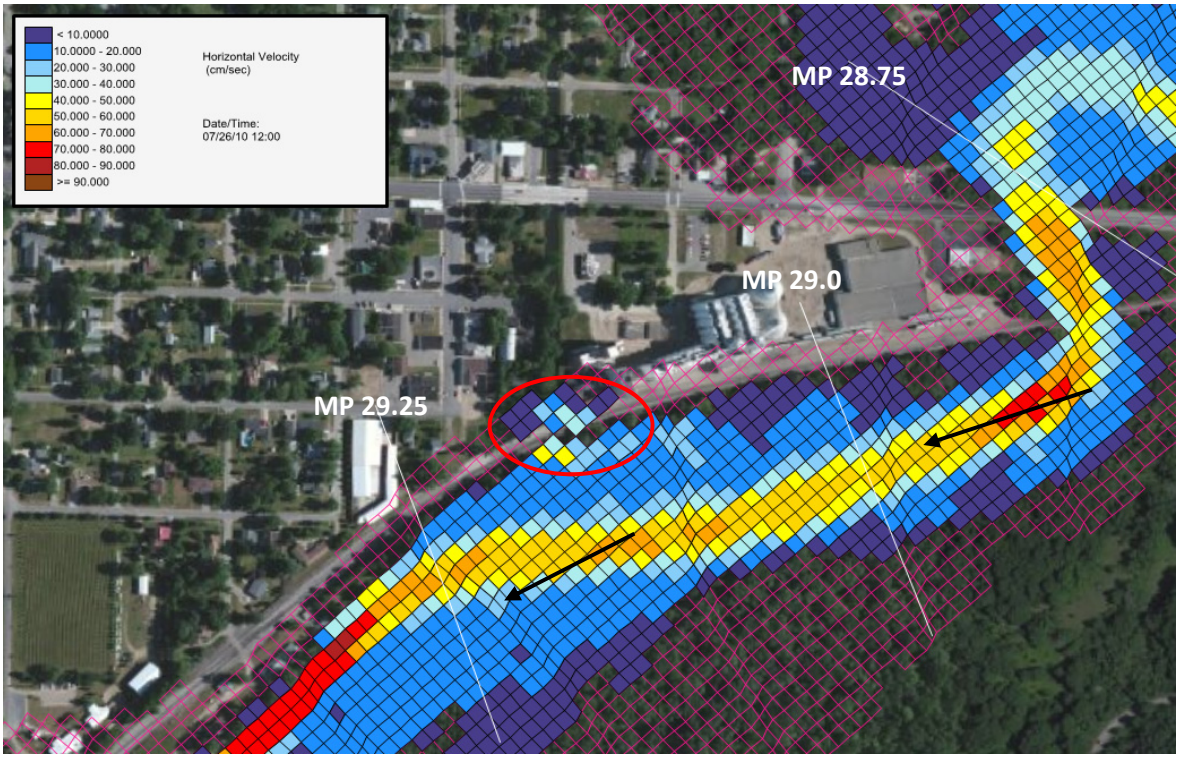

Figure 2. Limited connectivity of Augusta Creek in the 2012 Enbridge floodplain grid due to roadway topography (red circle). Red outline shows extent of floodplain model grid. Black arrows show general direction of flow.

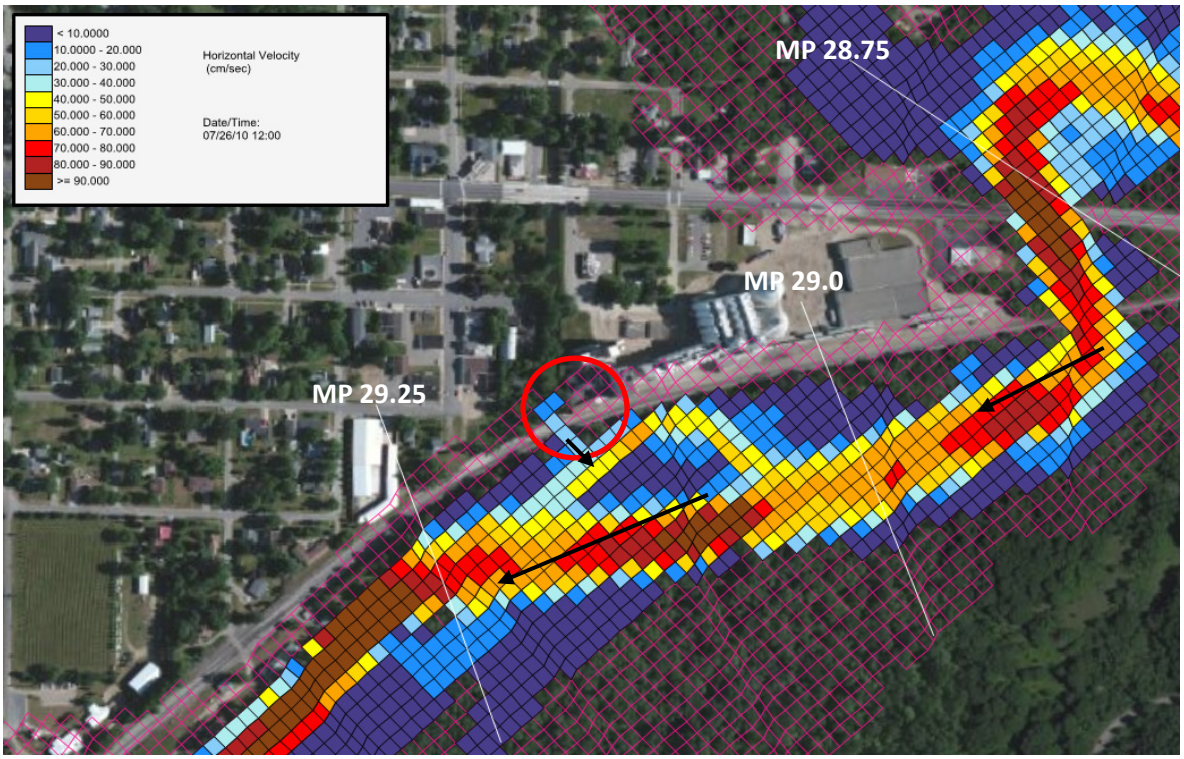

Figure 3. Augusta Creek flowing into the Kalamazoo River in the updated model with updated bathymetry and topography. Red outline shows extent of floodplain model grid. Black arrows show general direction of flow.

3.2 Updated Boundary Conditions

Numerical models require specification of conditions such as flow and sediment concentration at model boundaries. The following sections describe how the boundary conditions were developed based on available data.

3.2.1 Flows

In the 2012 Enbridge model, flow boundary conditions were imposed at the upstream boundary of the main stem, as well as at downstream tributary locations that discharge into the Kalamazoo River. The uppermost flow boundary for the riverine and floodplain model domains is on the Kalamazoo River near Marshall, MI at the I-69 Bridge, which is located above the confluence of Talmadge Creek and the Kalamazoo River. The Marshall USGS Station (USGS 04103500) provides historical flow data for this location at 15-minute intervals. The gage is located approximately 1.5 miles upstream of the I-69 bridge. No time lag was applied to the USGS gage data for use as a model boundary condition.

Boundary condition time series were developed for four simulation periods in the updated model (Table 3). Two periods were retained from the runs that were prepared by Tetra Tech, which included the July 2010 flooded spill period (See Figure 4 for the hydrograph of the Kalamazoo River near Battle Creek, USGS 04105500) and high base flow October to November 2011 (Figure 5). Additional simulation periods added to the updated model included an April to May 2013 high flow event (Figure 6) and a July 2013 low flow condition (Figure 7). Two of the periods were simulated with the floodplain grid and two were simulated with the riverine grid (Table 3).

The July 2010 period represents the period of flood flow immediately following the oil spill. The discharge in the river increased quickly reaching a peak of 3,000 cfs in approximately three days and then receded over a period of nine days. April 2013 had a similar peak flow, but occurred over a longer time period with a double peak. The peak flow of approximately 3,300 cfs was reached after 11 days and then flow receded over a period of 20 days. These two periods are quite different in duration, but are typical for summer and spring storm characteristics. Summer storms are usually short and intense which was the condition in July 2010 which produced a short duration flood event, while spring rains are typically sustained over a longer period in Michigan as was the case in the spring of 2013. In both cases, peak flows were slightly less than a 5 year flood (3,660 cfs) at the Kalamazoo River near Battle Creek gage (USGS 04105500, Personal Communication, Faith Fitzpatrick, 8/21/2013).

The October to November 2011 event was a high base flow period which is representative of fall conditions. The discharge on October 28, 2011 was 782 cfs, which was higher than the October monthly average of 501 cfs. The minimum flow of 555 cfs was reached approximately nine days later and is slightly less than the November monthly average discharge of 591 cfs (USGS, 2014).

The July 2013 event occurred during the summer low flow period. The flows were typically less than 500 cfs reaching a low of 352 cfs, well below the monthly average flow rate in July for the Kalamazoo River near Battle Creek Gage of 501 cfs (USGS, 2014). This period was chosen so the model behavior could be evaluated at a flow condition that was lower than the elevated baseflow of the October-November 2011 period.

Table 3. Model simulation time periods.

Run	Start Date/Time	End Date/Time	Description	Grid
July to Aug 2010	7/23/2010 0:00	8/4/2010 0:00	Oil spill flood	Floodplain
Oct to Nov 2011	10/28/2011 0:00	11/9/2011 0:00	High base flow	Riverine
Apr to May 2013	4/5/2013 0:00	5/16/2013 0:00	High flow	Floodplain
July 2013	7/11/2013 0:00	7/19/2013 0:00	Low flow	Riverine

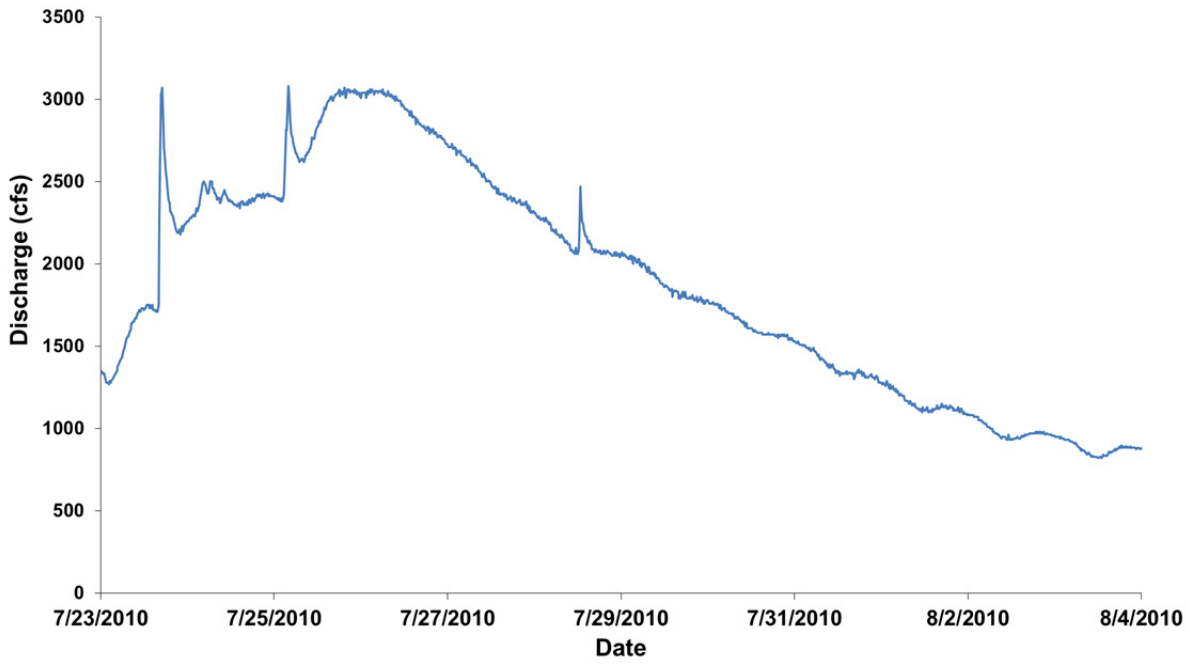

Figure 4. Hydrograph at the Kalamazoo River near Battle Creek gage (USGS 04105500) July to August 2010.

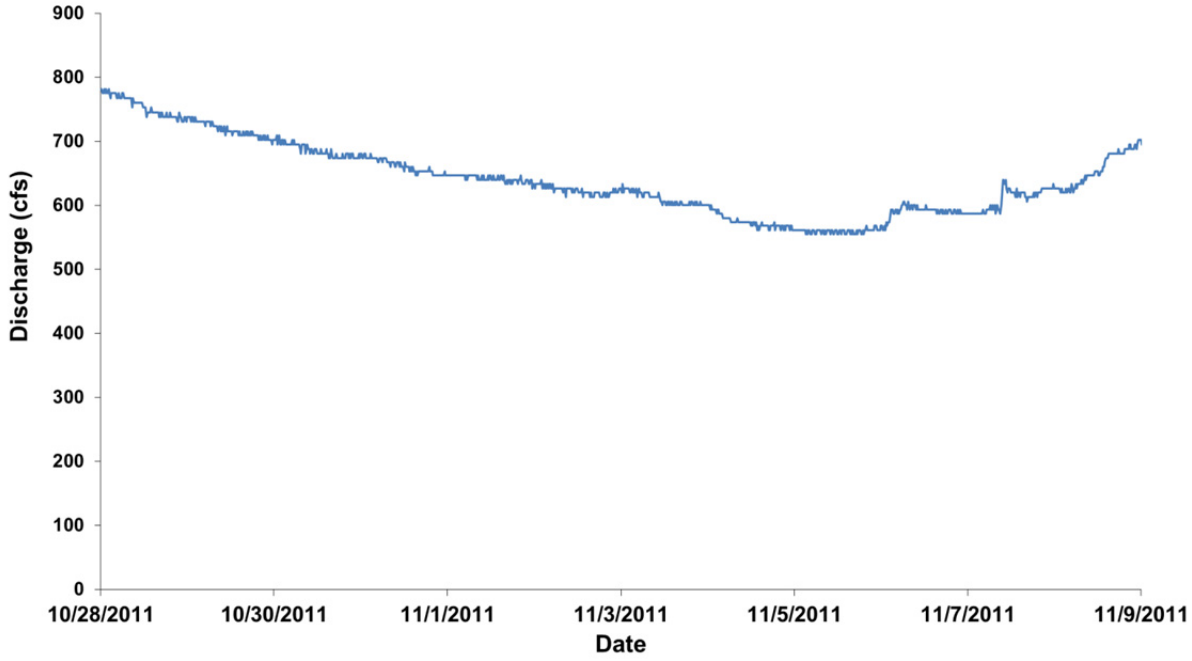

Figure 5. Hydrograph at the Kalamazoo River near Battle Creek gage (USGS 04105500) October to November 2011.

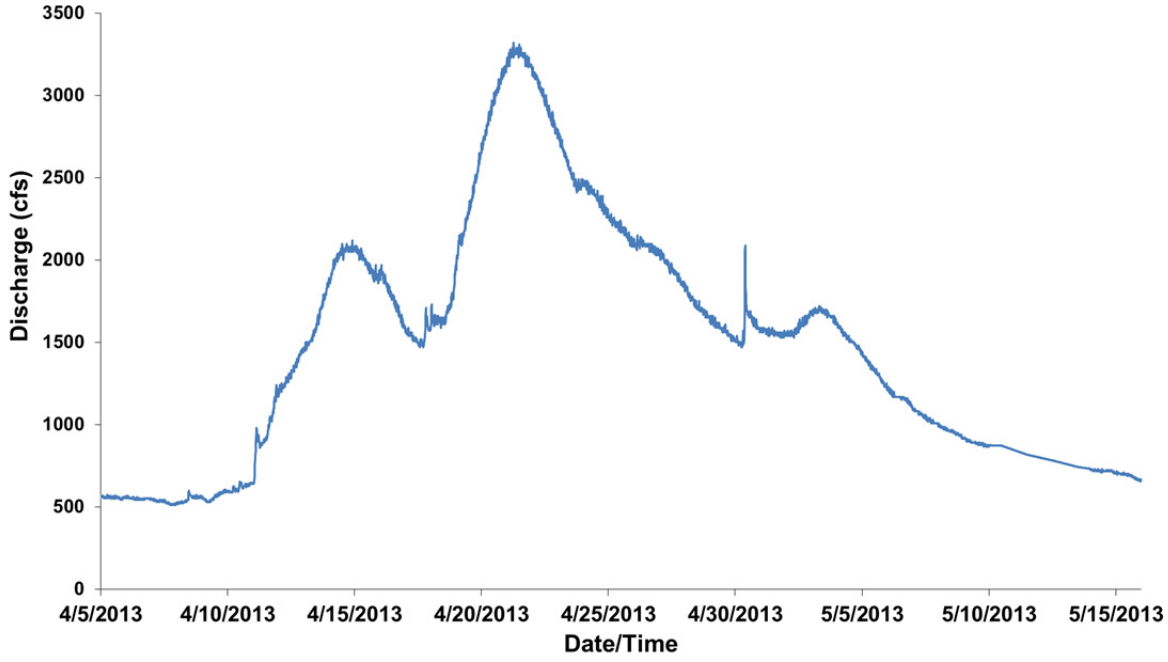

Figure 6. Hydrograph at the Kalamazoo River near Battle Creek gage (USGS 04105500) April to May 2013.

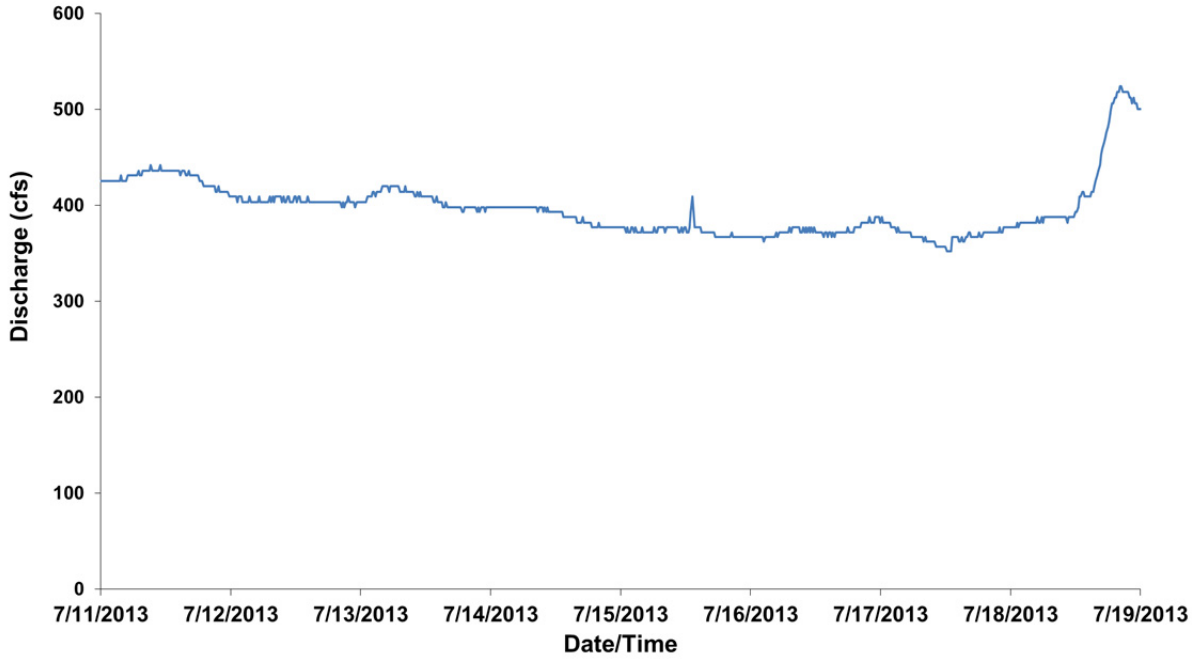

Figure 7. Hydrograph at the Kalamazoo River near Battle Creek gage (USGS 04105500) July 2013.

3.2.2 Tributary Inflows

Tributaries are an important source of flows to the Kalamazoo River main stem, and make up a critical part of the development of flow boundary conditions. The tributaries included Battle Creek as well as other smaller tributaries. The USGS gage for Battle Creek is approximately 3 miles upstream of the confluence of the Kalamazoo River and Battle Creek. Additional tributaries were included in the model to simulate all of the watershed flows that contribute flow in the simulated reach. These additional flows include the following tributaries:

- Talmadge Creek
- Bear Creek
- Harper's Creek and Minges Brook
- Battle Creek
- Wabascon Creek
- Sevenmile Creek
- Augusta Creek
- Gull Creek

Tributary flows were updated from the 2012 Enbridge model inputs with revised tributary flow estimates calculated by USGS staff on a 15-minute basis for the October to November 2011 riverine simulation and the July to August 2010 floodplain simulation. Flow estimates were also developed for the new simulation time periods, April to May 2013 and July 2013. The Flow Anywhere method was used to estimate flows for tributaries with no gages (Reneau et al., 2014).

The tributary flow estimates included estimates of flows from unaccounted for areas (watershed area that were not accounted for within one of the eight tributaries listed above) and a balancing

term. The balancing term allowed the tributaries to produce a volume of flow consistent with the flow that passes the downstream gages near Battle Creek and at Comstock. There were separate unaccounted area flows and balancing term flows calculated for tributaries located both upstream and downstream of Battle Creek. For both the upstream and downstream tributaries, unaccounted flows were distributed among the tributaries by a drainage area ratio at each 15 minute input interval. The balancing term was distributed in the same manner for the upstream tributaries.

During some 15-minute input intervals, the balancing term for flows downstream of Battle Creek was negative due to volume changes in Morrow Lake resulting from dam operations. For this reason, balancing term flows in this downstream reach were computed and distributed differently from the upstream balancing term flows. For the downstream tributaries, the tributary flow volume and the balancing term flow volume were added together over a modeling period (e.g. October 28 –November 9, 2011) along with the volume change in Morrow Lake. As shown below, the total volume was divided by the total tributary volume to get a scaling factor. Each tributary flow estimate was then multiplied by the scaling factor at every 15-minute input interval to increase all of the tributary flows by a uniform percentage throughout the modeling period.

$$\sum V_{Tribs} + \sum V_{Balance} + \Delta V_{ML} = Total\ \ volume$$

$$SF = \frac{Total\ volume}{\sum V_{Tribs}}$$

Where:

$\sum V_{Tribs}$ = Sum of volume produced by lower tribs in a modeling period

$\sum V_{Balance}$ = Sum of volume of the flow balancing term in a modeling period

ΔV_{ML} = Volume change in Morrow Lake in a modeling period

SF = Scaling factor

In comparison with 2012 Enbridge model inputs, the tributary flow updates addressed the issues of negative tributary flows (Figure 8), and unusually large flows in some tributaries, most likely due to the placement of all unaccounted for flow into one tributary (Figure 9). Gaged tributaries generally matched as expected (Figure 10).

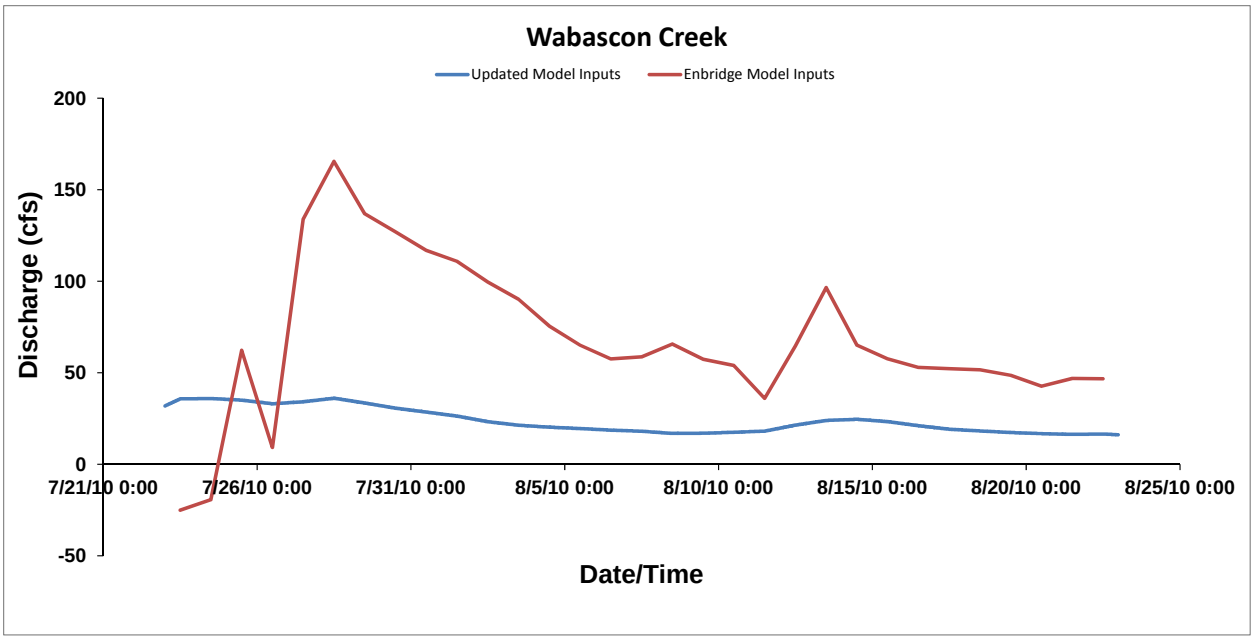

Figure 8. Improvements to tributary flow input, addressing negative flows and excessive peak flows in 2012 Enbridge model inputs (Wabascon Creek from July to August 2010 simulation).

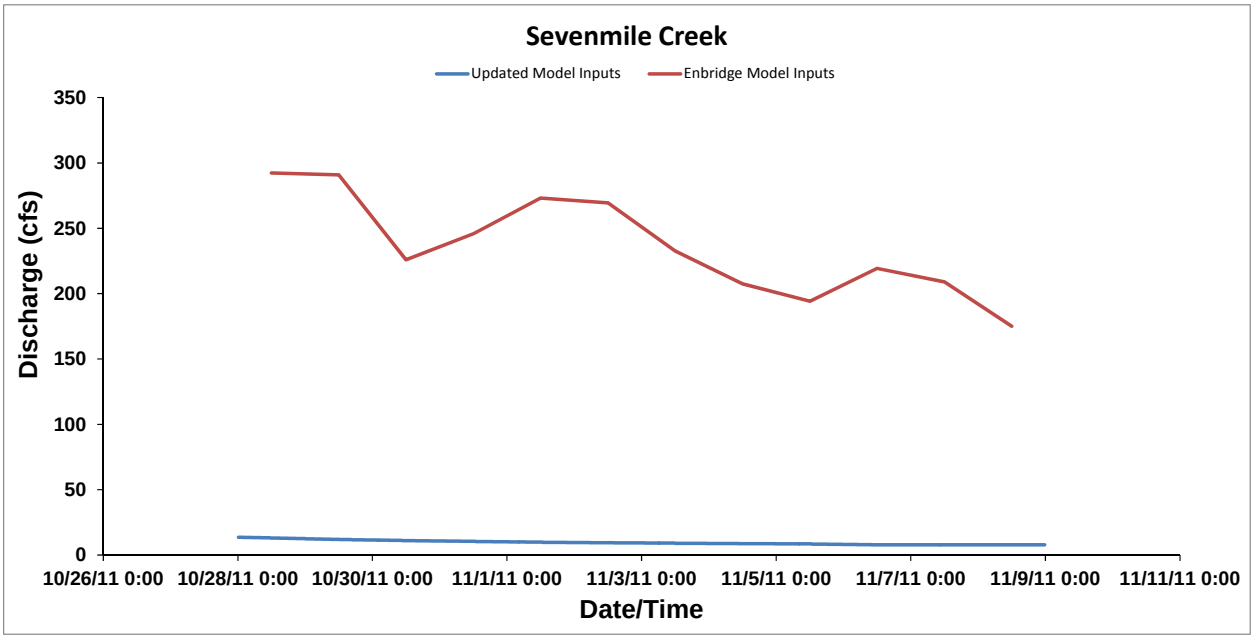

Figure 9. Unreasonably large flows in small tributaries in 2012 Enbridge model inputs (Seven Mile Creek from October to November 2011 simulation).

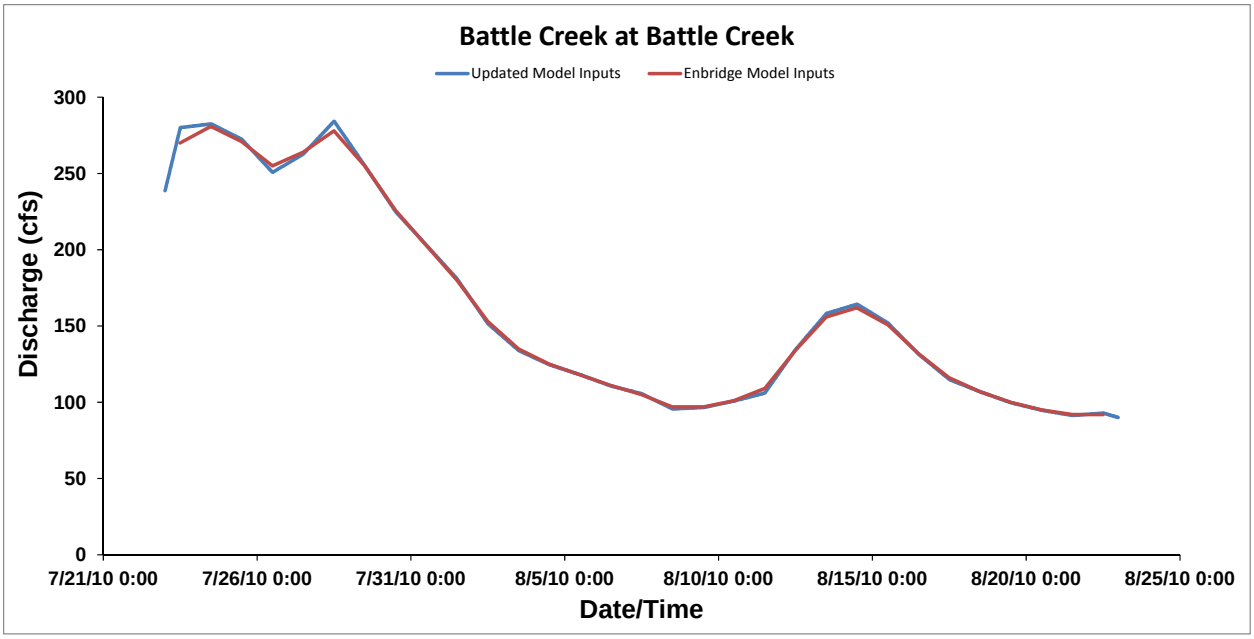

Figure 10. Close match between models in gaged tributaries (Battle Creek from October to November 2011 simulation).

3.2.3 Suspended Sediment Rating Curve

Following refinement of the mainstem and tributary flow inputs described in the previous sections, updated sediment loading estimates were based on new data collected in 2013-2014 (Reneau et al., 2014). Tributaries were classified according to watershed and stream characteristics to determine groundwater and surface water dominance, with consideration given to primary storage provided by swamps, wetlands, and reservoirs. A panel regression analysis (Soong et al., 2015) was used to estimate the coefficients of a power law rating curve for each tributary of the form:

$$SSC = 10^{a} \times Q^{b}$$

where,

SSC = suspended sediment concentration (mg/L)

Q = tributary discharge (cfs)

The estimated coefficients, a and b, were applied to calculate sediment concentrations at 15 minute intervals based on the tributary flow estimates described in Section 3.2.2. The calculated sediment concentration time series was then used to create the SEDZLJ sediment inputs for each tributary in the updated model. The estimated values for coefficients a and b are summarized in Table 4.

Table 4. Updated sediment rating curve coefficients used for each tributary (Soong et al., 2015).

Tributary	a	b
Kalamazoo River at Marshall (u/s BC) 4103500	1.9426	-0.2030
Battle Creek at Battle Creek 4105000	-0.1612	0.603
Talmadge Creek ungaged	-0.1612	0.603
Bear Creek ungaged	-0.1612	0.603
Minges Brook-Harper ungaged	-0.1612	0.603
Sevenmile Creek ungaged	-0.1612	0.603
Gull Creek ungaged	1.5785	-0.5439
Augusta Creek 04105700	2.2785	-0.5439
Wabascon Creek ungaged	2.2785	-0.5439

The updated sediment rating curves are presented in Figure 11. Some of the creeks were assigned the same rating curve, but concentrations applied to the model at any given time step are not the same because the concentration depends on the discharge in the creek.

The 2012 Enbridge model sediment rating curve is also presented in Figure 11. Note that the concentrations predicted by this curve are dependent only on the flow at Marshall, and all of the tributaries had the same solids concentration as the upstream boundary in the 2012 Enbridge model. The sediment load was broken into three classes in the Enbridge model: 15% clay, 50% silt, and 35% sand, and the maximum concentration of the rating curve was capped at 120 $mg \cdot L^{-1}$. The rating curve was based on a limited number of data points that were collected at a gage upstream of the Marshall gage in the 1970s (Tetra Tech, 2012).

The 15/50/35 particle size distribution was retained from the 2012 Enbridge model, although the size range represented by each modeled size class varied to some degree (Section 3.4). The tributary sediment loads in the updated model were split into 15% clay/fine silt, 50% medium to coarse silt, and 35% very fine sand. Particle size data collected by USGS in 2012 – 2014 included locations on the Battle Creek and Augusta Creek tributaries. Data for these tributaries supported this particle size distribution, with data-based sand fractions ranging from 20% to 60%, clay/fine silt size fractions generally less than 25%, and the remainder falling in the medium to coarse silt size (Reneau et al., 2014).

The upstream sediment load input at Marshall was 30% clay/fine silt, 60% medium to coarse silt, and 10% very fine sand in the updated model. The USGS data included samples at Marshall, which averaged approximately 15% clay/fine silt, 55% medium to coarse silt, and 30% sand; however, with consideration of the data likely reflecting some aggregated small particles within the larger size fractions (Reneau et al., 2014), this small adjustment to a finer distribution at the upstream boundary was not deemed inconsistent with the data, and it prevented excessive deposition of the upstream load near the boundary of the model.

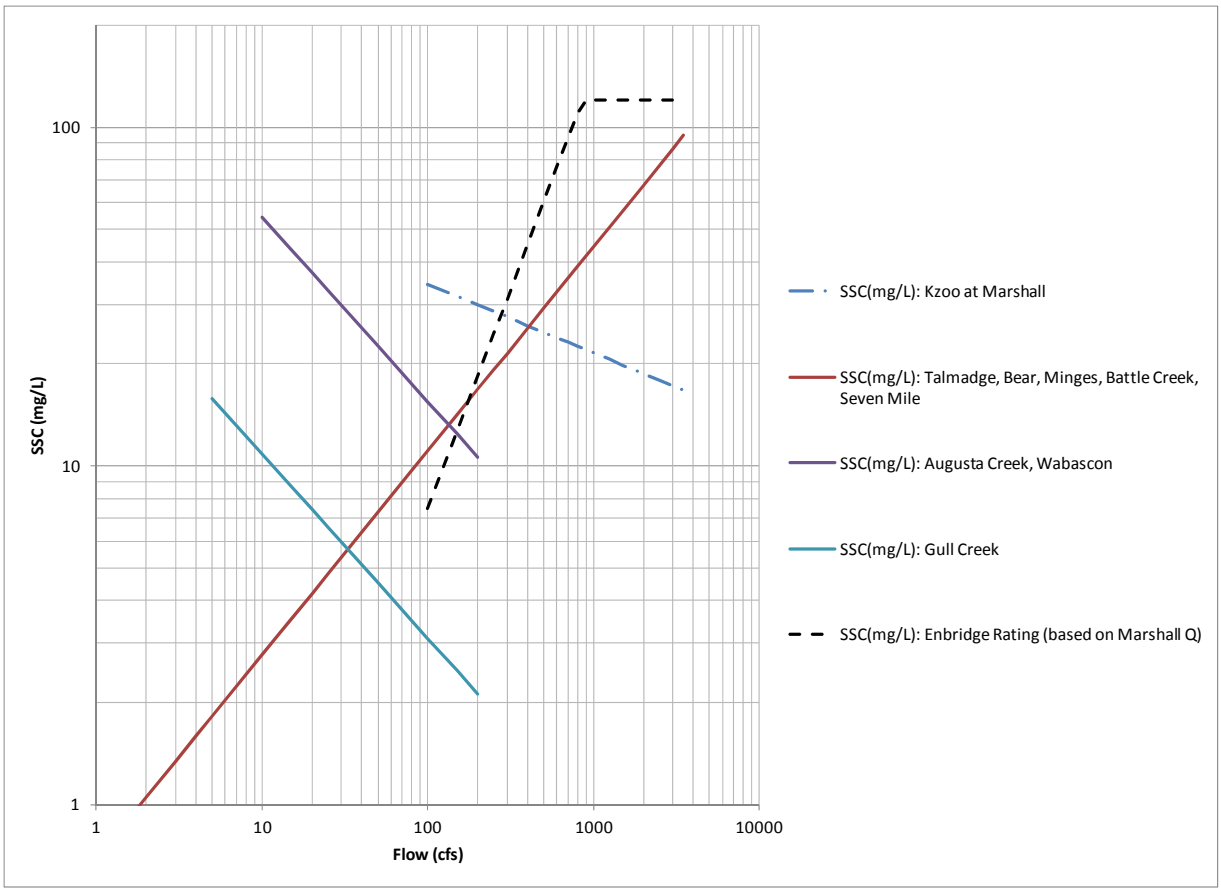

Figure 11. Sediment rating curves developed by USGS compared with the sediment rating curve used for 2012 Enbridge model (dashed black line).

3.2.4 Stage Discharge Relationships and the Downstream Boundary– The Three Dams

The dam rating curves were updated at Ceresco Dam and at Kalamazoo River Dam using the HEC-RAS model updated by Weston in 2014 (Johnson and Weston Solutions, 2014). The dam rating curves represent total flow across the width of the dam and consequently estimated flow must be divided by the number of model grid cells comprising that width. The number of grid cells at Ceresco Dam and Kalamazoo River Dam were different in the riverine and floodplain models. The same rating curves were used for the riverine and floodplain models, and scaled by dividing the total discharge by the number of grid cells to which the rating was applied. This scaling was not done in the 2012 Enbridge model, resulting in inaccuracy in the stage-discharge relationships being applied to the riverine and floodplain models (Figure 12 and 13).

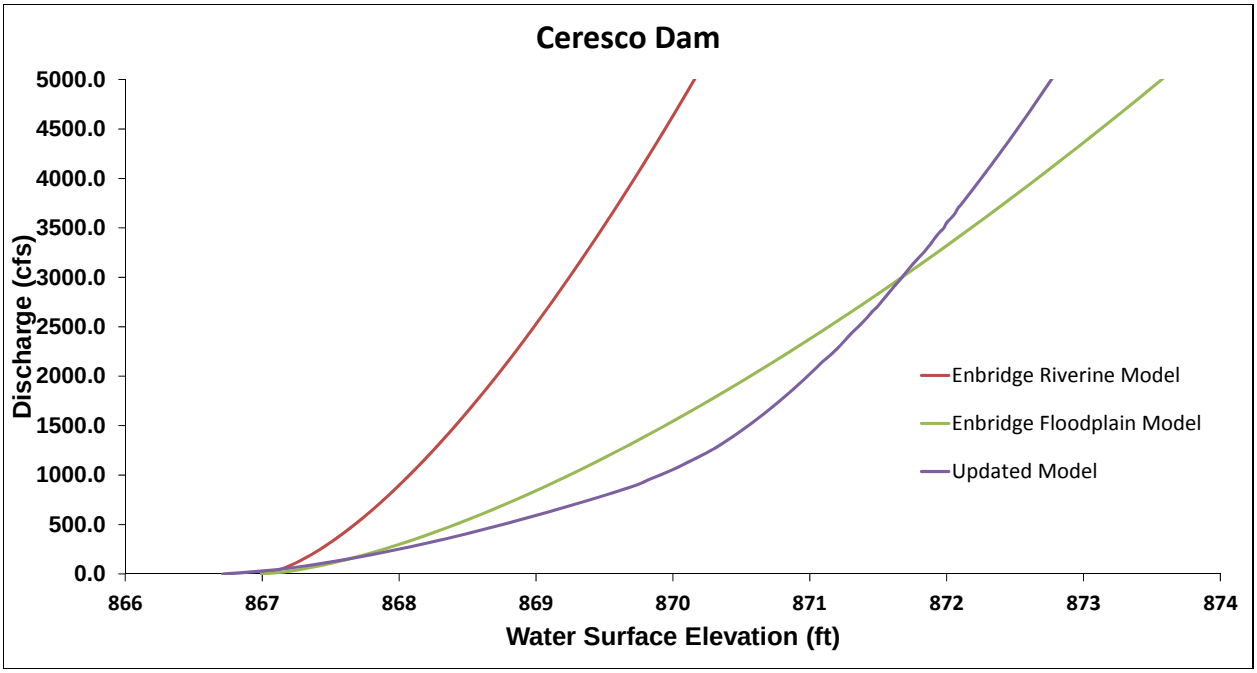

Figure 12. Dam rating curves at Ceresco Dam.

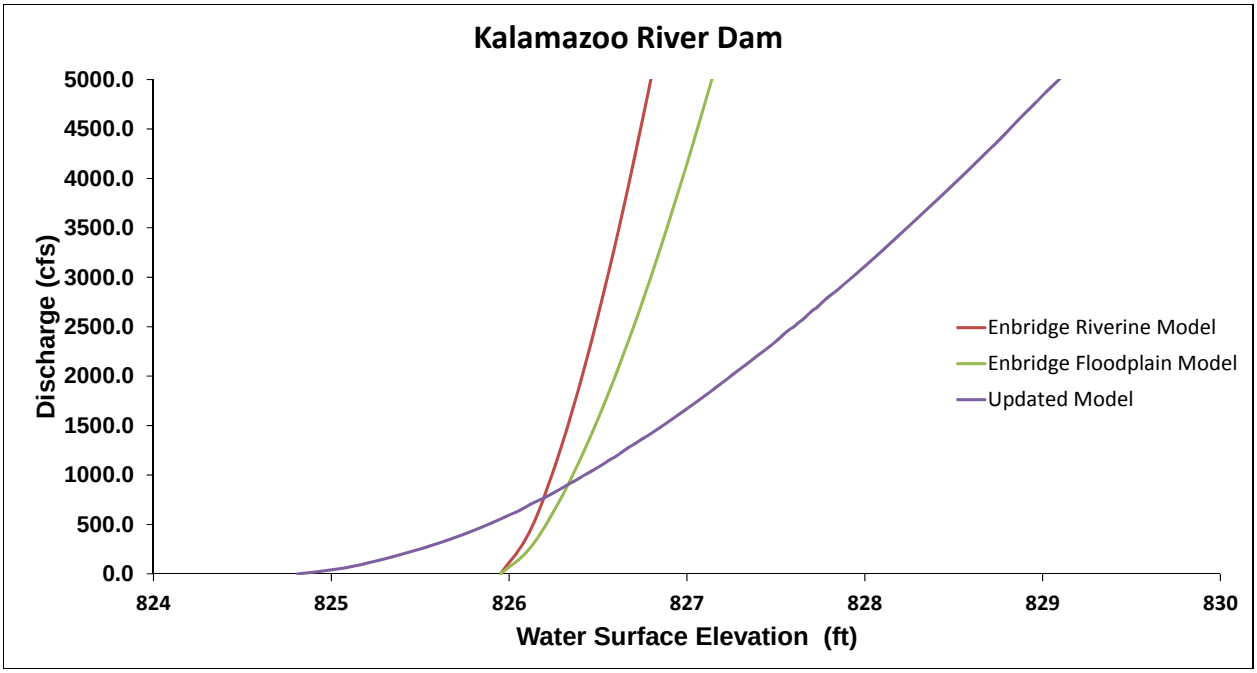

Figure 13. Dam rating curves at Kalamazoo River Dam.

The 2012 Enbridge model used a stage-discharge rating curve at Morrow Lake for their downstream boundary condition. Because of the complexity of dam operations at the Morrow Lake Dam, which include passage of flows through a combination of turbines, tainter gates, and overflow weirs, all of the updated model simulations simply drive the boundary condition at this location

with headwater elevations measured at Morrow Lake. The headwater elevation data were obtained from the following sources:

- USGS stage recorder data at Mile Post 38.55. USGS data were used for the July 2013 low flow and the April – May 2013 high flow model simulations.
- STS Hydro Power data collected upstream of the Dam. STS data were used for the October – November 2011 high base flow and the July – August 2010 oil spill flood simulations.

The data collected by STS were reported relative to the NGVD29 datum and were adjusted to NAVD88 for use in the model. The adjustment factor was -0.137 meters and was obtained from NOAA (http://www.ngs.noaa.gov/cgi-bin/VERTCON/vert_con.prl).

3.3 Hydraulic Parameters

After updating the hydrodynamic model with improved bathymetry and topography, tributary flow inputs, dam stage-discharge ratings, and Morrow Lake stage data, the model input for roughness height was evaluated.

3.3.1 Channel

The Enbridge model had a channel roughness (universal logarithmic velocity profile roughness height, Z_o) of 2 cm in the riverine model. The channel roughness was lowered to 5 mm in the updated model because of the resulting improvements in water surface elevations and velocities in comparison with measured data.

In the updated floodplain model a channel roughness of 0.2 mm was applied to the river channel compared to channel roughness of 2 cm in the Enbridge model. This low channel roughness was used in part to compensate for the apparent momentum losses related to poor grid alignment with the river channel, as described in Section 2.4. This lower channel roughness allowed model predictions to be more consistent with measured water surface elevation and velocity data that were collected by USGS in April 2013 (discussed further in Sections 4.2 and 4.5).

The tributary channel cells in the updated floodplain model were also given a channel roughness of 0.2 mm. In the 2012 Enbridge model these tributary channel cells were assigned the same roughness as the adjacent floodplain cells.

In the concrete channel portion of the floodplain grid just downstream of the Mill Ponds area a roughness of 0.1 mm was used, which is a representative roughness for concrete (Chow, 1959).

3.3.2 Floodplain

Roughness applied to floodplain grid cells in the updated model remained the same as that used in the floodplain portion of the grid in the 2012 Enbridge model. LimnoTech tested the model with a lowered floodplain roughness and found there was not a significant improvement in channel velocity and water surface elevations in model-to-data comparisons. In addition there were very little velocity data in the floodplain to justify revising the roughness.

3.4 Sediment Transport Inputs

The updated sediment transport model was run as part of the riverine model for the October to November 2011 and July 2013 time periods. These two scenarios were used to evaluate sediment transport behavior for in-bank flow conditions and to provide the framework for simulation of oiled sediments. New inputs for the updated sediment transport model were developed for sediment size classes, settling velocities, critical shear stresses and streambed substrates.

3.4.1 Sediment Size Classes

The updated sediment transport model was expanded from three sediment size classes to five. The 2012 Enbridge model included three classes specified as clay, silt, and sand (Tetra Tech, 2012). The updated model expanded to two sand classes (very fine sand and fine to medium sand) in order to better capture the wide range of settling velocities amongst sand-sized particles (Table 5). The updated model also refined the characterization of the two smaller size classes, clay and silt, from the 2012 Enbridge model, defining these as clay/fine silt and medium to coarse silt, respectively. Additionally, the updated model included a coarse sand/gravel size particle, which played a significant role in armoring the surface of the sediment bed against unrealistic erosion depths in higher energy areas of the river (see Section 3.4.4 for details). Modeled erosion was limited in the 2012 Enbridge model by constraining the model so that it could not erode beyond the top 10 cm of the bed.[1]

Table 5. Updated model sediment size classes.

Updated Model Sediment Size Class	Wentworth Scale Diameter Range (µm)[1]	Characteristic Particle Diameter Selected for Updated Model (µm)
Clay / Fine Silt	< 15	6
Medium to Coarse Silt	15 – 63	30
Very Fine Sand	63 – 125	75
Fine to Medium Sand	125 – 500	200
Coarse Sand / Gravel	500 – 4000	1500

[1] Wentworth scale presented in Lick (2009)

[1] This constraint of the 2012 Enbridge model was mentioned in Tetra Tech's (2012) report on the Enbridge model within a discussion of sediment bulk density, "The initial sediment layer of 0.1 meter thickness was the only mobile layer, therefore values [for bulk density] below the initial layer did not influence model results" (p. 16). The statement was unclear as to whether this was a finding of the model, or a restriction imposed on the model. LimnoTech determined the erosion limitation was imposed on the 2012 Enbridge model by specifying an inconsistency in the model inputs for sediment mass and volume. The 2012 Enbridge model was set up to run out of sediment mass in the top bed layer (causing erosion to cease) without running out of sediment volume. Due to the remaining volume, the model would never begin to access sediment mass present in the deeper layers of the bed.

3.4.2 Settling Velocities

Settling velocities are computed internally within the updated model based on the formula proposed by Cheng (1997). The computed settling velocity is a function of particle density and particle diameter. Particle density is hard-coded to be 2.65 g/cm^3. The characteristic particle diameter for each modeled sediment class is shown in Table 5, and the resulting settling velocities are shown in Table 6. The 2 m/day settling velocity for clay/fine silt class and the 50 m/day settling velocity for the medium to coarse silt class are the same as those used in the 2012 Enbridge model for the clay and silt classes. The sand class in the 2012 Enbridge model settled at approximately 1,000 m/day. The sand classes in the updated model bracket this value, with the very fine sand settling at approximately 300 m/day and the fine to medium sand settling at approximately 1600 m/day.

Table 6. Settling velocities for each sediment size class.

Updated Model Sediment Size Class	Updated Model Settling Velocity (m/day)	2012 Enbridge Model Sediment Size Class	2012 Enbridge Model Settling Velocity (m/day)
Clay / Fine Silt	2	Clay	2
Medium to Coarse Silt	50	Silt	50
Very Fine Sand	305	--	--
Fine to Medium Sand	1,670	Sand	~ 1,000[1]
Coarse Sand / Gravel	12,885	--	--

[1] Internally computed by EFDC

3.4.3 Critical Shear Stress for Erosion and Deposition

Each sediment size class included in the updated model is assigned a critical shear stress. The critical shear stress is a threshold for erosion or deposition. In the updated model, when the bed shear stress is above the threshold for a size class, sediments of that size can erode; and when the bed shear stress is below the threshold, sediments can deposit. The critical shear stress for each sediment size class is shown in Table 7. The critical shear stress inputs used in the updated model are typical of values reported in the literature (e.g., USGS (2008), Table 7). Values used in the 2012 Enbridge model are also shown in Table 7, although there are differences in the way each model uses the critical shear stresses. This is discussed below, as it highlights some important differences between the Enbridge model and the updated model.

Table 7. Critical shear stress for each sediment size class.

Updated Model Sediment Size Class	Updated Model Critical Shear Stress (Pa)	2012 Enbridge Model Sediment Size Class	2012 Enbridge Model Critical Shear Stress (Pa)
Clay / Fine Silt	0.05	Clay	0.4
Medium to Coarse Silt	0.05	Silt	0.4
Very Fine Sand	0.1	--	--
Fine to Medium Sand	0.15	Sand	0.12[1]
Coarse Sand to Gravel	0.82	--	--

[1] Internally computed in EFDC

Figure 14 illustrates various forms of flow resistance. Total bed shear stress is the sum of grain stress and form drag. Grain stress reflects the near-bed stress felt by particles at the bed surface. Form drag results from larger-scale elements of flow resistance such as bedform resistance from dunes or ripples and bank and planform resistance in sinuous river reaches. Grain stress is always less than (or possibly equal to) total bed stress. In the 2012 Enbridge model, grain stress is typically around 10% of total bed stress, whereas in the updated model, grain stress is typically around 20% of total bed stress. The difference is primarily attributable to the larger channel roughness height used in the 2012 Enbridge model as compared to the updated model, which results in a higher model-computed total bed stress.

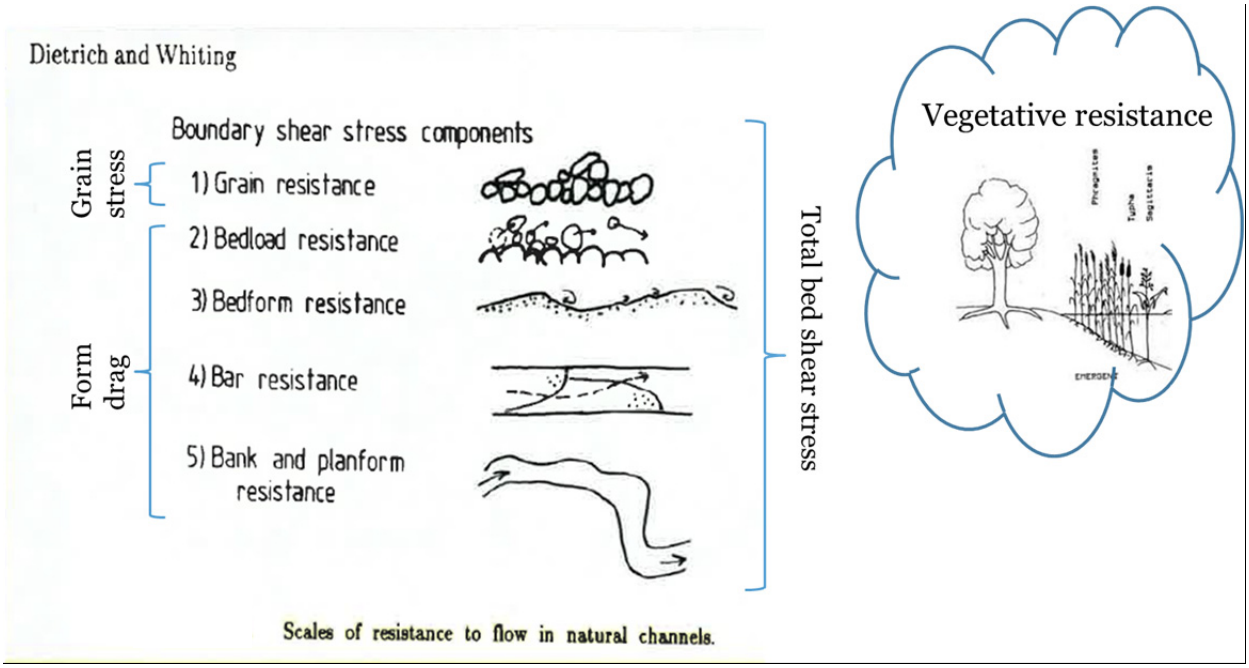

Figure 14. Flow resistance in natural channels (based on Dietrich and Whiting, 1989).

For purposes of determining deposition, the updated model compares the critical shear stress values shown in Table 7 against model-computed grain stress. For grain stresses less than the critical shear stress, deposition occurs. This differs from the 2012 Enbridge model, which compares critical shear stress to total bed stress when determining if deposition should occur. As an example, if a grid cell in the updated model has a grain stress of 0.06 Pa, then deposition of clay and silt particles would not occur (0.06 Pa grain stress > 0.05 Pa critical shear). Assuming the grid cell in the 2012 Enbridge model has the same grain stress of 0.06 Pa and has total bed stress 0.6 Pa, then deposition of clay and silt would also not occur in the 2012 Enbridge model (0.6 Pa total bed stress > 0.4 Pa critical shear). This example is intended to highlight how differences in the model algorithms can mitigate what appears to be a large difference in model inputs. This example is not intended to indicate that sediment deposition is the same in all locations for the 2012 Enbridge model and the updated model. In fact, there are significant differences in deposition computed by the models. Examples of these differences are shown in Section 5.

In terms of erosion, both models erode based on grain stress, which means that the updated model has the *potential* to erode clay and silt particles at a much lower grain stress than the 2012

Enbridge model. For example, assuming a grid cell has a grain stress of 0.2 Pa in both models, clay and silt would not erode from that cell in the 2012 Enbridge model (0.2 Pa grain stress < 0.4 Pa critical shear), but *could* erode in the updated model (0.2 Pa grain stress > 0.05 Pa critical shear). While this simple example accurately depicts erosion determination in the 2012 Enbridge model, there are a couple of model framework differences between the models that make this example too simplistic for determining whether or not erosion would occur in the updated model.

Erosion is strictly particle-based in the 2012 Enbridge model. Anywhere a clay or silt particle is present in the sediment bed, the model will erode those particles if grain stress exceeds 0.4 Pa. In the updated model, the threshold for erosion first considers bulk properties of the sediment bed. For example, medium to coarse silt particles may be present in a bed surface grid cell containing a mix of silt, sand, and larger gravel-sized particles. The critical shear for this sediment mix might be 0.6 Pa, in which case the medium to coarse silt particles present in the grid cell would not erode until grain stress reaches 0.6 Pa.

To further explore the example above, if the grain stress applied to this grid cell in the updated model were 0.7 Pa, then erosion from the bed would occur, but the coarse sand/gravel particles present in the bed would be left behind because their critical shear for erosion (0.82 Pa, Table 7) was not exceeded. In other words, in order for a particular sediment class to erode in the updated model, the grain stress must exceed the critical shear stress of both the bulk sediment bed and of the individual sediment class. This is one of the means by which the sediment bed can armor in the updated model – the surface of the bed can become enriched with larger, more difficult to erode particles. No armoring mechanism was applied in the 2012 Enbridge model.

3.4.3.a VEGETATIVE RESISTANCE

Vegetative resistance is also shown in Figure 14. This resistance applies to flow through vegetated areas such as the Kalamazoo River floodplain. The vegetation provides flow resistance without imparting a shear stress to the sediment bed. Vegetative resistance can be simulated with the EFDC hydrodynamic model; however, neither the 2012 Enbridge model nor the updated model explicitly included this. The 2012 Enbridge model includes flow resistance due to vegetation by increasing the hydrodynamic roughness (Z_o) of grid cells in the floodplain of the floodplain model grid. While this can provide a reasonable hydrodynamic model result, the model "sees" this extra resistance as coming from the sediment bed and overstates total bed shear stress. In the 2012 Enbridge model, since deposition is tied to total bed shear stress, the increased Z_o for floodplain grid cells may cause an understatement of floodplain deposition. For the updated model, only hydrodynamics were simulated with the floodplain model grid.

3.4.4 Streambed Substrate

As discussed above, the updated model utilizes properties of the bulk sediment bed in addition to properties of the individual sediment classes that comprise the bed. Characterization of the streambed was based on the sediment type and geomorphic surface mapping developed by Tetra Tech for Enbridge, which used poling data and physical data from streambed characterization cores (Tetra Tech, 2012). Four generalized sediment categories were used to represent the streambed in

the updated model, with the assignment of those categories linked to the Tetra Tech mapping of the bed as shown in Table 8.

Each of the Tetra Tech sediment types (SED_CATs) were applied to a single updated model bed type with the exception of the sand and silt SED_CATs. The sand and silt categories were split, based on Tetra Tech's geomorphic surface categories (SURF_CATs), between the Gravel / Sand /Silt bed type and the Sand / Silt bed type. SURF_CATs associated with higher energy flow areas, where the presence of some gravel was expected, were assigned to the Gravel / Sand / Silt bed type (e.g., SED_CAT = Sand and Silt, SURF_CAT = Thalweg). Most of the sand and silt SED_CATs were assigned to the Sand / Silt bed type, which assumed no gravel.

The Hardpan sediment type was used to represent portions of the river classified as "Gravel and larger". The Hardpan sediment type allows deposition and subsequent erosion of deposited material, but it does not allow for erosion into the parent bed of these very coarse-grained areas. Field evidence and geomorphic mapping showed that submerged oil was associated with deposits of fine-grained sediments in the Kalamazoo River; therefore, these high-energy flow areas classified as Hardpan are not expected to contain significant amounts of oiled sediments. Preventing net erosion from these areas of the model is not expected to adversely impact either the sediment transport or OPA model results. Further, bedload is often the primary transport mode for gravel and larger particles. If these Hardpan areas were to be modeled with an erodible parent bed, then bedload transport should be activated in the model. Because of the focus on transport of fine-grained sediments, which are transported in suspension, bedload transport was not simulated in either the 2012 Enbridge model or the updated model.

Table 8. Assignment of sediment bed types to the updated model.

Updated Model Sediment Bed Type	Tetra Tech SED_CAT	Tetra Tech SURF_CAT Exclusions
Hardpan	Gravel and larger	None
Gravel / Sand / Silt	Sand and gravel	None
Sand / Silt	Sand, Sand and silt, Sand over silt, Silt over sand	Include with Gravel / Sand / Silt sediment type: Thalweg, Near bank high energy, Channel deposit, Island, Island deposit, Cutoff channel (Sand SURF_CAT only), Anthropogenic deposit, Anthropogenic thalweg
Fine-grained	Soft sediment, Organic	None

In addition to the categories shown in Table 8, the 2012 Enbridge model also had an "Unknown" SED_CAT, which included the engineered channel near Battle Creek, islands, areas immediately behind the dams in Morrow Lake and the Mill Ponds, and several backwater areas, oxbows, and tributary confluences. These areas were assigned a sediment type in the updated model based on the conditions of the area. The engineered channel was assigned to Hardpan, islands and areas immediately behind the dams were assigned to Gravel / Sand / Silt, and the remaining unknown areas (largely backwater and other quiescent areas) were assigned to the Fine-grained sediment type.

3.4.4.a Model Bed Layers

The sediment bed in the SEDZLJ model consists of parent bed layers, along with the potential for active and deposition layers on top of the parent layers (Figure 15). The model is initialized with only parent layers present. As the sediment transport simulation progresses, a thin active layer can form at the sediment – water interface. The active layer thickness is computed by the model based on d50, shear stress and the amount of material available to form the active layer. The active layer forms when a grid cell receives deposited sediments from the water column or when erosion from the parent bed leaves larger-sized particles behind that could not be eroded at the applied shear stress. Due to being a thin layer (typically less than a couple of millimeters thick), the active layer quickly responds to changing hydrodynamic and sediment loading conditions in the river, which allows it to armor the surface of the sediment bed, protecting deeper layers from erosion. The deposition layer is used by the model to accumulate deposited sediments in excess of the amount needed to fill the active layer. This allows the parent layers to remain intact until such time as sufficient shear stress is applied to erode the active and deposition layers (if present) and cause erosion of the parent layers.

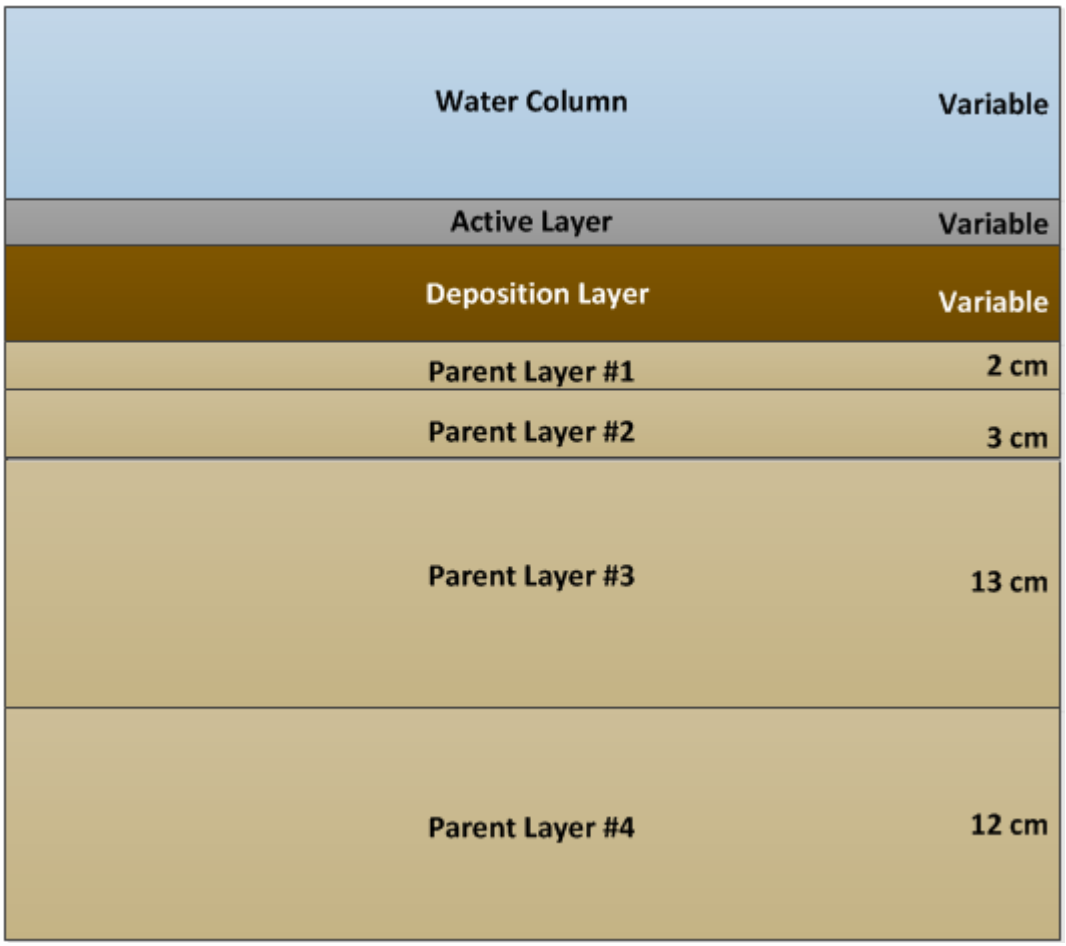

Figure 15. Updated model sediment bed layers.

3.4.4.b Bed Layer Properties

For each of the sediment bed types, the updated model requires inputs for particle size distribution, wet bulk density, critical shear stress for erosion, and erosion rate. These inputs are specified for each depth interval of the modeled sediment bed.

Specification of the sediment bed model inputs was guided by a combination of site-specific data, literature values, hydrodynamic characteristics, and the response of the sediment model to various inputs. Although the available data were insufficient to fully calibrate the sediment transport model, a few data sets (listed in Table 1) were available to either guide inputs directly or to constrain inputs by providing data targets for the model output. Sedflume data were used to specify sediment bed properties, and suspended sediment data (Reneau et al., 2014) provided a target for the resulting sediment transport.

Sedflume data were collected at nine locations during 2013, primarily focused in Morrow Lake (including the delta and neck) (Perkey et al., 2014). These data were used to directly specify sediment bed inputs for grid cells in Morrow Lake, downstream of the 35th Street Bridge. The process of applying Sedflume data to model grid cells is described in Section 3.4.5. Outside of Morrow Lake, the generalized sediment bed types were assigned as described above using the sediment bed type and geomorphic surface mapping developed by Tetra Tech. Model inputs for each bed type are shown in Table 9. Sedflume data helped guide these inputs, with the most direct application being the use of the Sedflume core SF-1 to define the values for the Fine-Grained bed type, albeit with somewhat different layer thicknesses. Properties of the Sand / Silt bed type relied heavily on the Sedflume core SF-9 data (below the top 1 cm). These two Sedflume cores were the only cores with erosion data collected outside of Morrow Lake.

The erosion rates are based on an equation of the form

$$E = A\,\tau^{n}$$

where E is the erosion rate (cm/s), τ is the shear stress (Pa), and A and n are constants. This is the same equation used to fit the Sedflume data (Perkey et al., 2014). The constant, n, was set to 2.5 for the Gravel / Sand / Silt and the Sand / Silt sediment bed types. A value of 2 to 3 is common (Lick, 2009), and 2.5 approximates the average for the Kalamazoo River Sedflume data (Perkey et al., 2014). Another property of the Sedflume data that was carried into the sediment bed type inputs is the trend of increasing critical shear stress with depth especially for the Fine-Grained bed type.

Table 9. Properties of updated model sediment bed types (parent layer).

Bed Property	Gravel/Sand/Silt	Sand/Silt	Fine-Grained
Sediment class size distribution (constant with depth):			
% Clay / Fine Silt	10	10	10
% Medium to Coarse Silt	25	45	55
% Very Fine Sand	10	20	20
% Fine to Medium Sand	30	25	15
% Coarse Sand / Gravel	25	-	-
Wet bulk density (g/cm^3):			
0 - 2 cm	1.80	1.30	1.15
2 - 5 cm	1.80	1.30	1.15
5 - 18 cm	1.80	1.45	1.15
18 - 30 cm	1.80	1.60	1.20
Critical shear stress (Pa):			
0 - 2 cm	0.5	0.4	0.1
2 - 5 cm	0.7	0.4	0.4
5 - 18 cm	0.9	0.8	0.8
18 - 30 cm	1.2	1.2	1.0
Erosion rate constant, *A*:			
0 - 2 cm	2.00E-05	3.00E-03	1.24E-02
2 - 5 cm	2.00E-05	3.00E-03	7.07E-03
5 - 18 cm	1.00E-05	2.00E-03	1.99E-03
18 - 30 cm	5.00E-06	1.00E-03	4.84E-04
Erosion rate constant, *n*:			
0 - 2 cm	2.5	2.5	2.74
2 - 5 cm	2.5	2.5	2.66
5 - 18 cm	2.5	2.5	2.49
18 - 30 cm	2.5	2.5	2.98

3.4.5 Direct Application of Sedflume Data

Within Morrow Lake, Sedflume data were used to characterize the sediment bed. The general approach of assigning Sedflume cores was to replace the Sand / Silt and the Fine-grained sediment bed types described above with data from one of the Sedflume cores. The Gravel / Sand / Silt bed type was generally not replaced by Sedflume data because none of the cores were collected in gravel sediments. A few exceptions are discussed below. The Sedflume data are described in Perkey et al. (2014). A map of the core locations taken from that report is reproduced here as Figure 16.

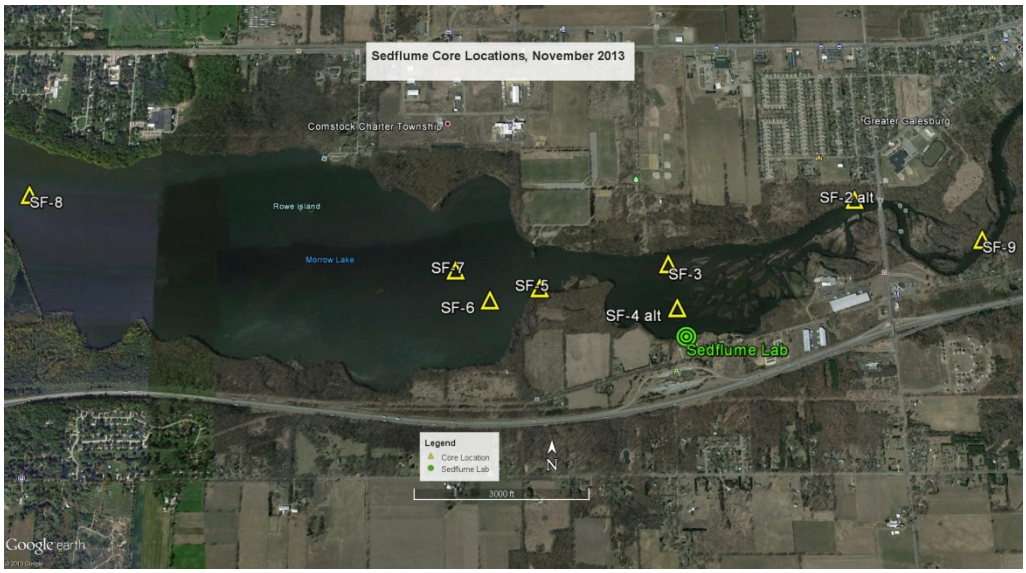

Figure 16. Sedflume core locations (Perkey et al., 2014).

Consideration was given to the coring locations and the characteristics of each core in deciding how to map the Sedflume data onto the model grid within Morrow Lake. The lake was divided into four regions, and the Tetra Tech SURF_CAT mapping was used to assign cores within each region. The process is described in Table 10.

Table 10. Mapping of Sedflume cores.

Morrow Lake Region	Sediment Bed Type Being Replaced	Sedflume Core Assigned	Tetra Tech SURF_CAT
Western Morrow Lake, west of MP38.5 / Rowe Island area	Fine-Grained Sand / Silt	SF-8	All SURF_CAT in the region
Fan, MP38.5 to MP37.75	Fine-Grained Sand / Silt	SF-6	Former Channel
		SF-5	Remnant Terrace, Backwater
		SF-7	All others
Neck, MP37.75 to MP37.5	Fine-Grained Sand / Silt	SF-6	All SURF_CAT in the region
Delta, MP37.5 to MP36.5	Fine-Grained	SF-5	All SURF_CAT in the region
	Sand / Silt	SF-3	All (except for Sand SED_CAT areas, which were retained as Sand / Silt bed type)

One exception to the mapping rules shown in Table 10 was made for the Sand SED_CAT within the delta. The generalized Sand / Silt bed type, with the properties shown in Table 9, was retained for these areas, rather than assigning SF-3.

In some portions of fan, neck, and delta, the Gravel / Sand / Silt bed type was also replaced with a Sedflume core. These are areas that were originally assigned to the gravel bed type as part of the river-wide mapping process using SED_CAT and SURF_CAT assignments, but are not expected to contain any significant gravel content within Morrow Lake:

- Fan:
  - Sand and silt (SED_CAT) – Thalweg (SURF_CAT) assigned SF-6
- Neck:
  - Silt over sand (SED_CAT) – Island deposit (SURF_CAT) assigned SF-6
  - Sand and silt (SED_CAT) - Thalweg (SURF_CAT) assigned SF-6
- Delta:
  - Sand and silt (SED_CAT) – Thalweg (SURF_CAT) assigned SF-6
  - Sand and silt (SED_CAT) – Island deposit (SURF_CAT) assigned SF-3
  - Silt over sand (SED_CAT) – Island deposit (SURF_CAT) assigned SF-3

Figure 17 shows the results of the Sedflume mapping. This figure is clipped near MP38.5. The western portion, not shown in the figure, was assigned SF-8. Figure 17 shows the Sedflume core assignments, as well as areas where one of the generalized bed types described in Tables 8 and 9 were retained.

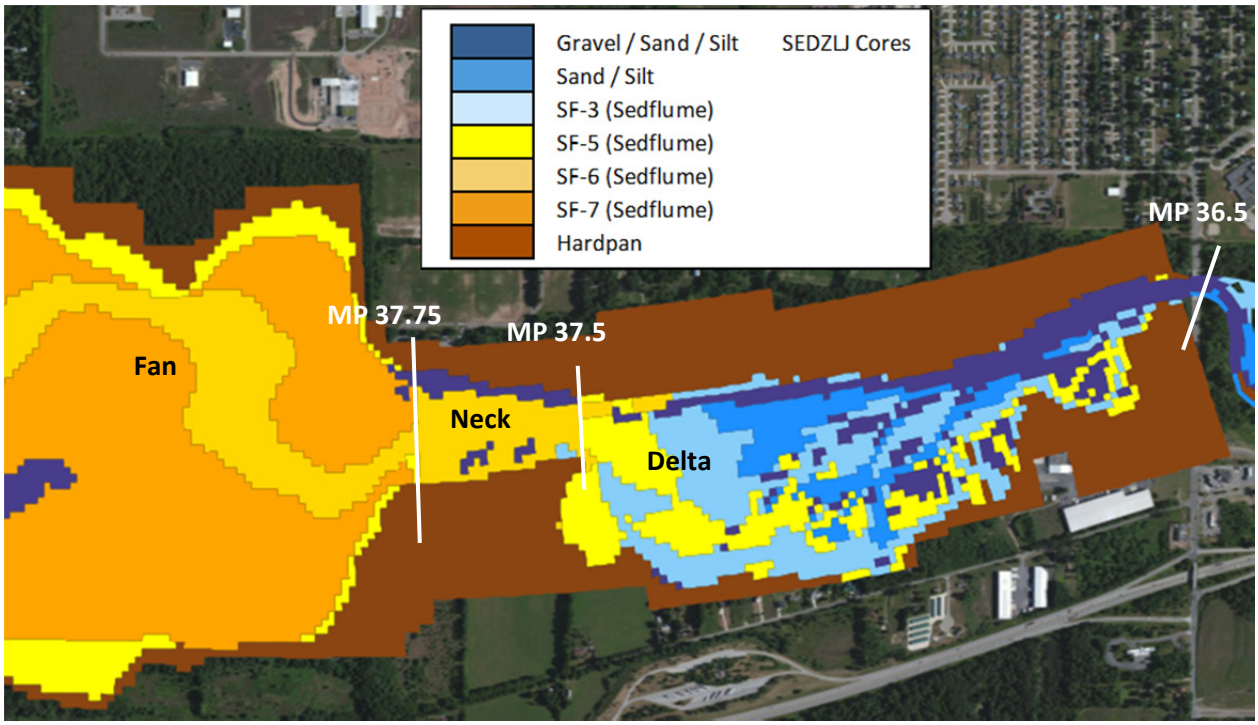

Figure 17. Model core assignment in Morrow Lake.

At each Sedflume core location, data are available for various depth intervals, with the thickness of each interval dictated by the properties of the core and the operating procedures of the Sedflume operator. The updated model used consistent depth intervals for all grid locations (0 – 2 cm, 2 – 5 cm, 5 – 18 cm, and 18 – 30 cm). The Sedflume data were mapped to the model depth layers using a "closest fit" approach, rather than a formal interpolation scheme. As an example, the uppermost

interval of data for Sedflume core SF-5 applied to 0 – 5.5 cm. Data for this interval were applied to both the 0 – 2 cm and the 2 – 5 cm layers in the model.

3.4.6 Adjustment of Sediment Transport Inputs

While data were insufficient to calibrate the sediment transport model, inputs were adjusted in order to obtain acceptable results from the model. Results were deemed acceptable based on consistency with the range of observed suspended sediment data and based on qualitative evaluations of results. For example, when simulating low- to moderate-flow conditions, coarse sand and gravel should not accumulate in bed locations that are known to contain only clay and silt, and deep scour holes should not form where none existed previously.

In order to achieve acceptable sediment transport results, erosion rates were reduced from the values directly measured with the Sedflume device and from those presented in Table 9 above. This adjustment impacts the rate at which sediments erode from the bed, but does not directly impact whether or not erosion occurs. A factor of 10 reduction in erosion rate was applied to all Sedflume cores and the three general bed types shown in Table 9. Without this adjustment, the sediment transport results were deemed to be too variable in time, with quick spikes of large suspended sediment concentration followed by rapid declines to unacceptably low suspended sediment concentrations as the bed armored.

Reasons why adjustment from the measured Sedflume rates may be necessary include differences in spatial scale between Sedflume and model grid cells and differences in temporal scale, with rapid changes in applied shear stress in the Sedflume device versus relatively slow changes in a natural system. The reduction in erosion rates for the Gravel/Sand/Silt bed type appeared to have the most significant impact on modeled sediment transport, suggesting that the model could benefit from a more complete characterization of these coarse-grained areas and how they are represented in the sediment transport model. With this adjustment to the rate of erosion, the sediment transport model generated acceptable results, which are shown in Section 5, providing a useful tool for characterizing areas of erosion and deposition and for serving as the framework for the OPA model of oiled sediments.

Blank page

4 Model to Data Comparisons

As discussed in Section 3, several data sets were collected in the three years following the July 2010 oil spill. Those data were used to support updates to model inputs (Section 3) and for comparison to model outputs. Model to data comparisons for the hydrodynamic model are the focus of this Section. Data available to check against sediment transport model output were much more limited. Those data are discussed in Section 5 as part of the model application.

4.1 Summary of Available Data

Data were collected by various entities and model to data comparisons considering stage, velocity and discharge were performed as summarized below in Table 11.

Discrete stage data were collected by Enbridge in October to November of 2011, using staff gages located at several locations in the main stem of the Kalamazoo River (Tetra Tech, 2012). In the spring to fall of 2013, continuous stage recorders were deployed by USGS at five locations: Ceresco Dam, the Mill Ponds area, the 35th Street Bridge, and two locations on Morrow Lake (Reneau et al., 2014).

Mean daily discharge records were available at USGS gages at the Kalamazoo River at Comstock (near the downstream model boundary) and the Kalamazoo River near Battle Creek gage. Both stage and discharge data were used to develop a balanced calibration of the hydrodynamic model to known conditions, over the range of events for which data were available.

The floodplain and riverine models were also compared against velocity data. Velocity data were collected by Enbridge at various locations in the main stem of the river in October-November 2011. In April of 2013, additional data were collected by Stephen Hamilton (Michigan State University) in the floodplain, and by USGS at various channel and impoundment transects throughout the spill affected reaches of the river. Velocity data provided a way to check and refine the hydrodynamic model calibration, providing insight into cross-sectional variation in velocities at critical sections of the river channel.

Some perspective on the elevations of floodwaters during the July to August 2010 period was obtained by reviewing an oil mark survey that was executed by Enbridge in the fall of 2010. The oil mark survey data were considered the least reliable water surface elevation data set in terms of quantitative elevation data. The 2012 Enbridge model results showed significant variations from the surveyed oil marks, with differences between model and data commonly +/- 2 feet or more (Tetra Tech, 2012). Uncertainties in the timing of when an oil mark was left and in determination of a single elevation from a smeared oil mark likely contributed to the difficulty in matching model results to these data.

For the updated model, the oil mark data were used as a qualitative check on flood extent. Although the elevations may be uncertain, the presence of an oil mark is a clear indication that the floodwaters extended to that location during the July 2010 oil spill. The model updates (bathymetry, topography, channel roughness, etc.) resulted in a somewhat reduced flood extent as compared to the 2012 Enbridge model. In terms of comparison to the oil marks, the reductions in flood extent did not result in a mismatch to the oil mark locations. In other words, areas flooded in the 2012 Enbridge model, but not in the updated model, were not supported by oil mark data.

The remaining datasets and model to data comparisons are described in greater detail in the following sections.

Table 11. Summary of model simulations and associated hydraulic data.

Model Simulations	Velocity	Water Surface Elevation	Discharge at gages
July-Aug 2010	None	Oil Mark Survey	Comstock and Battle Creek
Oct-Nov 2011	Enbridge collected point velocities	Staff gage data	Comstock and Battle Creek
April 2013	Michigan State University (floodplain) and USGS (river and impoundment) point velocities and transects	Stage Recorders	Comstock and Battle Creek
July 2013	None	Stage Recorders	Comstock and Battle Creek

4.2 USGS Stage Recorders

4.2.1 Floodplain Model

Stage recorder data collected by the USGS were used to calibrate the hydrodynamics of the floodplain model (Reneau et al., 2014). During the calibration of the model for simulations of the April 2013 period, it was found that the model was generally over predicting water surface elevations. The floodplain grid channel roughness was initially set at 5 mm, consistent with the updated riverine model. Reduction of the roughness value resulted in a significant increase in the quality of the comparison to water surface elevation data, with an optimal comparison at a channel roughness of 0.2 mm. This lowered roughness was likely necessary to account for apparent losses of momentum related to a lack of alignment between the grid and river in several locations, as described in Section 3.3. This improvement is especially apparent at the Mill Ponds and 35th Street stage recorders (Figure 18 b and c). The 35th Street stage recorder location was emphasized in the calibration because it is also a point where the model has received all tributary inputs and flows are fully developed. The model agreed closely with stage data at this location, providing an indication that the model is accurately characterizing total flow. Similarly, a close comparison was also observed when the model was compared to the USGS gage discharge data downstream at Comstock (See Section 4.4).

Water surface elevations at the Ceresco Dam were relatively insensitive to the change in roughness values described above because the stage recorder was located close to the dam, where the stage

discharge relationship governs water surface elevations (Figure 18 a). With either roughness (5 mm or 0.2 mm) the model to data comparison shows an approximately 0.5 foot difference or less between the model and the data for the entire simulation period, indicating that the updated rating curve is behaving as expected (See Section 3.2.4).

The last two stage recorders were located at Morrow Lake (Figure 18 d and e). The stage recorder at mile post 38.55 served as the downstream boundary condition for the July 2013 and April 2013 runs (See Section 3.2.4). As expected, the stage recorder data closely matches the model output at this location, as the model is forced to follow this elevation. The water level at mile post 37.8, a short distance upstream, is also driven by the downstream boundary, and the modeled water surface elevation at this location also closely matches the stage recorder data.

4.2.2 Riverine Model

Figure 18 also presents the water surface elevation output from the riverine model period of July 2013 in comparison with the stage recorder data. Model to data comparisons for this application period were also judged to be acceptable, with differences limited to less than 0.5 feet at all locations. Staff gage readings that were recorded in October to November 2011 were also used to check the updated model results against water surface elevation data (Section 4.3), but ultimately, no adjustment from the 5 mm channel roughness initially selected for the updated riverine model was needed.

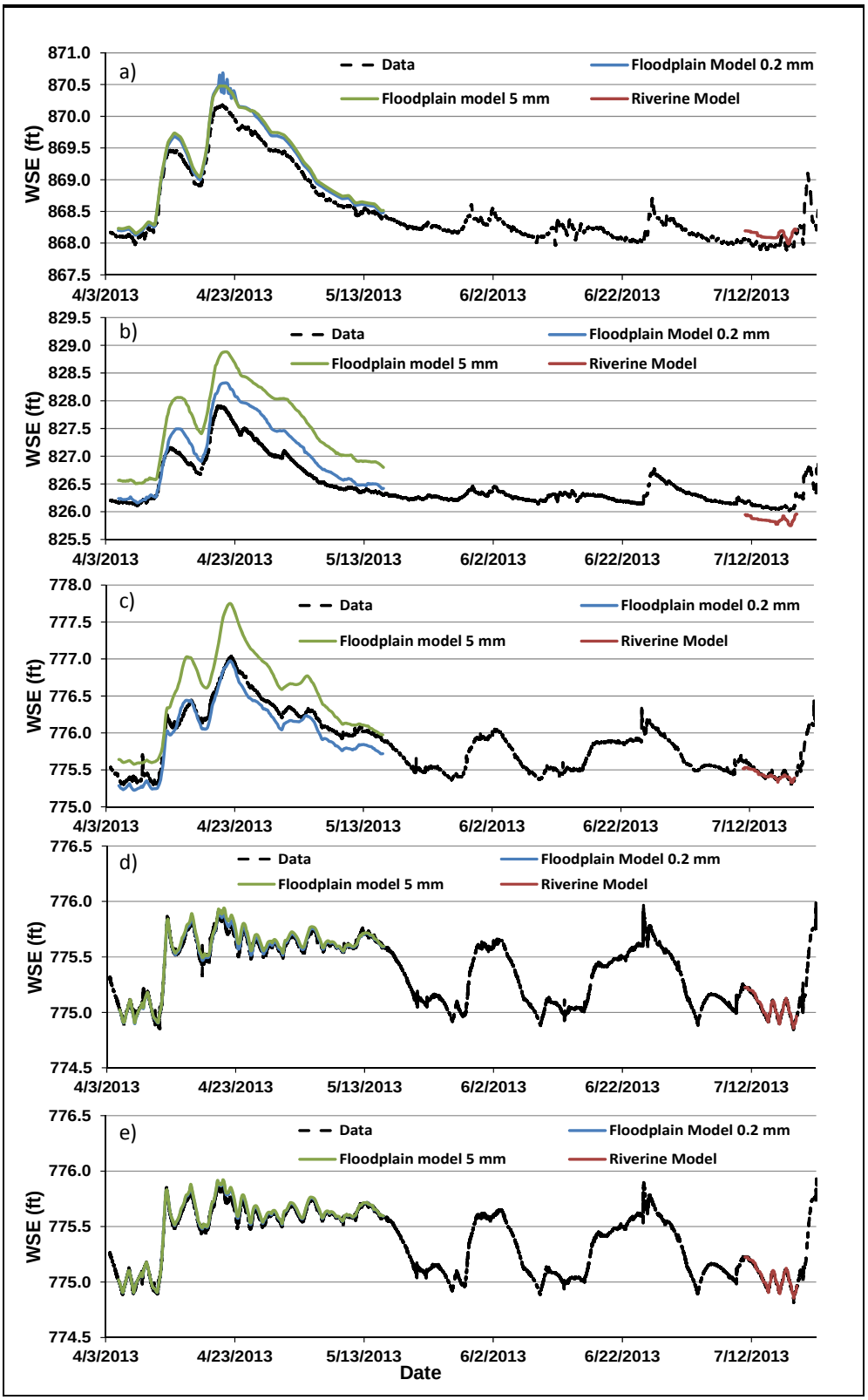

Figure 18. Stage recorders versus models at: a) Ceresco Dam; b) Mill Ponds area; c) 35th Street; d) River Mile 37.8 (Morrow Lake); and e) River Mile 38.55 (Morrow Lake). The floodplain model is compared at a 0.2 mm and a 5 mm channel roughness. The riverine model shows 5 mm channel roughness only.

4.3 Staff Gage Readings

Enbridge collected staff gage readings at numerous locations[2] in October to November 2011 and these data were used to supplement the calibration of the modeled water surface elevations, primarily by providing additional information about model performance for a time period and locations for which USGS stage recorder data do not exist (Figure 19). The staff gage data provide a way to assess the appropriateness of all the hydraulic model updates influencing updated model results, including the roughness, the dam rating curves, the bathymetry, and the tributary inputs.

At Ceresco Dam (Figure 20), the updated model and the 2012 Enbridge model show relatively small differences at the staff gage locations, but large differences in water surface elevations away from the gages. The updated model shows a smoothing of the water surface elevation profile, primarily due to the updated bathymetry (See Section 3.1). The water surface elevation has also changed at the dam due to the updated stage discharge relationship (See Section 3.2.4).

The Mill Ponds area (Figure 21) also shows a smoothing of the water surface elevation profile, again due to updated bathymetry. At this flow, the updated model water surface elevation has changed only slightly at the dam from the 2012 Enbridge model despite the updated stage-discharge relationship. A change in water surface elevation can be observed at Raymond Road and upstream of the road primarily due to the bathymetry updates. The water surface profile from the Mill Ponds area to the Morrow Lake Delta (Figure 22) also shows some changes resulting from model updates, although differences at the staff gage locations are relatively small.

Overall, while the updated model and the 2012 Enbridge model tend to predict similar water surface elevation results at the staff gage locations for the October to November 2011 time period, the updated model yields those results with improved bathymetry, improved dam rating curves, improved tributary flows, and an updated roughness height. These model updates result in more reliable predictions of water surface elevations throughout the system and for other time periods and lead to better predictions of discharge and velocity, which are discussed in the next sections.

[2] Staff gage data were obtained from Figure 4-3 of the Enbridge model report (Tetra Tech, 2012). Data were reported for gages at mile posts 2.25, 5.25, 10.0, 15.0, 16.75, 21.5, 27.0, 30.0, 35.0, and 38.0. The mile post locations associated with gage data in this LimnoTech model update report were based on surveyed gage locations and the latest mile post shapefile. Slight differences from the Enbridge reported locations relate only to the mile post labeling and do not reflect inaccuracies in matching the gage locations to the model grid cells for model-data comparisons.

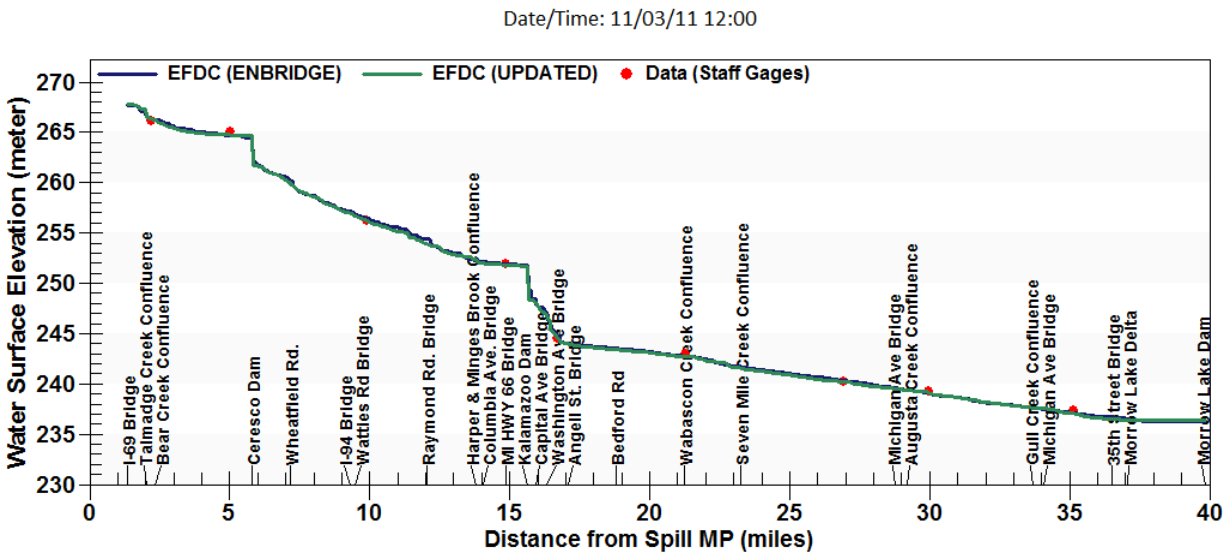

Figure 19. The 2012 Enbridge model and the updated model WSE profile for the entire river November 3, 2011.

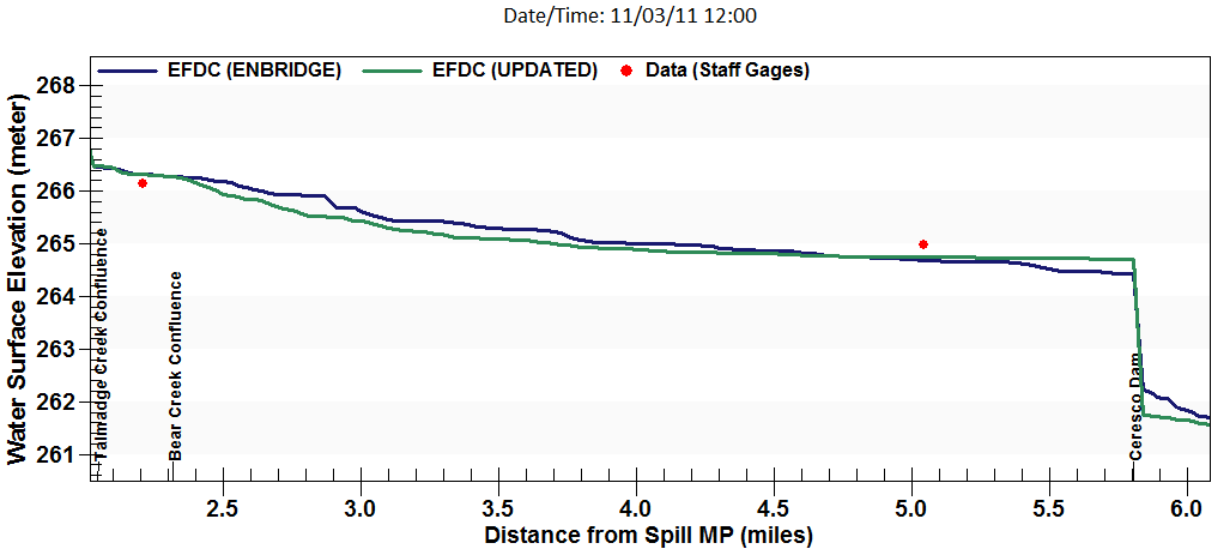

Figure 20. The 2012 Enbridge model and the updated model WSE profile at Ceresco Dam November 3, 2011.

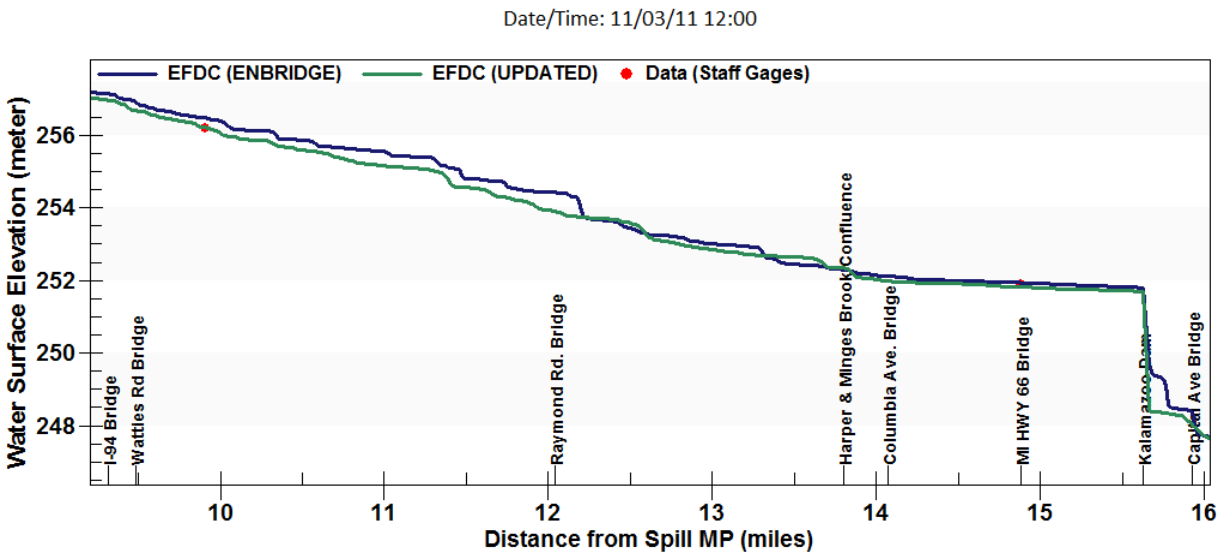

Figure 21. The 2012 Enbridge model and the updated model WSE profile at the Kalamazoo River Dam and Mill Ponds area November 3, 2011.

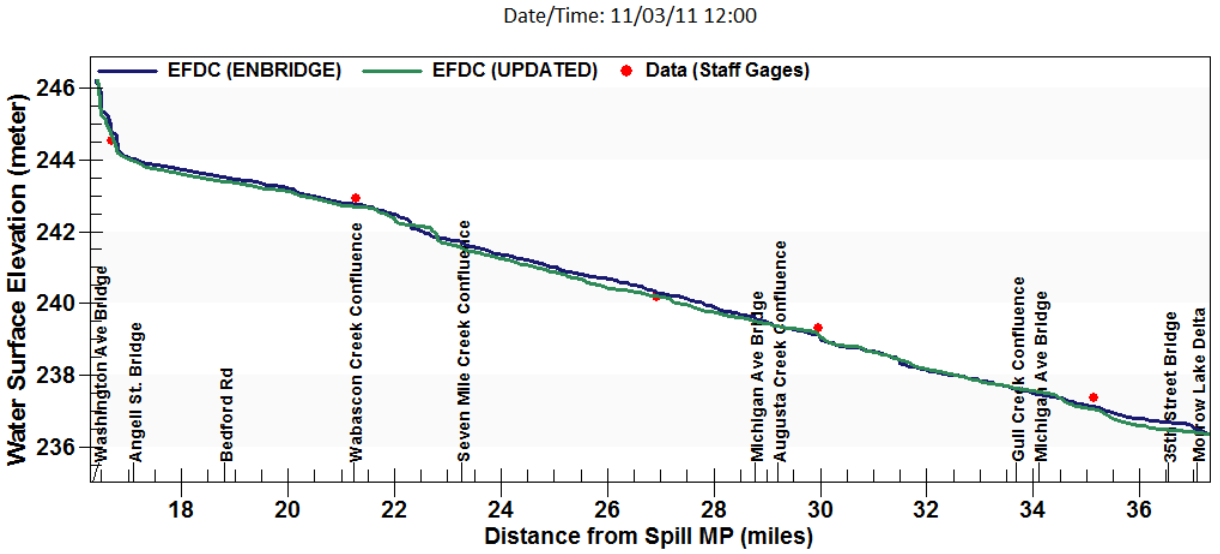

Figure 22. The 2012 Enbridge model and the updated model WSE profile from the Kalamazoo River Dam to the Morrow Lake Delta November 3, 2011.

4.4 Discharge at Gages and Tributary Inflows

Following calibration to stage data as described in the previous sections, updated model estimates of discharge were compared to discharges computed with the USGS stage-discharge relationship for the Kalamazoo River at Comstock and the Kalamazoo River near Battle Creek gages. For the April 2013 period, the model tracked the gage data closely (Figure 23 and Figure 24). The observed flows are consistent with the tributary flow inputs in terms of timing and magnitude, providing additional support for the channel and floodplain roughness values developed during the

calibration to stage. This was also true for the other modeled time periods which are presented in Appendix A.

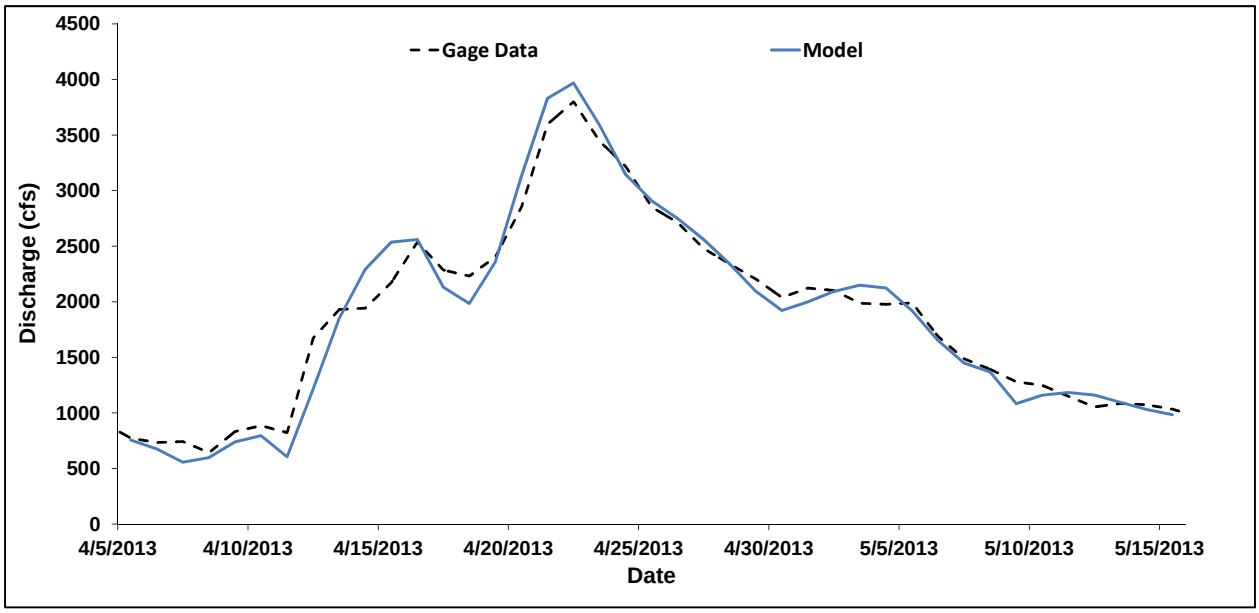

Figure 23. Model to data comparison at Comstock gage (USGS 04106000), April to May 2013, daily average discharge.

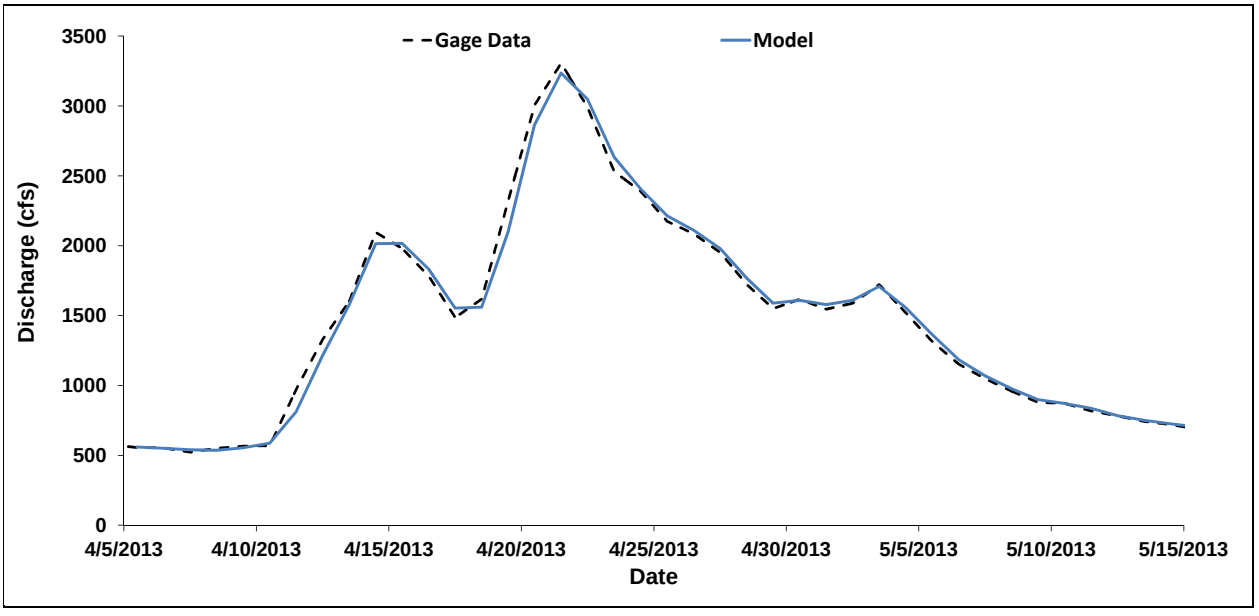

Figure 24. Model to data comparison at Kalamazoo near Battle Creek gage (USGS 04105500), April to May 2013, daily average discharge.

4.5 Velocity Measurement Comparisons

4.5.1 April 2013 USGS Velocity Data

Velocity transects were collected by USGS in April 2013 at various channel and impoundment transects throughout the spill affected reaches of the river[3]. Selected transects are included in Figures 25 to 28 and the remaining model to data comparisons are presented in Appendix B.

In general, the model closely agreed with the velocity data at the available points of comparison, as can be seen in Figure 25 for the Ceresco Dam area, where all four monitored transects are reasonably captured by the model. This agreement supports previous observations about the quality of the calibration and also suggests that the updated bathymetry and updated stage-discharge relationship were reasonable revisions to the model.

A similar result can be seen at the Mill Ponds area (Figure 26), where the updated model accurately characterizes the cross channel distribution of velocities and significant restrictions to flow imposed by the channel in this area.

The model reasonably captured the velocity data in the oxbow area of transects 21.31 and 21.36 (Figure 27). It appears that the flow split between the main stem of the river and the oxbow is captured well, as the velocities at both locations are of a reasonable magnitude. This agreement between the model and data support the updates to bathymetry and channel roughness made in this area.

The model also agreed with the velocity data at the Morrow Lake Neck and Delta (Figure 28). All six transects are reasonably captured by the model. The transect on the south side of the delta, in the main channel on the north side, the east-west transect between MP 37.25 and MP 37.5, and the three transects in the neck where the flow exits the delta are all well characterized by the model, demonstrating that the model described a reasonable distribution of flows across the delta, and provides further confirmation of changes made to the bathymetry and downstream boundary condition.

[3] Velocity transects collected at mile posts: 2.22, 5.03, 5.32, 5.62, 5.75, 7.18, 12.05, 13.89, 14.52, 14.71, 14.75, 15.17, 15.22, 15.24, 15.50, 18.83, 21.31, 21.36, 28.80, 34.12, 36.55, 37.14, 37.18, 37.55, 37.66, 37.25 – 37.50, 37.75

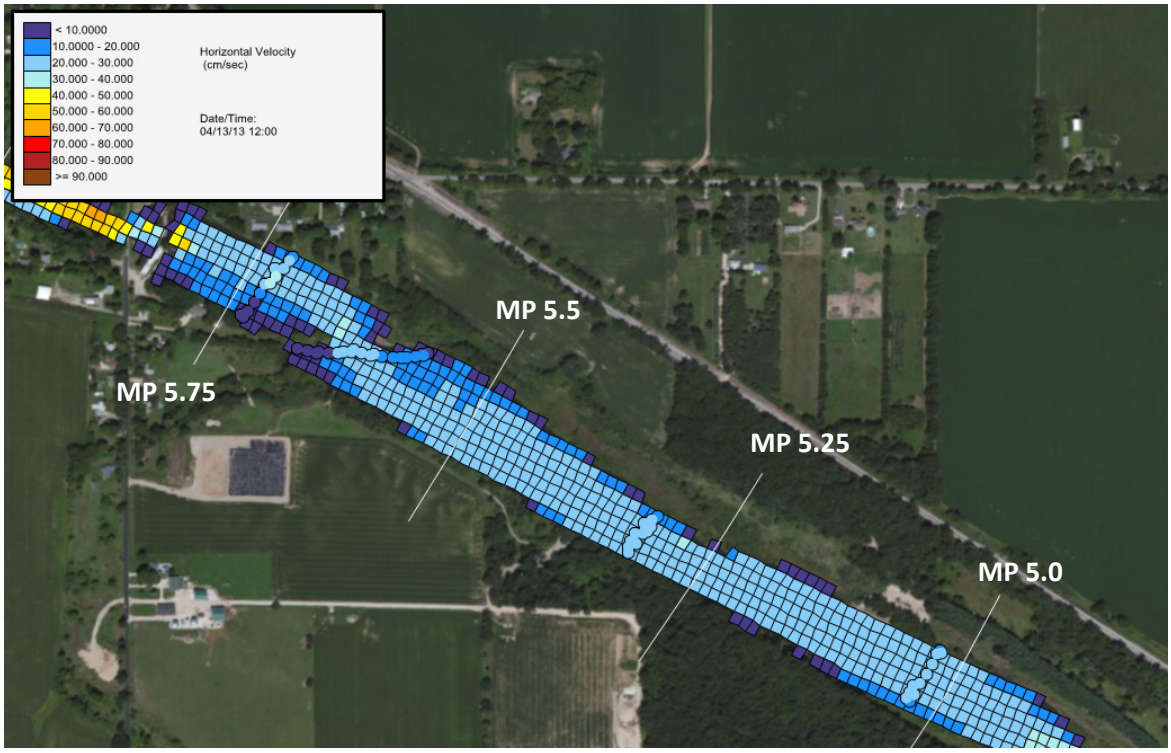

Figure 25. Model comparison with velocity data at Ceresco Dam April 13, 2013. Circles represent velocity measurements.

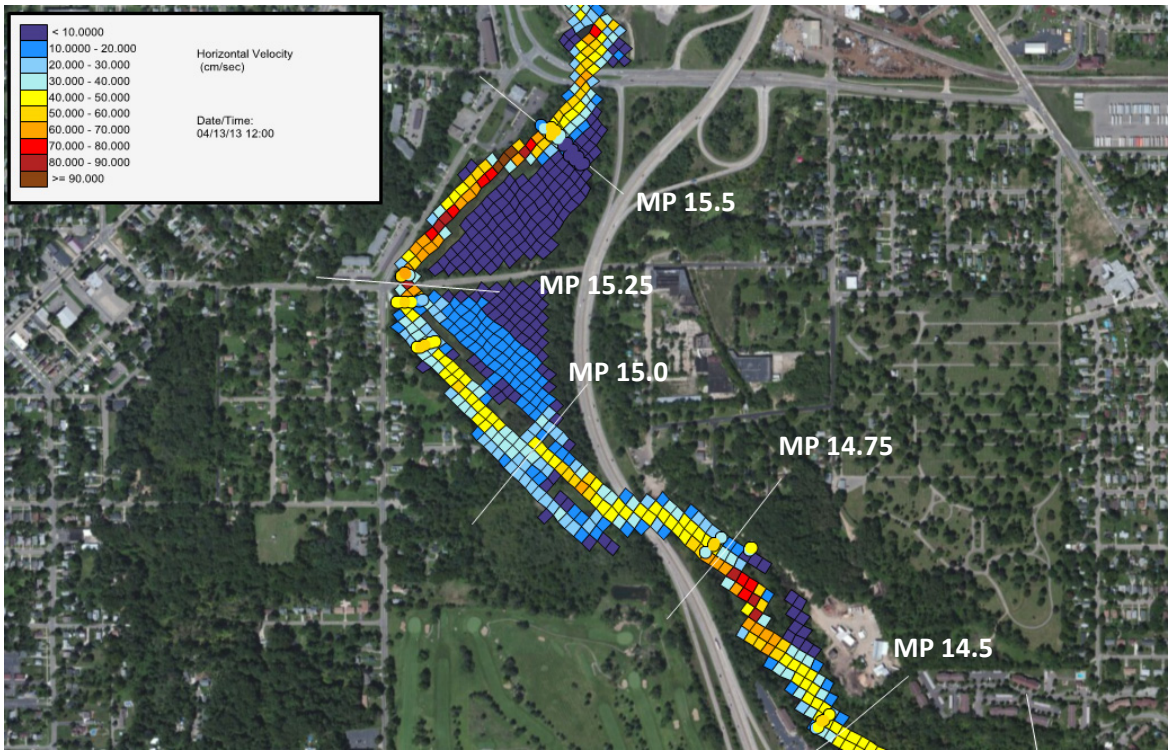

Figure 26. Model comparison with velocity data at Mill Ponds area April 13, 2013. Circles represent velocity measurements.

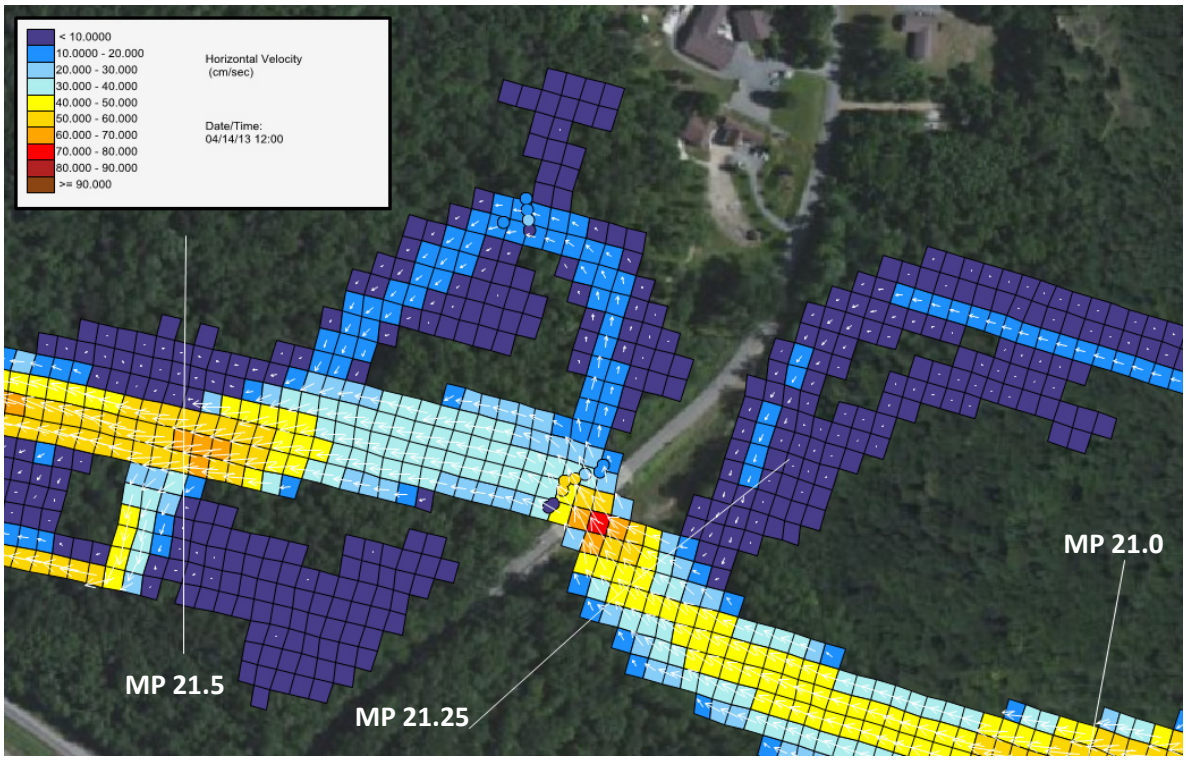

Figure 27. Model comparison with velocity data at transects 21.31 and 21.36. April 14, 2013. Circles represent velocity measurements. Velocity vectors shown as white arrows.

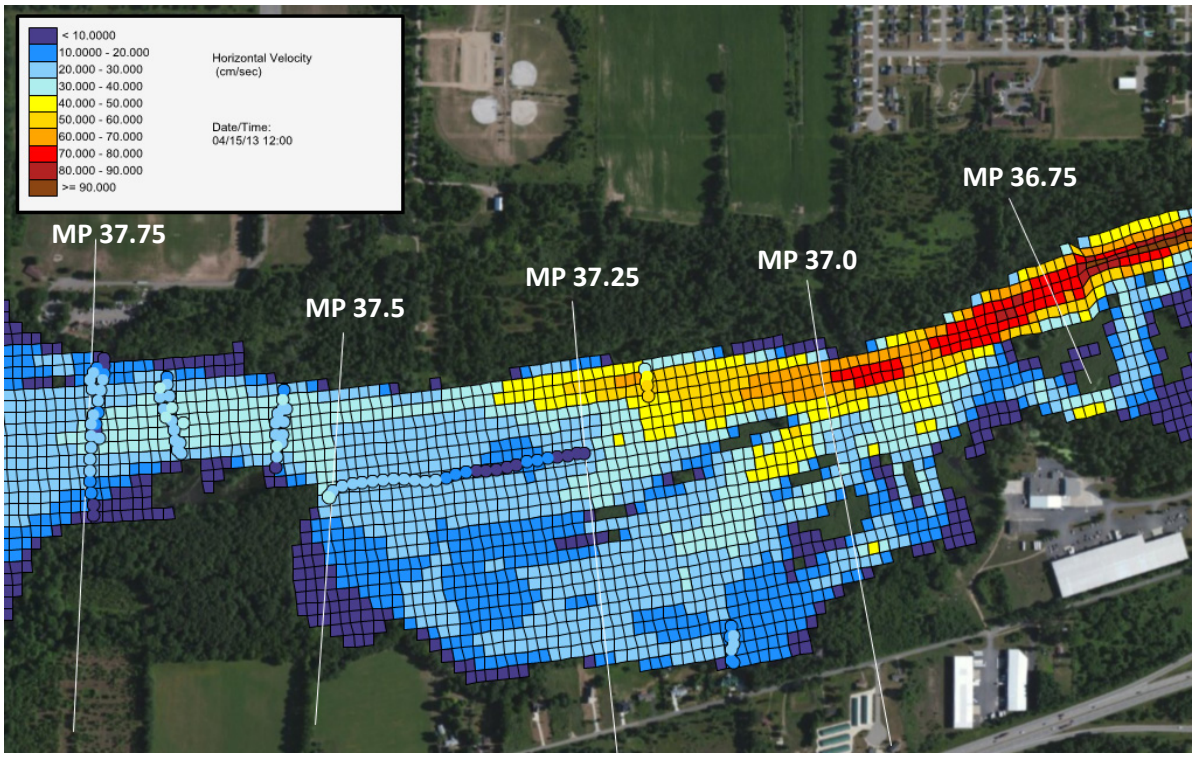

Figure 28. Model comparison with velocity data at transects at Morrow Lake Delta April 15, 2013. Circles represent velocity measurements.

4.5.2 April 2013 Michigan State University Velocity Data

Velocity data collected by Stephen Hamilton (Michigan State University) in the floodplain on April 21, 2013 were the only data describing velocities in the floodplain during flood conditions. These data were used to make a qualitative comparison with the numerical predictions of velocity in the floodplain, subject to the inability of a model of this scale to capture the small scale spatial variability of the data collected in the floodplain. Roughness characteristics in the model are averaged over individual cells spanning a broad area, and individual obstructions, such as trees and vegetation which can affect velocities are below the resolution of the model.

With this consideration, the velocities predicted by the model were judged to be reasonable (Figure 29). Sensitivity of the model to changes in floodplain roughness was evaluated by lowering the roughness values, which did not improve the comparison to the data, and ultimately the roughness values that were utilized in the floodplain of the 2012 Enbridge model were retained.

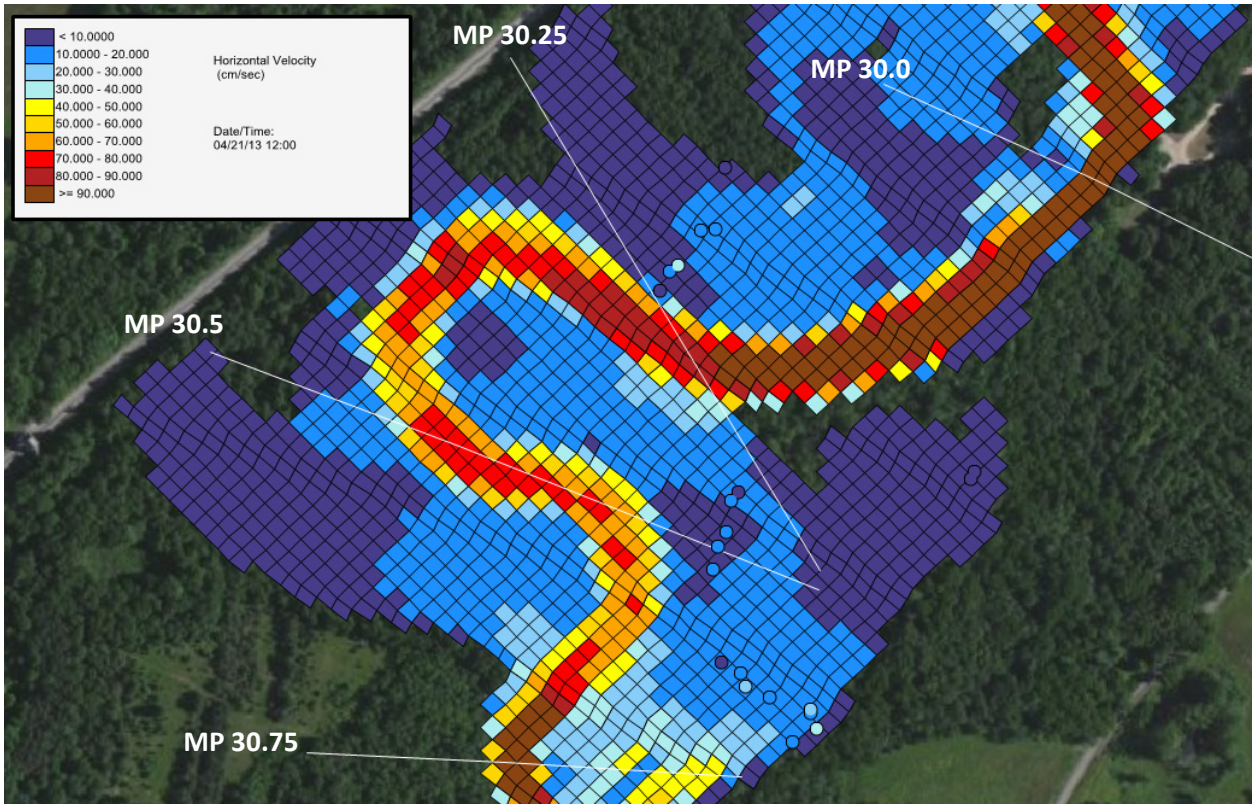

Figure 29. Model compared with floodplain velocity data collected by Stephen Hamilton April 21, 2013. Circles represent velocity measurements.

4.5.3 Fall 2011 Enbridge Velocity Data

The output from the October to November 2011 riverine simulation was compared to velocity data collected by Enbridge for the same period, and was used to develop a 1:1 plot of measured versus predicted velocity. Point-to-point comparisons generally show improvement in the updated model velocity estimates over the 2012 Enbridge model (Figure 30). Examination of the statistical

distribution of model to data differences (residuals) shows a narrowing of the range of computed residuals overall with the updated model, and a general decrease in bias. These effects were quantified through regression analysis of model to data comparisons of the 2012 and updated models. Linear regression of model versus data-based velocity using an unconstrained linear model showed an improvement in low-range bias in the updated model predictions of velocities, as indicated by a decrease in the regression intercept (0.167 to 0.106), and also showed an improved overall quality of fit (r^2 = 0.71 for Enbridge model, 0.78 for updated model). A separate regression with a forced zero intercept was used to provide a more general indication of bias, and also showed improvement with the updated model, with an increase in slope from 0.75 to 0.77 (relative to an ideal of 1.0), and a corresponding improvement in quality of fit (r^2 = 0.90 for Enbridge model, 0.93 for updated model).

While the model was not explicitly calibrated to the velocity data described here, the model updates discussed previously in Section 3, including improved tributary flow inputs, dam configurations, channel roughness, and channel bathymetry, resulted in improved velocity predictions.

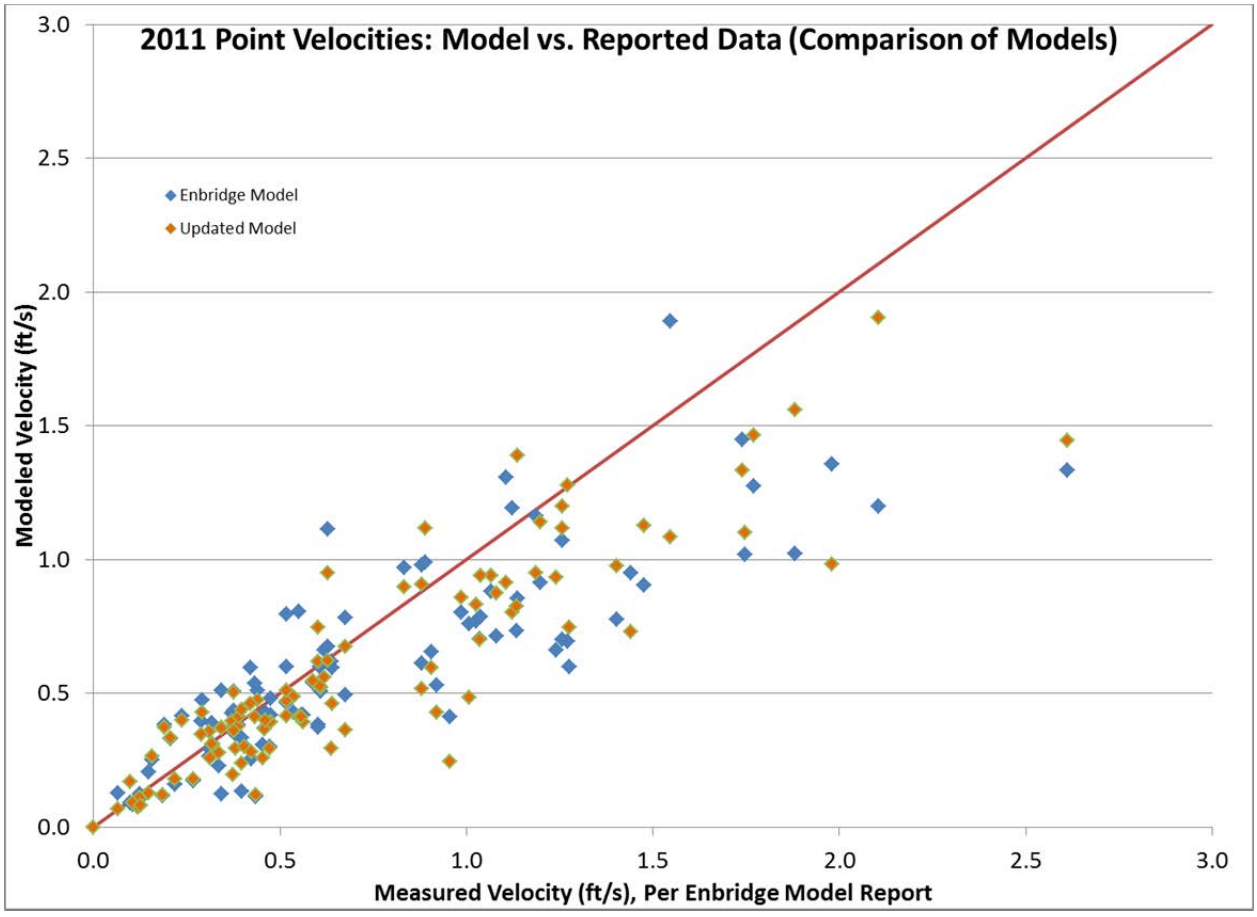

Figure 30. Comparison of 2012 Enbridge model and updated model with measured velocities, October to November 2011 elevated baseflow conditions.

Blank Page

5 Model Applications

Application of the updated model is described in this section through presentation and discussion of model results for multiple flow conditions. Model results for the full 38-miles of river between Marshall and Kalamazoo are presented through longitudinal profiles. More detailed examinations of model applications are provided by mapping the model results for Morrow Lake delta and the Ceresco impoundment, two areas of importance for oiled sediments. Hydrodynamic model applications are presented in Section 5.1, followed by sediment transport model applications in Section 5.2 to demonstrate the effect of the hydrodynamic behavior on sediment transport.

5.1 Hydrodynamic Model – Representative Flow Scenarios

The hydrodynamic model was applied under four characteristic flow event conditions (Section 3) to allow for review of model performance under a range of flows, and to explore the performance of the model with respect to critical determinants of sediment transport model performance, including velocity distribution and predicted grain and total shear stress. Application of the hydrodynamic model described in this section focuses on the October to November 2011 elevated baseflow event and the July to August 2010 spill event. These simulation periods allow for comparisons between a moderate- and a high-flow condition, as well as comparisons between the updated model and the 2012 Enbridge model.

5.1.1 Hydrodynamic Model Application: October to November 2011 Elevated Baseflow

The late October to November 2011 baseflow condition period, described in Section 3.2, was a period of moderate flows elevated above the lowest baseflow conditions of late summer, yet not affected by measurable quick-flow response to antecedent precipitation. Flows were generally steady, with a slow decrease over most of the period. Velocity magnitude results from the updated hydrodynamic model applied to this period are shown in Figure 31 for November 3, 2011. The updated model shows generally higher velocities relative to the 2012 Enbridge model due to updates to bathymetry and decreased roughness relative to the 2012 model implementation. Modifications to roughness are described in Section 3.3, and were made to improve the model's representation of water surface elevation and velocity under both baseflow and elevated flow conditions. A point-to-point comparison of the two models with measured velocity data presented in the previous section (Figure 30) shows a general trend of improvement in model performance with the implemented model updates.

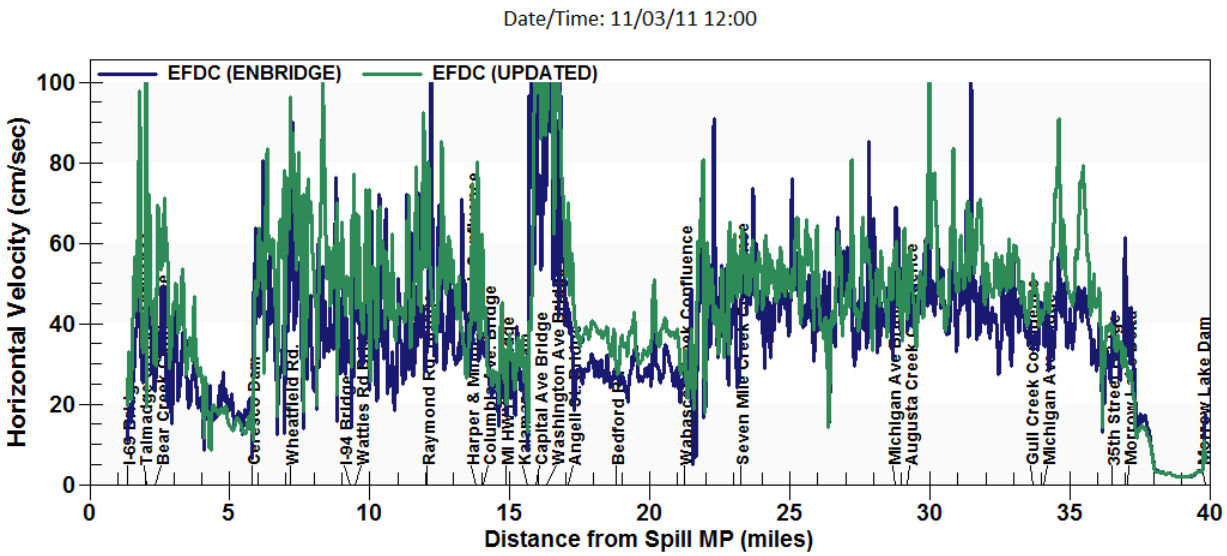

Figure 31. Comparison of predicted velocity magnitudes for the 2012 Enbridge model and the updated model, November 3, 2011 elevated baseflow conditions.

Example maps of velocity distribution in the Morrow Lake delta area are presented in Figures 32a and 32b. These illustrate both models' ability to represent velocity variation in the braided channel section of the delta area, with a primary flow pathway in the main channel along the north end of the delta, and slower but significant flows in the braids to the south. At this location and flow rate, the updated model indicates slightly lowered velocities relative to the earlier 2012 Enbridge model, due to a combination of factors including modifications to tributary inputs, bathymetric updates, dam rating curve updates, and modifications to roughness as described above. Superimposed velocity vectors on the updated model (Figure 33) illustrate the complexity of the flow pathways in this area and likely routes by which oiled sediments may have accessed this area and contributed to deposition of oiled material.

A primary hydrodynamic variable governing sediment deposition, transport, and erosion is the shear stress exerted on the bed, at both the near-bed scale (grain stress) and at the larger scale of major bedforms and other larger-scale contributors to drag at the bed (total stress). Visualization of bed shear stresses can provide insight into the critical characteristics of flow hydrodynamics as predicted by the models and their implications for prediction of sediment transport.

Figures 34a and 34b present grain stresses for the 2012 Enbridge model and updated model under the same conditions of elevated baseflow on November 3, 2011 described above. In both models, little or no erosion is expected because grain stress does not generally exceed a critical threshold for erosion: 4 dynes/cm^2 for the 2012 Enbridge model, and 1- 5 dynes/cm^2 for the parent bed of the updated model, depending on the Sedflume core or the generalized bed type used to represent the sediment bed in the delta (Figure 17 and Table 9; 1 Pa = 10 dynes/cm^2). Figure 35 shows total bed stress for the 2012 Enbridge model under the same conditions. As deposition in this model is primarily governed by a total stress threshold of 4 dynes/cm^2 above which no deposition occurs, deposition is predicted in this model only in areas shaded in light to darker shades of blue. In contrast, deposition in the updated model is governed by grain stress (Figure 34b), with a probability of deposition function that is nonzero at grain stresses below critical shear stress as

specified for the sediment classes (0.5-1.0 dynes/cm^2 Table 7, Section 3.4.3). Consequently, we would expect to see deposition in a broader area of the delta under this condition than is seen in the 2012 Enbridge model.

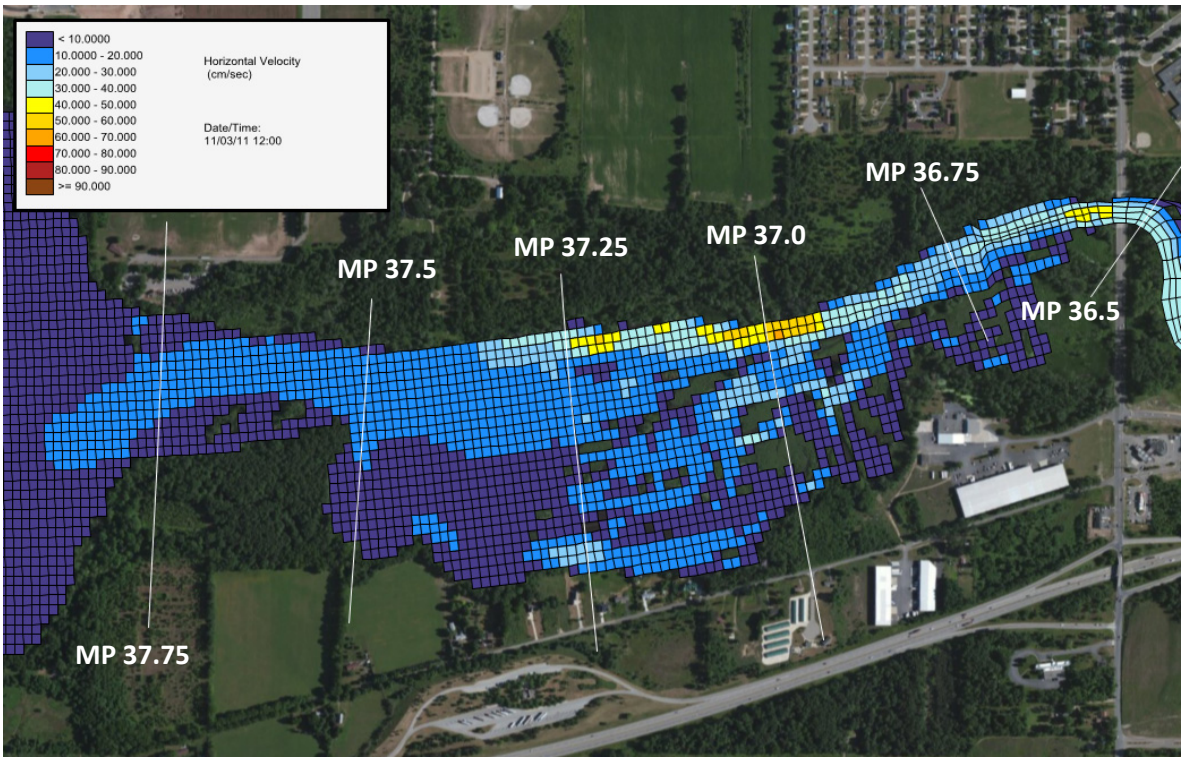

(a)

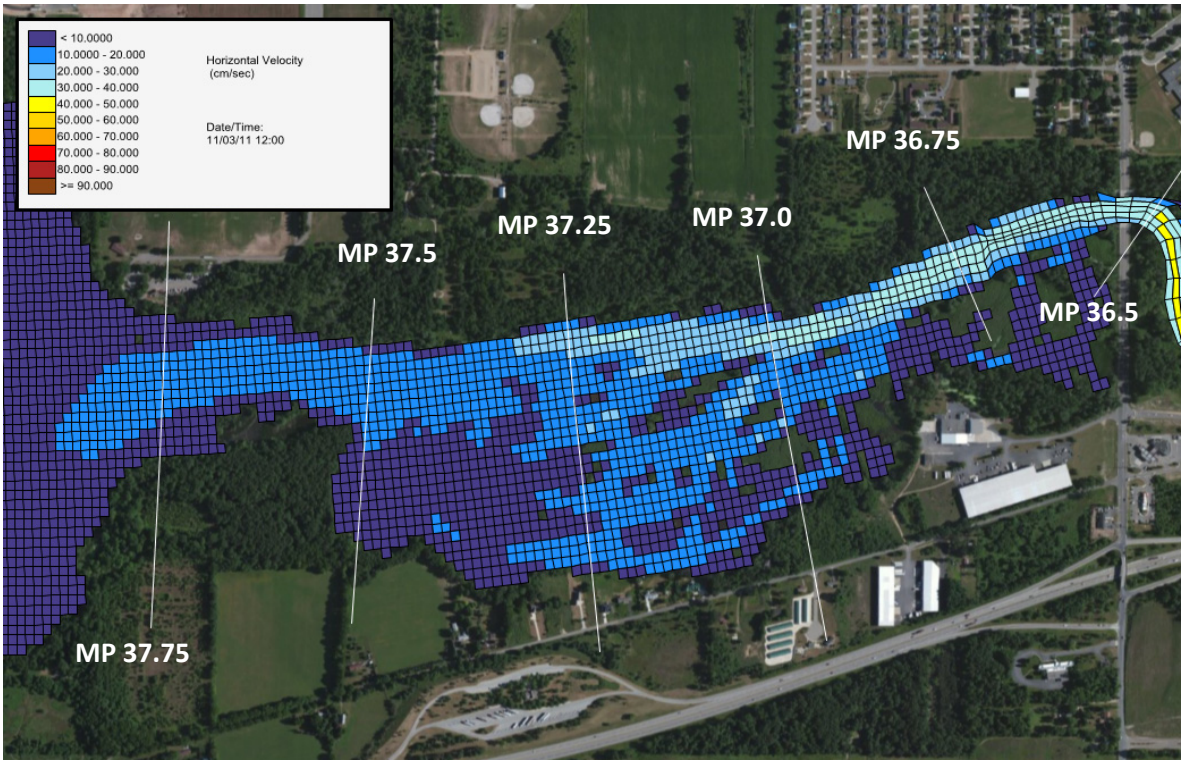

(b)

Figure 32. Predicted velocity distribution, Morrow Lake Delta, under November 2011 elevated baseflow conditions, (a) 2012 Enbridge model, (b) updated model

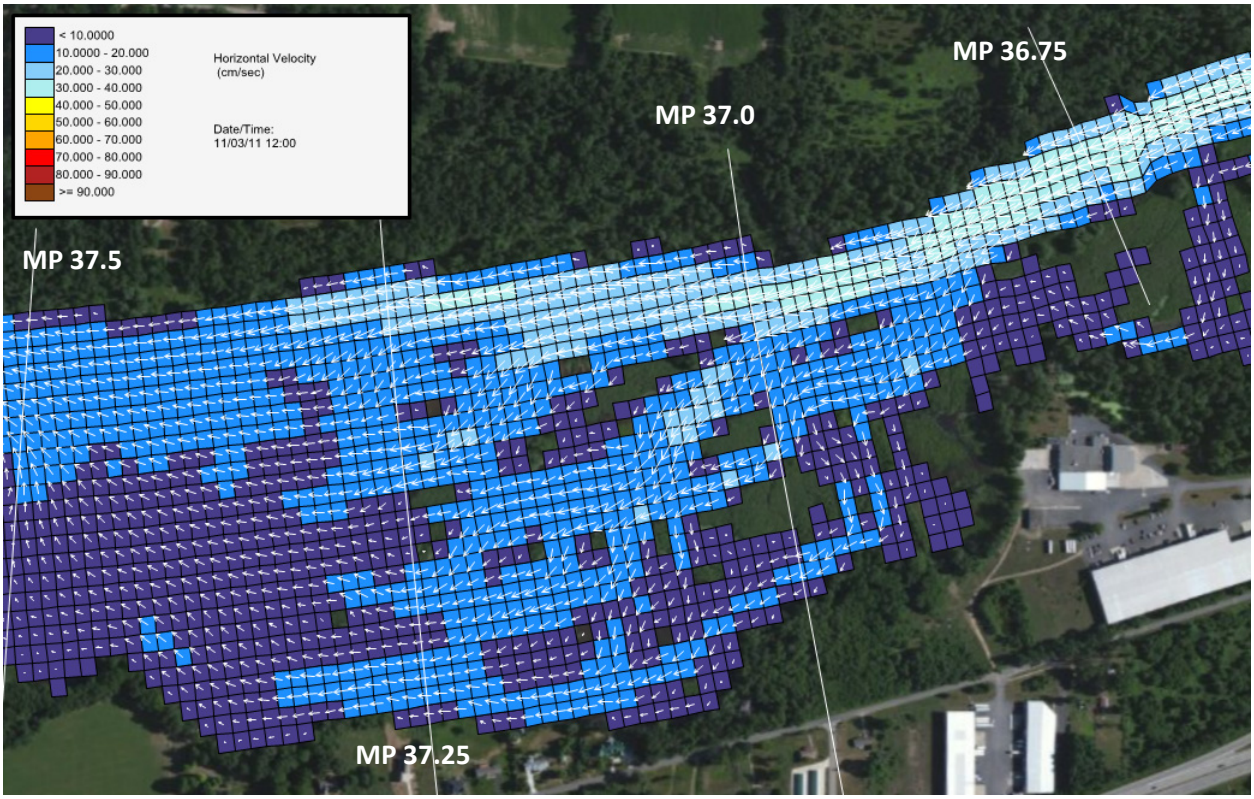

Figure 33. Predicted velocity distribution, Morrow Lake Delta, under November 2011 elevated baseflow conditions, with superimposed velocity vectors.

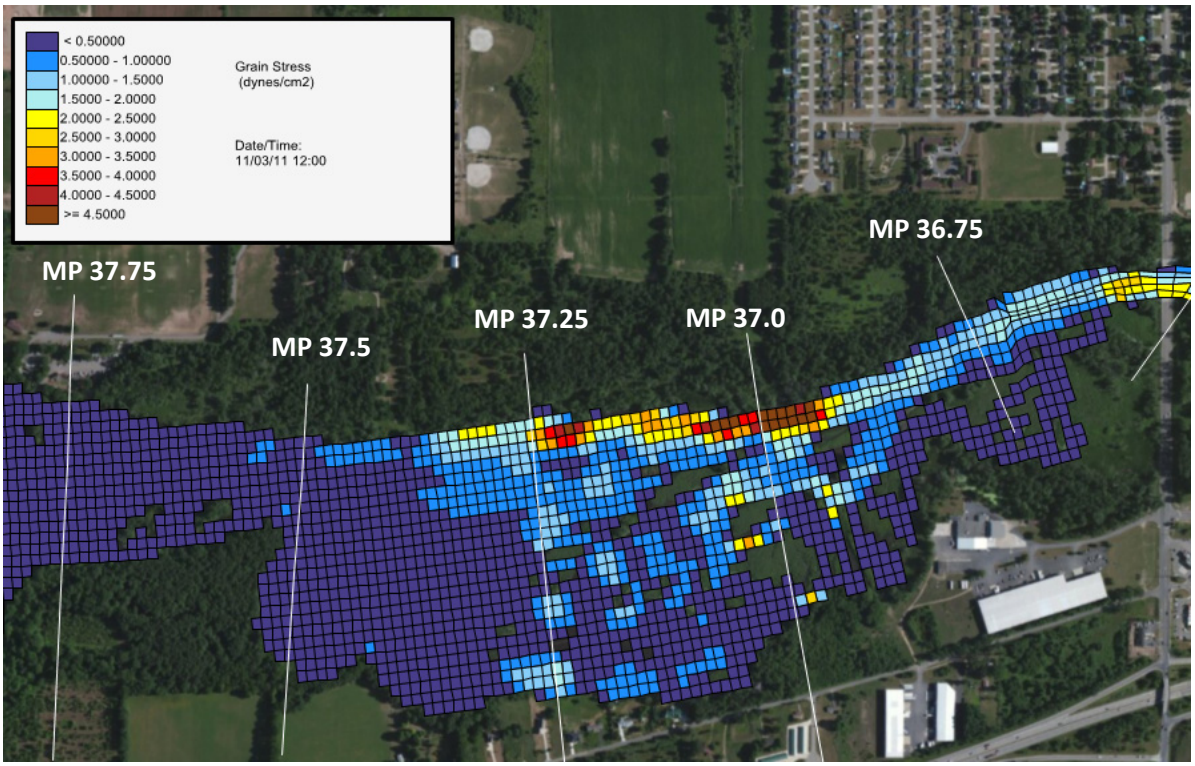

(a)

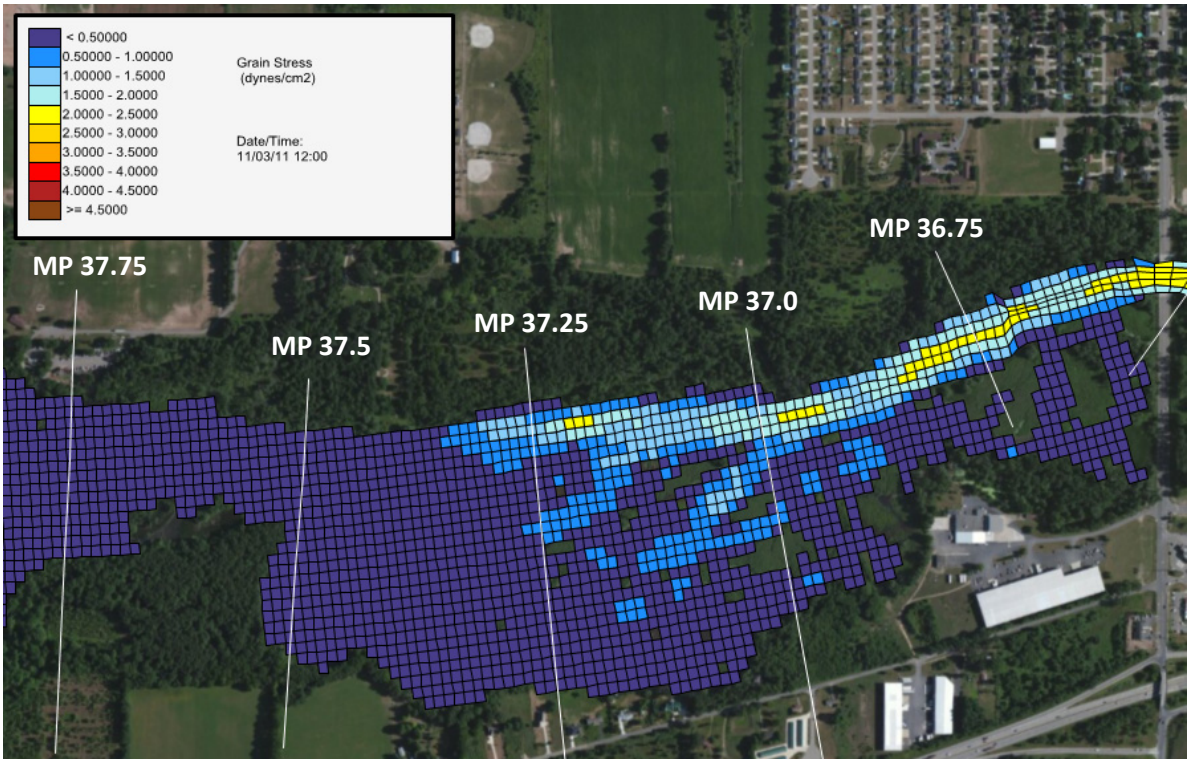

(b)

Figure 34. Predicted grain stress distribution, Morrow Lake Delta, under November 2011 elevated baseflow conditions, (a) 2012 Enbridge model, (b) updated model.

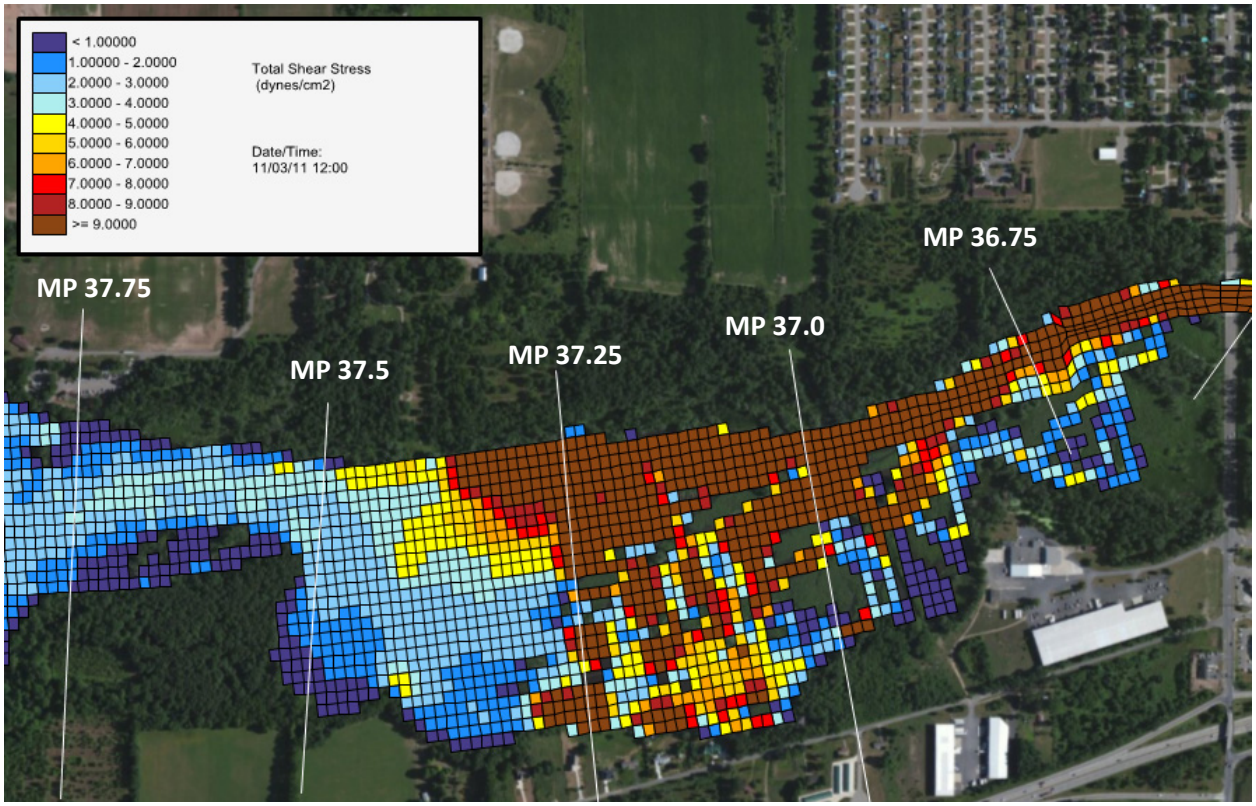

Figure 35. Predicted total stress distribution, Morrow Lake Delta, under November 2011 elevated baseflow conditions, 2012 Enbridge model.

Maps of velocity distribution in the Ceresco Dam area for November 3, 2011 are presented in Figures 36a and 36b. At this location and flow rate, the updated model predicted generally slower velocity than did the 2012 Enbridge model, primarily as a result of the improvements made in the stage-discharge relation at Ceresco Dam. The updated model simulates the relatively slow-moving backwater profile expected upstream of the dam, with velocities less than 0.5 ft/sec (15 cm/sec) for much of the area within approximately 0.75 miles of the dam. The observed decrease in velocity, compared to the 2012 Enbridge model, results in a noticeable decrease in predicted grain stress in the reach for the updated model, as shown in Figures 37a and 37b, but neither model predicts shear stresses in excess of critical shear for erosion to occur.

Total bed stress as predicted by the 2012 Enbridge model for this condition is shown in Figure 38. As described above for the Morrow Lake delta area, deposition in the 2012 Enbridge model is governed by a total stress threshold of 4 dynes/cm^2 above which no deposition occurs. In this reach, high assumed bed roughness combined with incorrect representation of the Ceresco Dam in the 2012 Enbridge model contribute to an elevated estimate of total bed stress, resulting in very limited potential for deposition in this reach (areas shaded in light to darker shades of blue). In contrast, deposition in the updated model is governed by grain stress (Figure 37b), with a probability of deposition function that is nonzero at grain stresses below critical shear stress for the sediment size classes in the model, ranging from 0.5 - 1.0 dynes/cm^2 for clays through very fine sand. Consequently, we would expect to see deposition at locations throughout the Ceresco Dam backwater area under this flow condition.

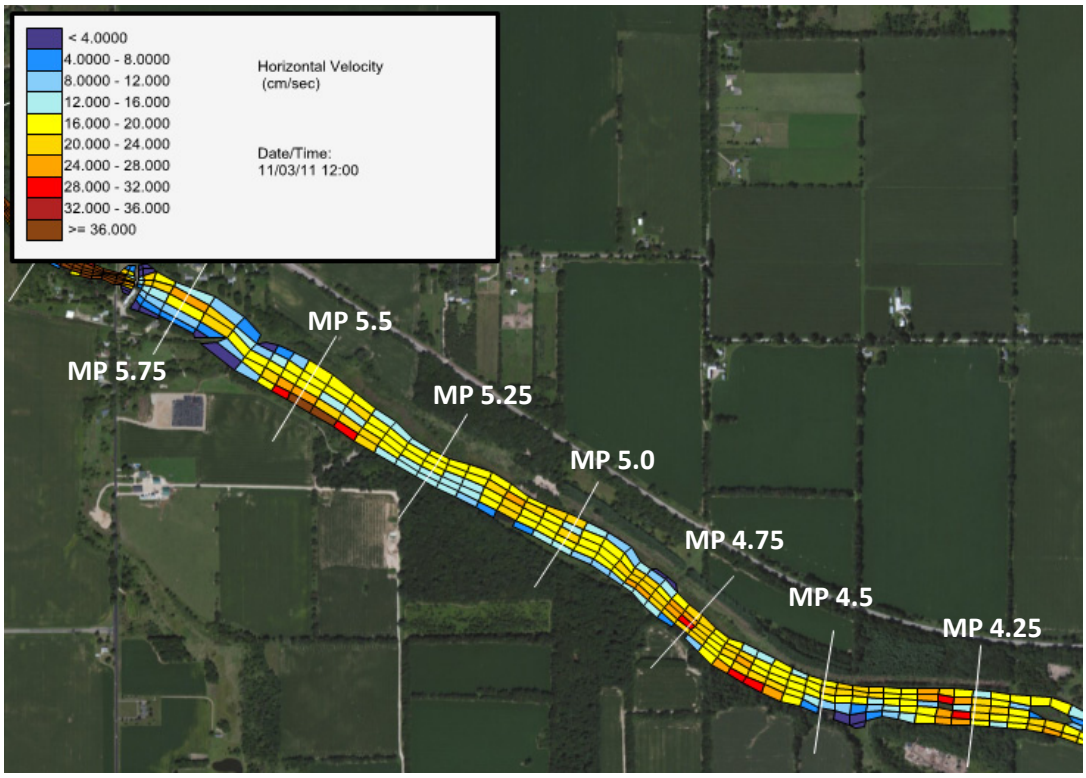

(a)

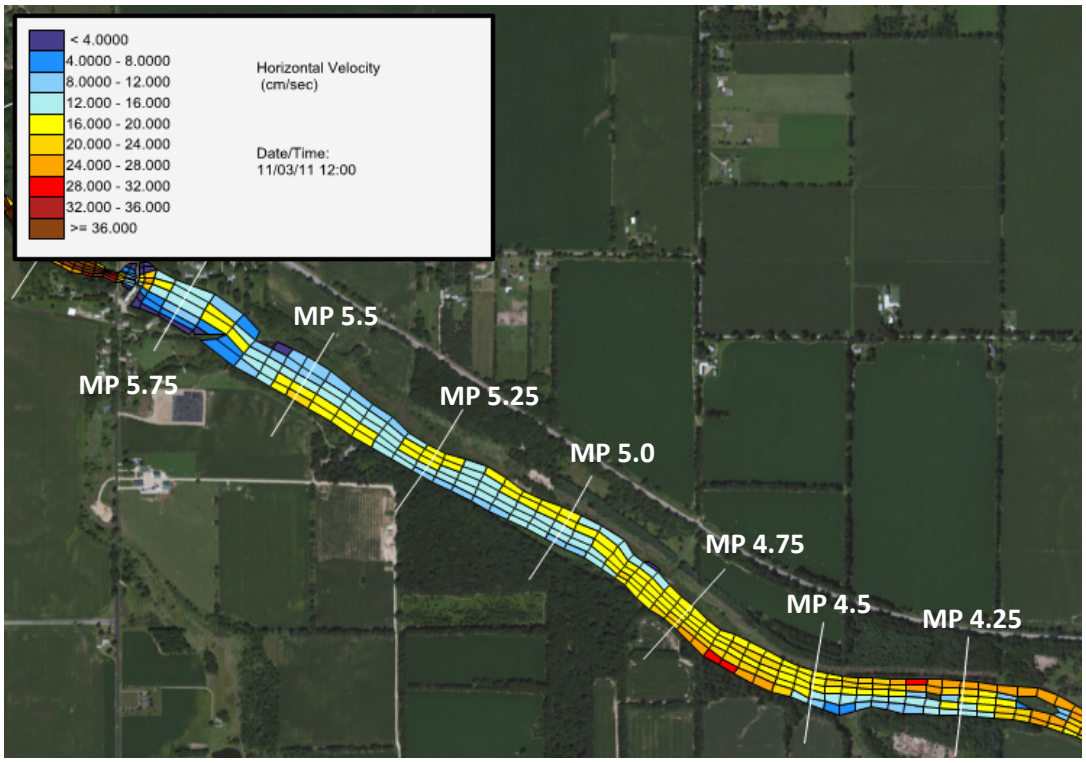

(b)

Figure 36. Predicted velocity distribution, Ceresco Dam Impoundment, under November 2011 elevated baseflow conditions, (a) 2012 Enbridge model, (b) updated model.

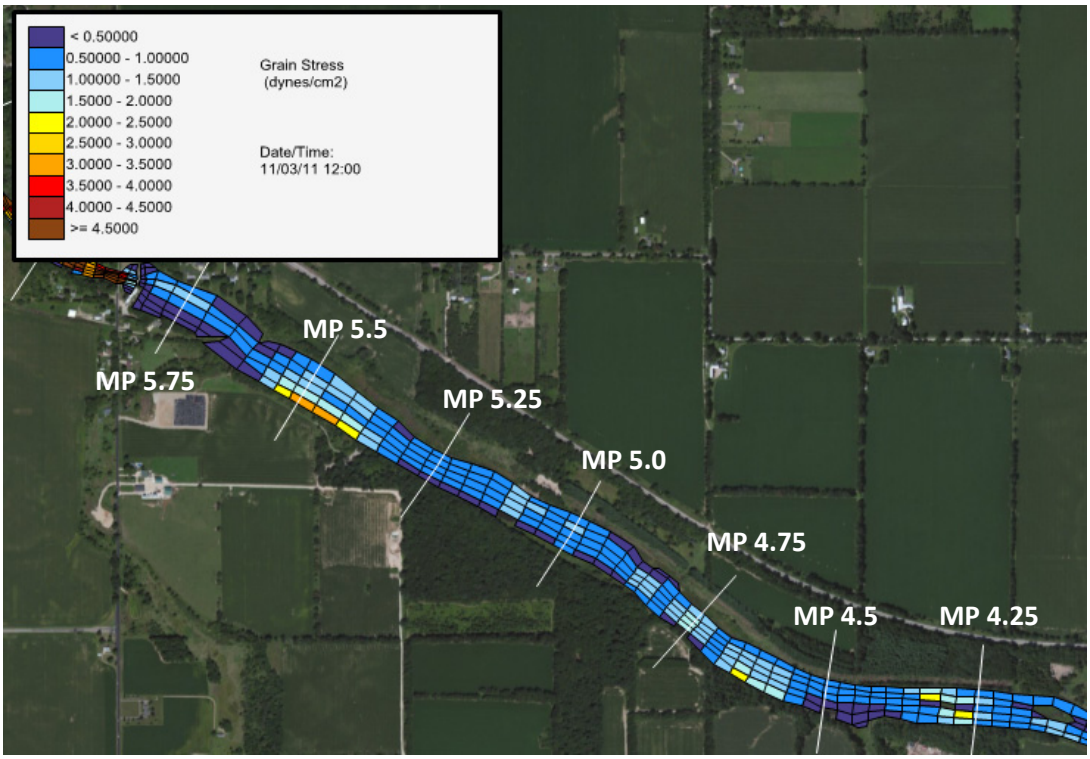

(a)

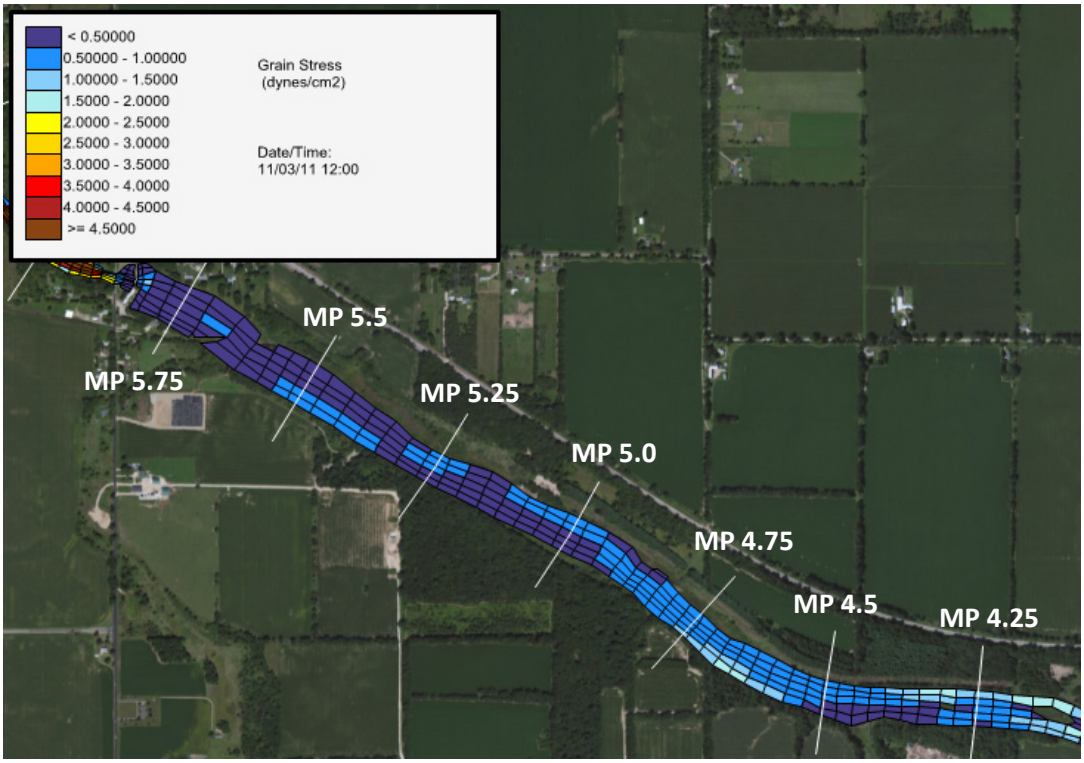

(b)

Figure 37. Predicted grain stress distribution, Ceresco Dam Impoundment, under November 2011 elevated baseflow conditions, (a) 2012 Enbridge model, (b) updated model.

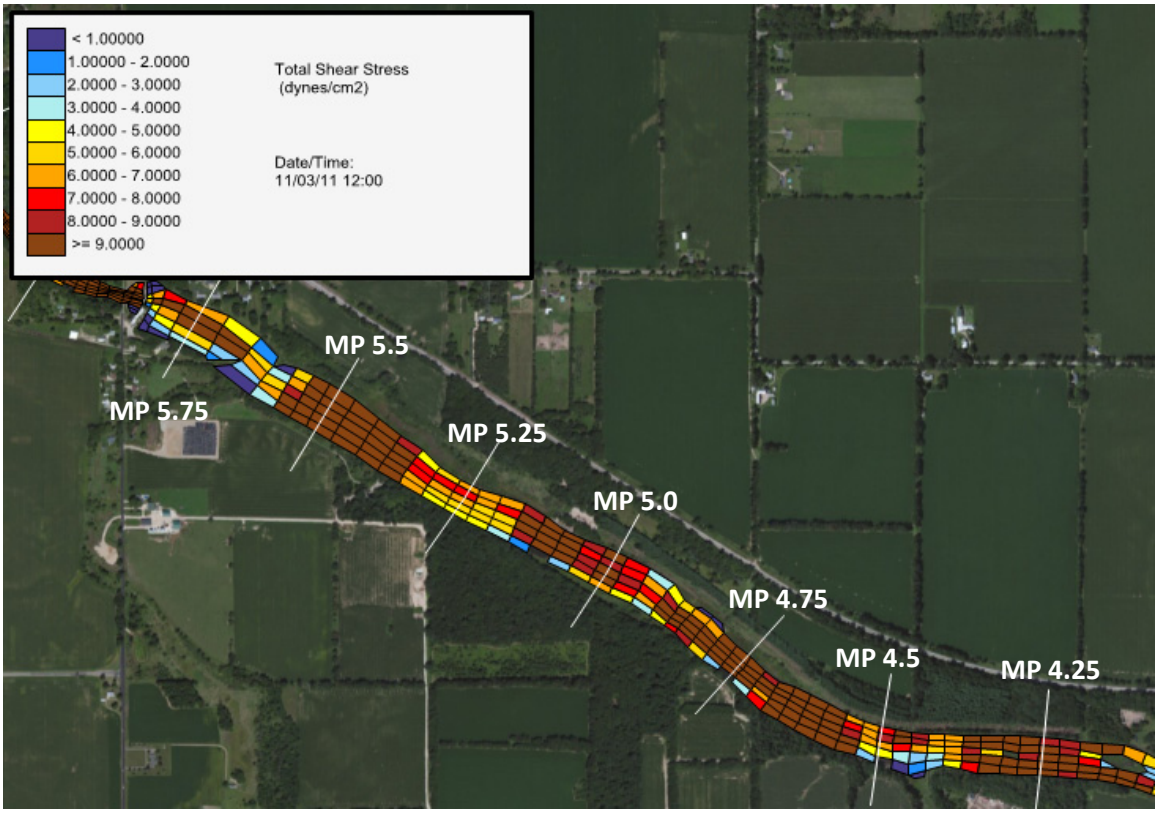

Figure 38. Predicted total stress distribution, Ceresco Dam Impoundment, under November 2011 elevated baseflow conditions, 2012 Enbridge model.

5.1.2 Hydrodynamic Model Application: July Oil Spill Event

The July to August 2010 oil spill was accompanied by heavy rains that contributed to the transport and emplacement of oil throughout Talmadge Creek and the Kalamazoo River. The hydrodynamics of this event were modeled using the floodplain model as developed by Enbridge and modified to reflect updates to bathymetry, tributary inputs, dam behaviors and roughness characteristics as described in Section 3. Flows simulated during this event peaked at more than 3,000 cfs and resulted in elevated velocities and shear stresses throughout the river. Velocities under peak event conditions at the delta are shown in Figure 39a for the 2012 Enbridge model, showing highly elevated velocities in the main channel of the delta and more moderate velocities in the braided distributary channels. Velocities predicted with the updated model, shown in Figure 39b, are significantly higher than those predicted by the Enbridge model, due primarily to modifications in computed tributary inflows and modifications to the Morrow Lake dam boundary conditions in the floodplain model that allow for more accurate characterization of flow delivered to the delta area. Peak velocities in the main channel and particularly in the narrow section passing underneath the 35th Street Bridge are elevated, approaching 1 m/s at the peak of the event.

Corresponding bed shear stresses (as grain stress) are shown for the two models in Figure 40a and 40b. As was observed for velocities, grain stresses are significantly elevated in the updated model relative to the 2012 Enbridge flood model, with stresses capable of eroding sediment through much of the delta area. The observed differences are primarily due to the difference in modeled

hydrodynamics, with more flow delivered to the delta at this point in the flood event with the updated model than with the 2012 Enbridge model. Differences in the methods by which the two models calculate grain stress contribute only slightly to the differences in predicted grain stress.

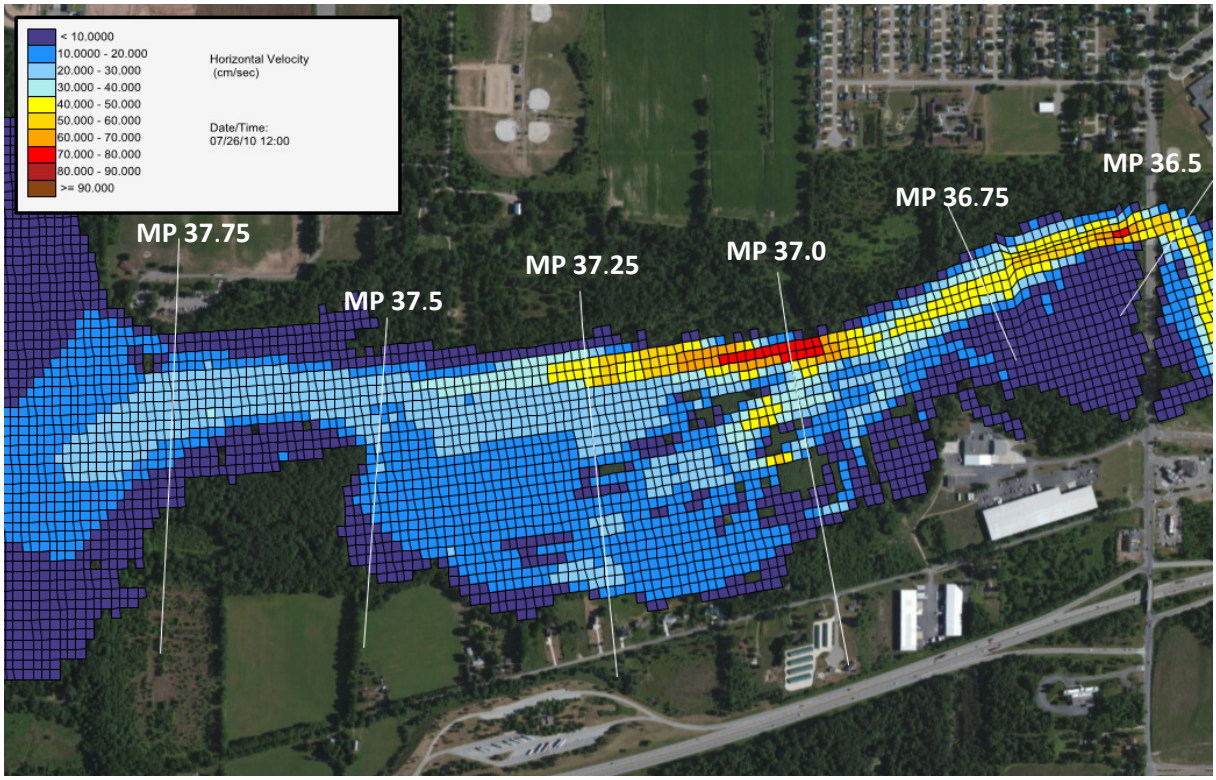

(a)

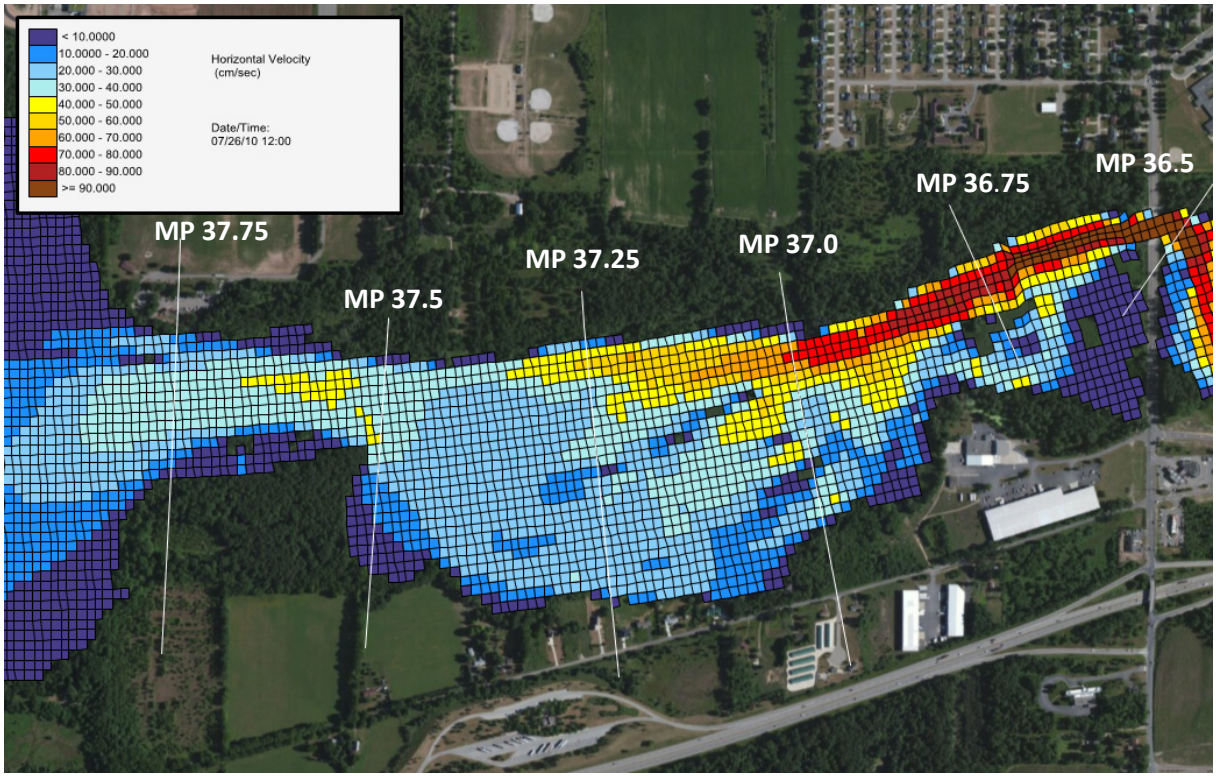

(b)

Figure 39. Predicted velocity distribution, Morrow Lake Delta, under July 26, 2010 peak high flow conditions, (a) 2012 Enbridge model, (b) updated model.

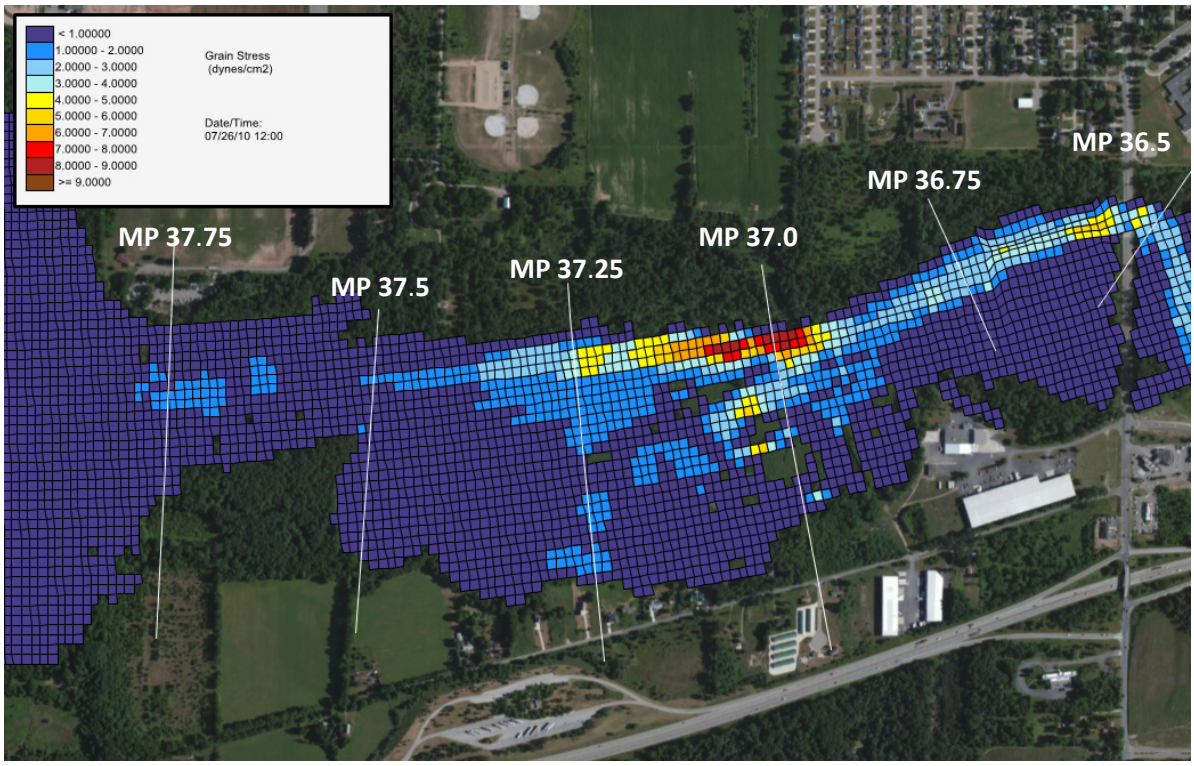

(a)

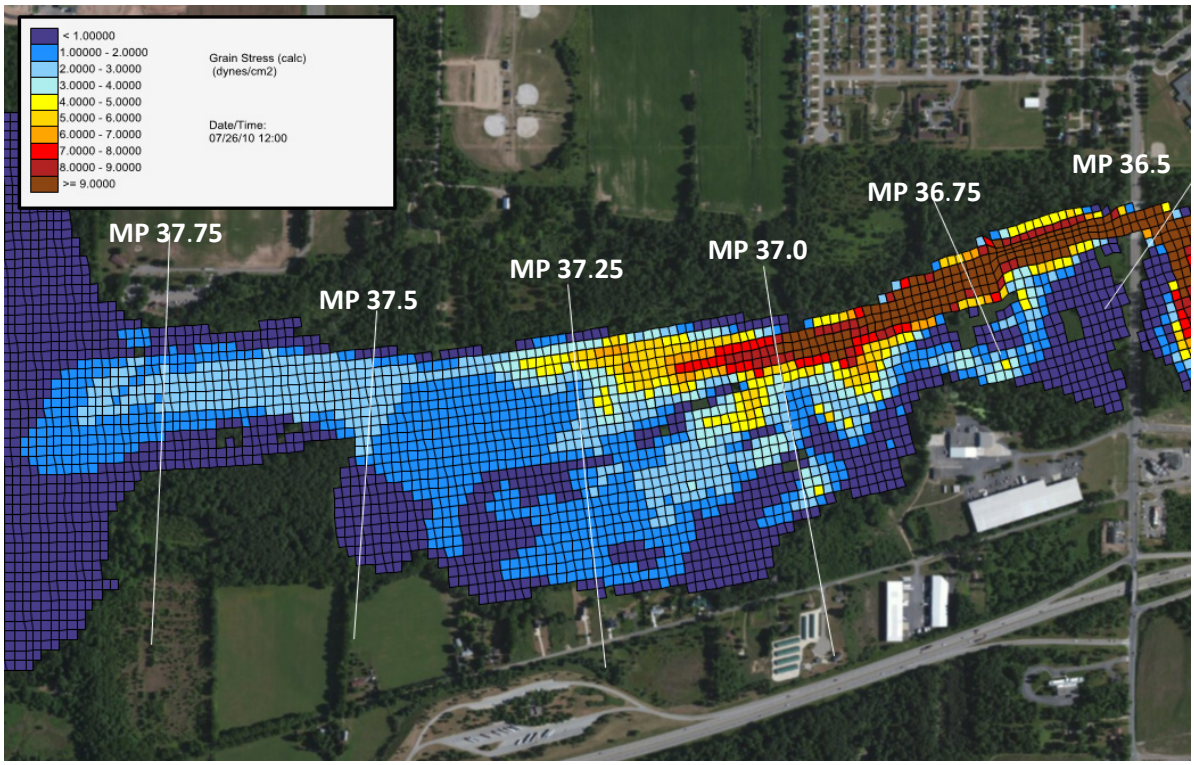

(b)

Figure 40. Predicted grain stress distribution, Morrow Lake Delta, under July 26, 2010 peak high flow conditions, (a) 2012 Enbridge model, (b) updated model.

5.2 Sediment Transport Model

The sediment transport model incorporates the effects of the hydrodynamic behavior described above into a prediction of sediment erosion, deposition, and net bed elevation change over the course of a simulation period. The data available for calibration of the sediment transport model are limited and are insufficient to fully constrain the model in its prediction of sediment transport and quantitative estimation of bed changes. However, the improvements to the flow inputs, bathymetry, bed roughness calibration and other hydrodynamic refinements have significantly improved the capacity of the model to simulate patterns of sediment movement in the Kalamazoo River system. Consequently, simulations depicting sediment transport are useful for integrating the substantial knowledge gained through the project about observed system hydrodynamics, river geomorphology and bank characteristics, sediment bed properties and particle size characteristics, and local measurements of bed erodibility and critical shear stresses made with Sedflume and in-situ flume studies. These simulations can also be related to known characteristics of the distribution and magnitude of oiled sediment deposition downstream of the Marshall spill.

The sediment transport model was run for the following cases:

- October 28 to November 9, 2011 elevated baseflow condition
- July 11 to July 19, 2013 low flow condition

Example results from the updated model are presented below for both of these simulation periods. Results for the October to November 2011 elevated baseflow condition include comparisons to the 2012 Enbridge model, which was run for the same period. The July 2013 low flow period occurred subsequent to the 2012 Enbridge model development.

5.2.1 Sediment Transport Model Application: October – November 2011 Elevated Baseflow

Model results for suspended solids are shown as longitudinal profiles in Figure 41. Overall, the updated model (green line) predicts higher suspended solids concentrations than the 2012 Enbridge model (blue line) for this point in time, November 3, 2011. The updated model exhibits greater large-scale longitudinal variation than the 2012 Enbridge model, with concentrations ranging from approximately 10 – 30 mg/L upstream of the Ceresco Dam and generally 40 – 60 mg/L downstream of Ceresco to the Morrow Lake delta. The updated model shows the expected decline in suspended solids through the Ceresco impoundment due to deposition within that reach. The 2012 Enbridge model exhibits more small-scale variations in suspended solids due to rapid changes in the model's prediction of sand concentrations, but overall, the 2012 Enbridge model results range from approximately 20 – 30 mg/L throughout most of the river upstream of Morrow Lake.

The USGS collected suspended sediment concentration data for various flow conditions during 2012 to 2014, but no data are available for the October to November 2011 simulation period. Six sampling events occurred during 2012 to 2014, with data collected at Marshall, near Battle Creek, and at Battle Creek and August Creek tributary locations (Reneau et al., 2014). Data for Marshall and the tributary locations were used to develop model inputs (Section 3), while data collected for the Kalamazoo River near Battle Creek provide a point of comparison for the model output.

Measured suspended sediment concentrations near Battle Creek ranged from 14 mg/L to 91 mg/L, with a mean concentration of 38 mg/L. This sampling station is between mile posts 16 and 17, between Washington Avenue and Angell Street (Figure 41), just downstream of the confluence with Battle Creek. Near this location, both models show rapid changes in suspended solids concentrations due to the influence of Battle Creek flows and solids loads. While the suspended sediment data are limited in terms of both number of samples and sampling locations, these data provide some constraint on the model output. For this time period, both models predict suspended solids concentrations within the range of the data.

The USGS sampling included particle size analysis for the suspended sediment samples (Reneau et al., 2014). Data collected at Marshall and at tributary locations were used to inform model inputs as described in Section 3. Particle size data for the Kalamazoo River near Battle Creek show predominantly medium to coarse silt and sands, which is generally consistent with the model results shown in Figure 42a for the 2012 Enbridge model and Figure 42b for the updated model at this sampling location.

Overall, the updated model results show a physically realistic representation of the suspended solids particle size distribution among the size classes considered in the model as it transitions between faster-moving river reaches and slower-moving controlled sections at each of the dammed reaches, Morrow Lake Delta, and Morrow Lake itself (Figure 42b). Medium to coarse silt (green line) is generally the most significant size fraction, but deposition in the impoundments results in shifts to more clay/fine silt. The contributions from sand size classes increase throughout the riverine reaches between impoundments.

The 2012 Enbridge model also shows silt as the most significant size fraction (blue line in Figure 42a), but shows less of a shift in particle size distribution through the impoundments such as Ceresco. Upstream of Morrow Lake, variations in particle size distribution in the Enbridge model result largely from the rapid changes in the sand contribution (orange line).

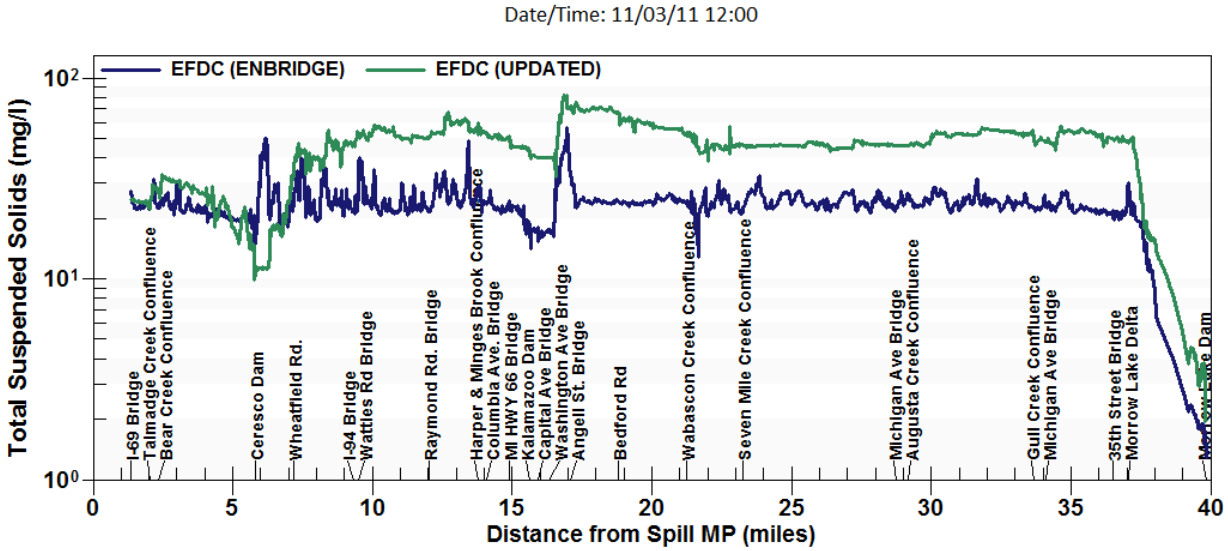

Figure 41. Predicted total suspended solids concentrations for November 3, 2011 elevated baseflow conditions, 2012 Enbridge model (blue) and updated model (green).

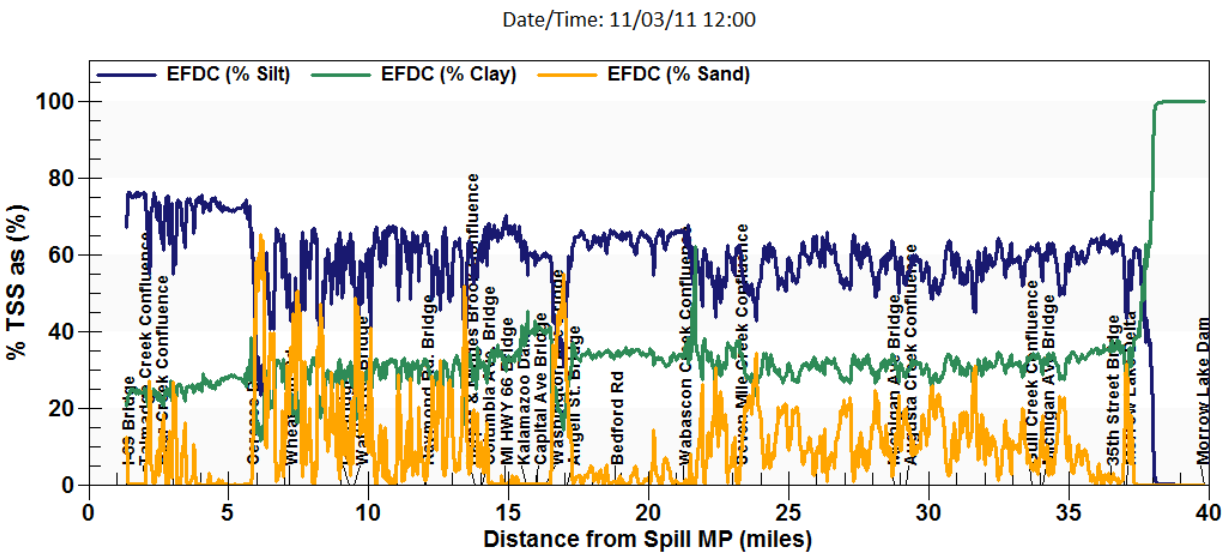

(a)

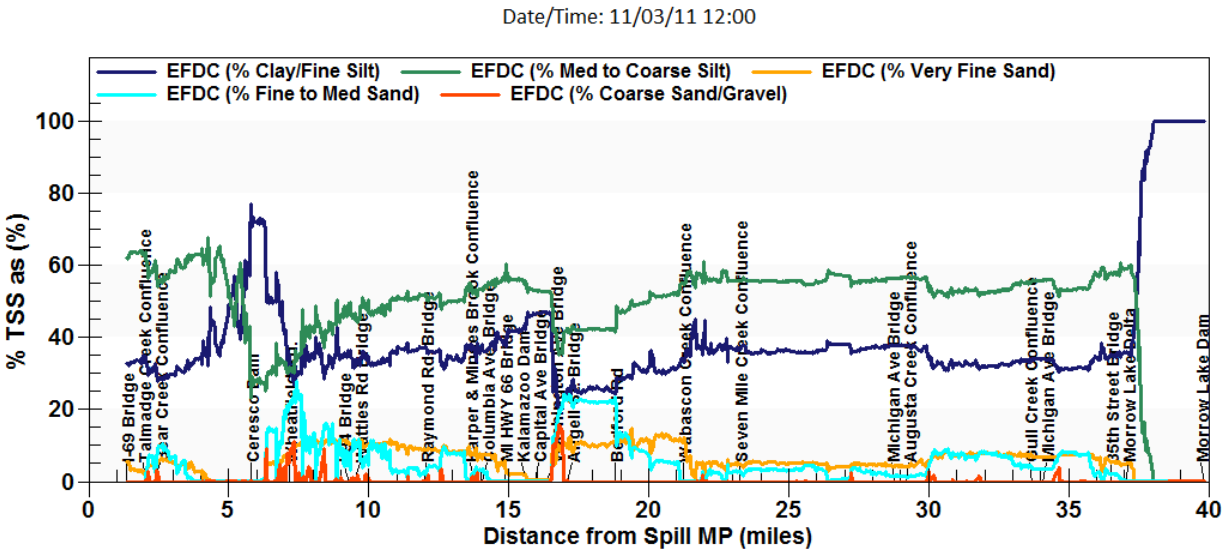

(b)

Figure 42. Predicted fractional contribution of different particle size classes to total suspended solids concentrations for November 3, 2011 elevated baseflow conditions, (a) 2012 Enbridge model, (b) updated model.

Sediment fluxes were also output from each model at the USGS gage location near Battle Creek and at 35th Street at the entrance to Morrow Lake delta. Daily average sediment fluxes are included in Table 12. Loads in both models decline through much of the simulation period in response to declining flow. Consistent with the results for suspended sediment concentrations, the updated model predicts larger sediment fluxes during this time period. The updated model shows an increase in sediment flux from Battle Creek to 35th Street, particularly during the higher flows early in the simulation period. The 2012 Enbridge model predicts declines in sediment flux through this reach early in the simulation and increases in sediment flux between these locations after November 1, 2011.

Table 12. October – November 2011 model-predicted sediment fluxes.

	Updated Model		2012 Enbridge Model	
Date	Kalamazoo Near Battle Creek (MT/day)	Kalamazoo at 35th Street (MT/day)	Kalamazoo Near Battle Creek (MT/day)	Kalamazoo at 35th Street (MT/day)
10/28/2011	198	482	188	105
10/29/2011	169	314	137	90
10/30/2011	150	228	104	78
10/31/2011	133	197	82	70
11/1/2011	117	167	69	66
11/2/2011	107	145	60	62
11/3/2011	96	121	53	55
11/4/2011	88	107	47	50
11/5/2011	80	95	42	46
11/6/2011	69	86	37	44
11/7/2011	61	75	33	41
11/8/2011	66	69	35	38

As described in Section 5.1, hydrodynamic and other refinements to the model resulted in a net decrease in estimated velocities and corresponding shear stresses in the Morrow Lake delta area for the October to November 2011 simulation period. Combined with the increase in sediment load delivered to the delta by the updated model, these changes result in a significant difference in estimated bed elevation change relative to the 2012 Enbridge model (Figure 43a and 43b), with a substantial increase in the extent and magnitude of deposited sediment throughout the delta area for the period simulated. While this prediction is not directly calibrated to data describing long-term bed evolution or short-term bed fluctuations, the results provide an illustration of the pathways and direction of sediment transport under a moderate flow condition, and conceptual insight into the behavior of the delta area as a transition from riverine to lacustrine conditions that acts to capture and retain sediment delivered from upstream. The distribution of retained solids predicted by the updated model is generally consistent with observations of retained oiled sediment mass throughout the delta, including areas in the southern portion of the delta, well off the main flow channel.

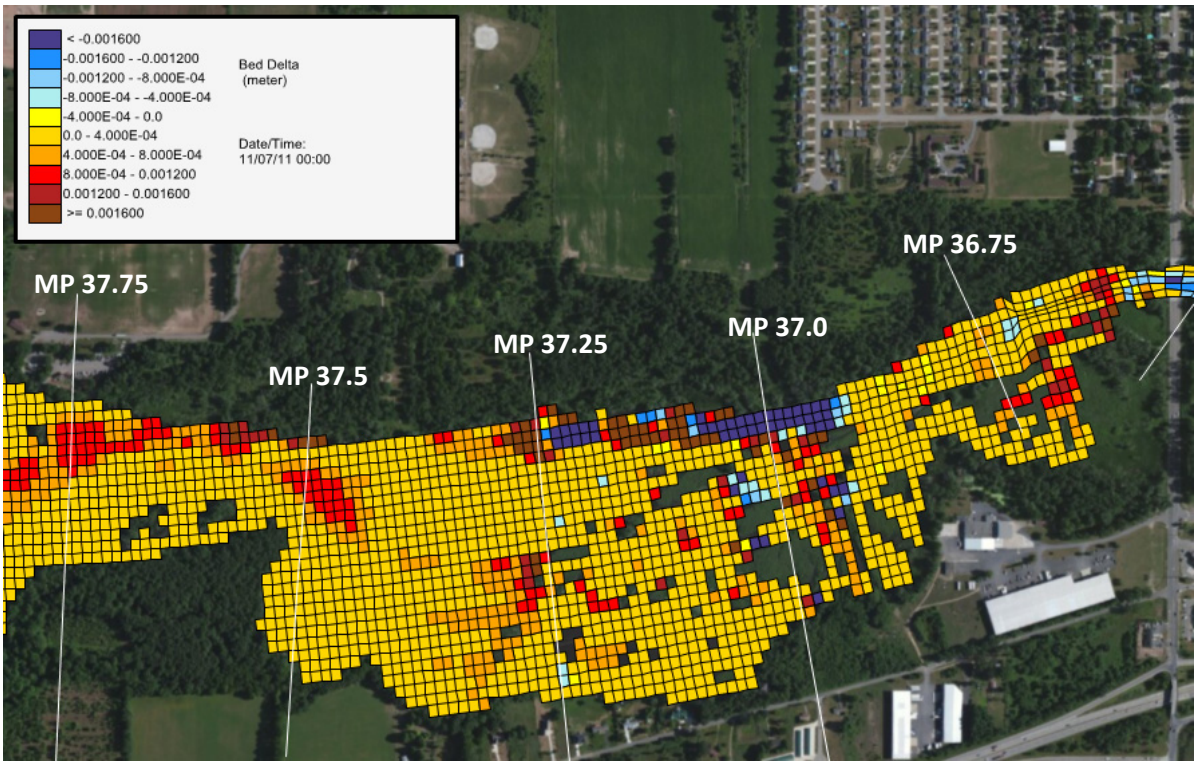

(a)

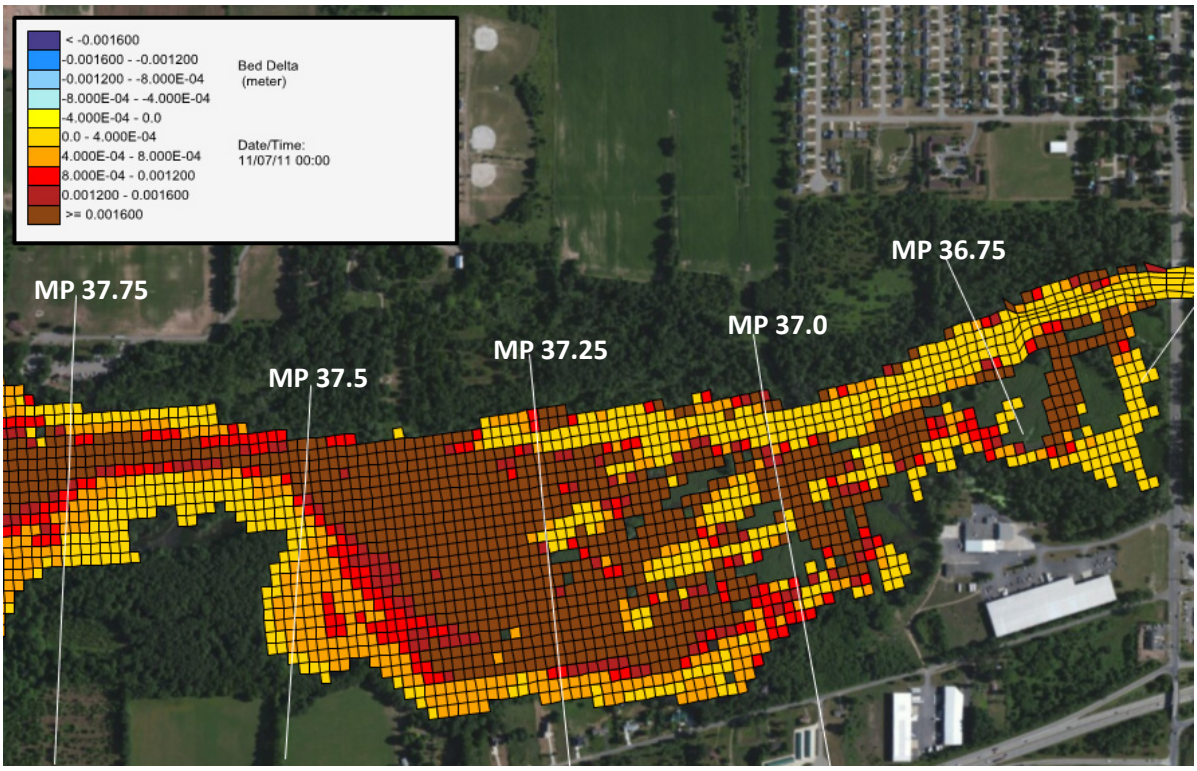

(b)

Figure 43. Predicted change in bed elevation, Morrow Lake Delta, under October to November 2011 elevated baseflow conditions, (a) 2012 Enbridge model, (b) updated model.

Predictions of sediment bed elevation change upstream of the Ceresco Dam also move from a prediction of a near static condition in the 2012 Enbridge model to a more dynamic representation of deposition in the updated model (Figures 44a and 44b). Refinements to the model hydrodynamics and representation of shear stress in the reach allow for a more realistic representation of deposition of solids upstream of the dam under the low to moderate flow conditions that prevailed during the period of the simulation. Again, while this is an uncalibrated sediment transport simulation, the results provide insight into likely patterns of deposition upstream of the dam, and the observed distribution of soft sediment under this condition is generally consistent with observations of oiled sediment areas characterized during the site investigation work.

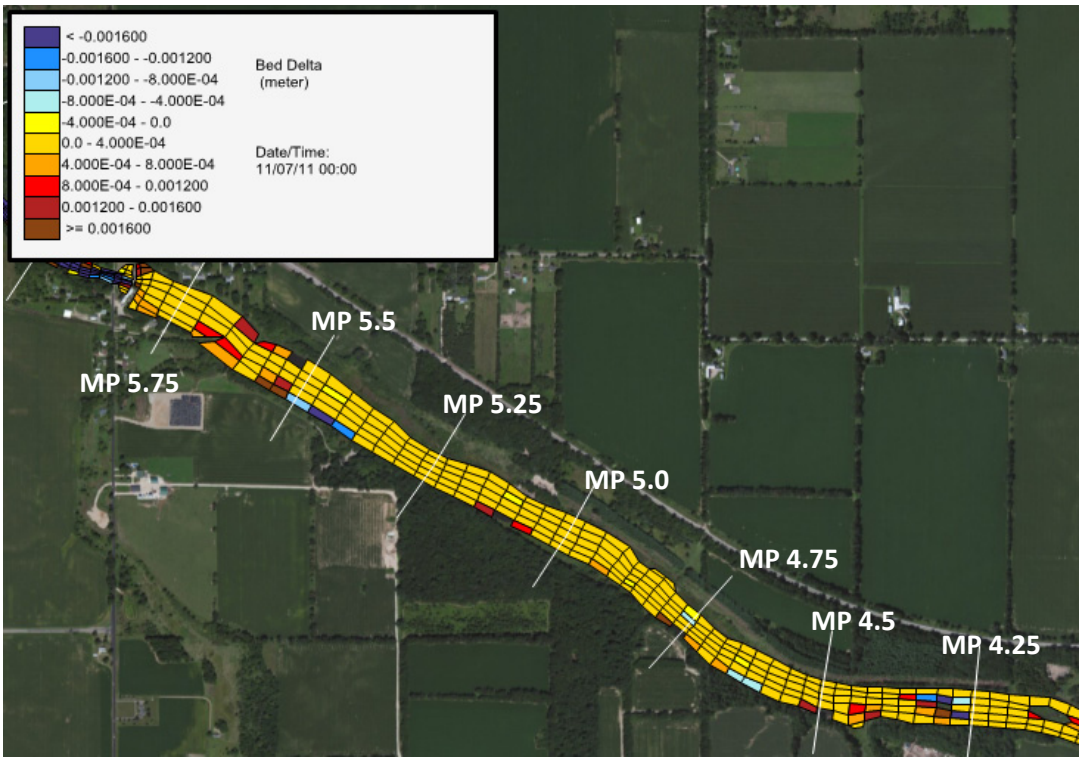

(a)

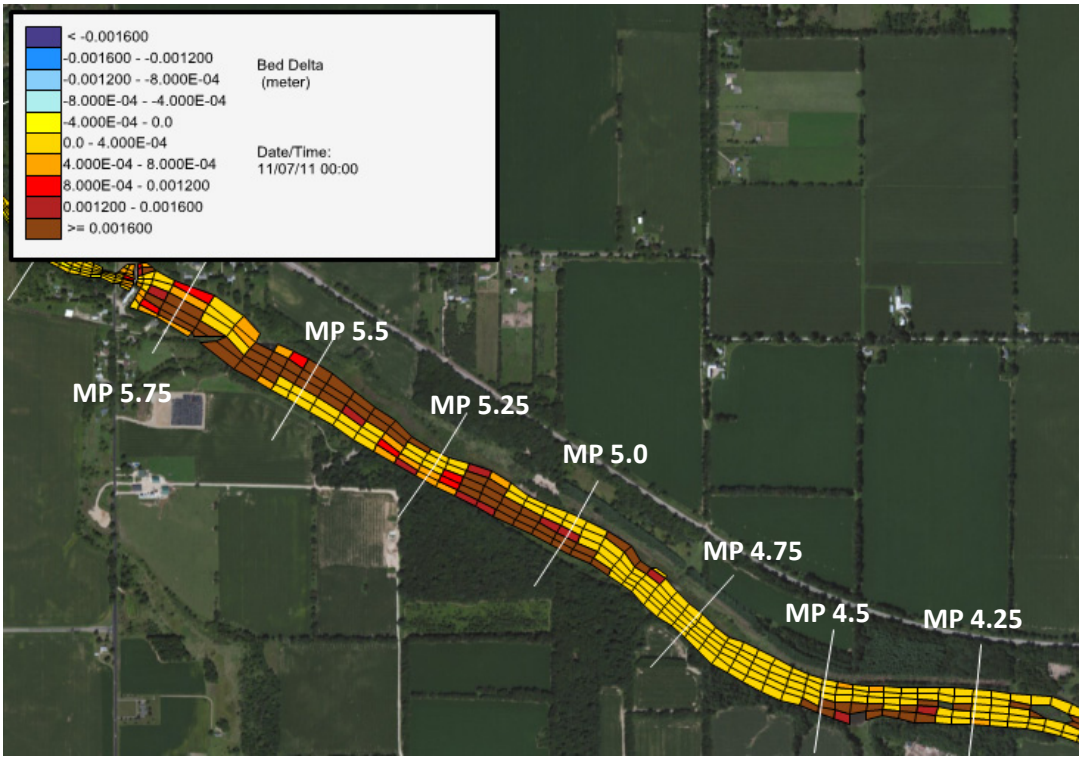

(b)

Figure 44. Predicted change in bed elevation, Ceresco Dam Impoundment, under October to November 2011 elevated baseflow conditions, (a) 2012 Enbridge model, (b) updated model.

5.2.2 Sediment Transport Model Application: July 2013 Low Flow

Results for the July 2013 low flow period are in many ways similar to those of the October to November 2011 period, with decreases in suspended solids through the impounded reaches, followed by increases in the riverine reaches between impoundments. The suspended sediment concentrations (Figure 45) are lower than those predicted for the October to November 2011 period (Figure 41), with increased deposition and reduced erosion resulting from the lower flows.

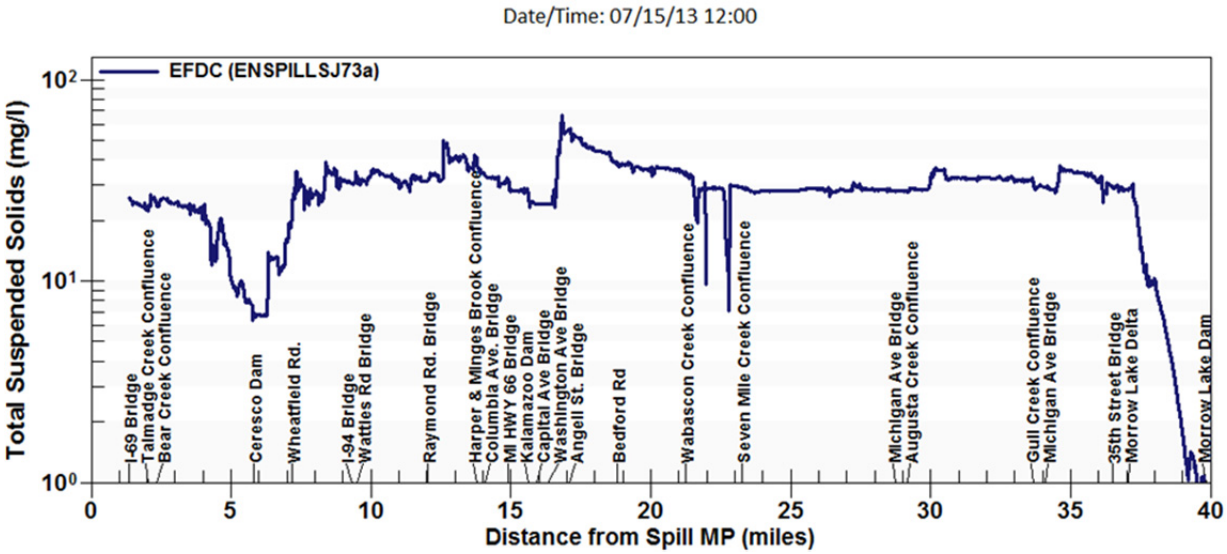

Figure 45. Predicted total suspended solids concentrations for July 15, 2013 low flow conditions.

Total sediment flux for July 11 – 18 averages 44 MT/day near Battle Creek and 49 MT/day at 35th Street. Daily average fluxes are shown in Table 13. As expected, sediment fluxes for this low flow period are significantly lower than those predicted by the updated model for the October – November 2011 high baseflow period (Table 12). For July 2013, the updated model predicts only small increases in sediment flux between Battle Creek and 35th Street, with no increase over the last 3 days of the simulation.

Table 13. July 2013 updated model-predicted sediment fluxes.

Date	Updated Model	
	Kalamazoo Near Battle Creek (MT/day)	Kalamazoo at 35th Street (MT/day)
7/11/2013	64	69
7/12/2013	54	68
7/13/2013	48	54
7/14/2013	42	51
7/15/2013	35	41
7/16/2013	36	34
7/17/2013	37	35
7/18/2013	35	36

Net sediment deposition for July 11 – 18 is shown in Figure 46 for the Morrow Lake delta and Figure 47 for the Ceresco impoundment. In comparison to the October to November 2011 high baseflow period, the updated model predicts less sediment deposition, as well as somewhat different deposition patterns. In the Morrow Lake delta (Figure 46), the depositional zone does not extend quite as far into the southern edges of the delta. Similarly, for the Ceresco impoundment, there is not as much deposition near the dam for July 2013 as for October to November 2011. These results highlight the fact that the oiled sediment conditions that exist in the Kalamazoo River reflect the integration of a series of many transport events that occur over a variety of flow conditions.

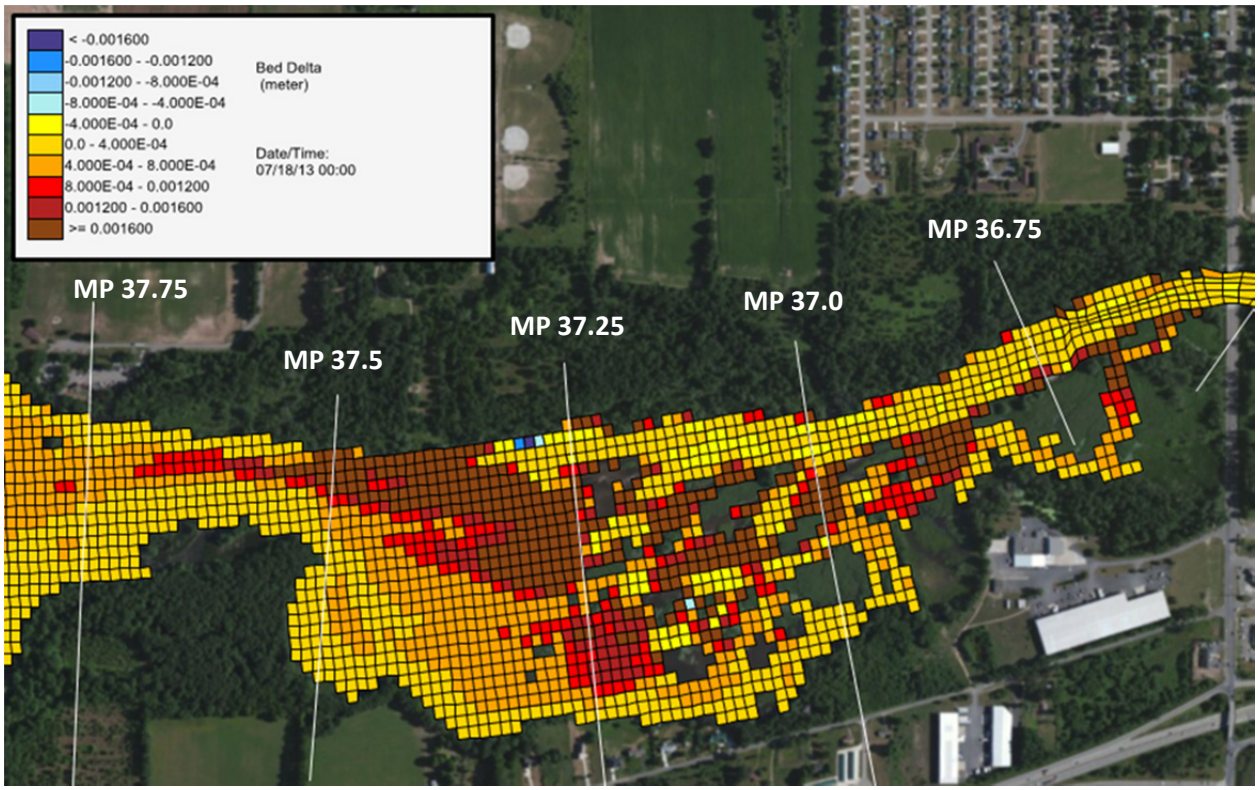

Figure 46. Predicted change in bed elevation, Morrow Lake Delta, under July 2013 low flow conditions.

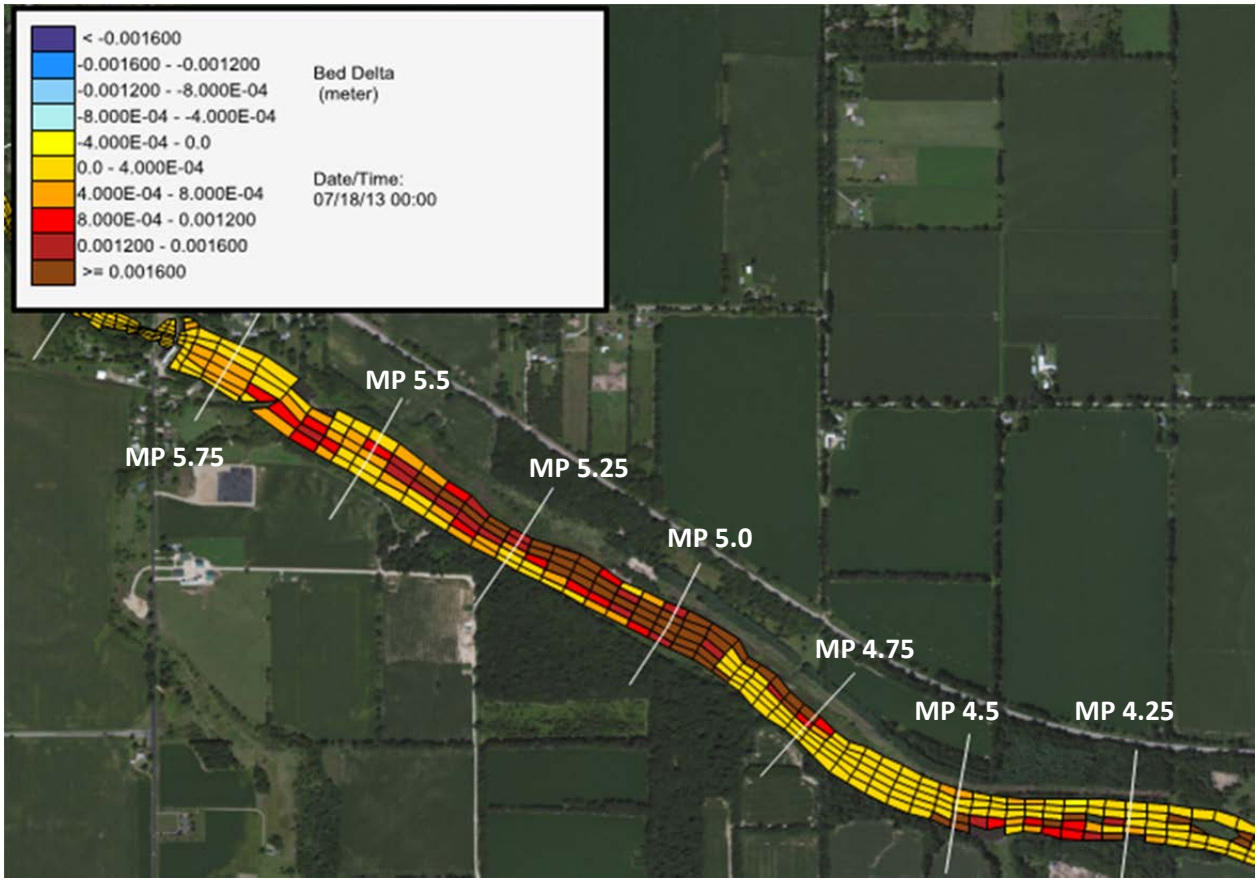

Figure 47. Predicted change in bed elevation, Ceresco Dam Impoundment, under July 2013 low flow conditions.

5.3 Conclusions and other Applications

The hydrodynamic and sediment transport models as developed under this effort benefitted from a significant improvement in the quality of the incorporated underlying datasets, resulting in a substantial enhancement in the parameterization and calibration of the models to available data. This includes improvements to the bathymetric data describing the river and floodplain, improved representation of tributary flow inputs, modified representation of the dams and other physical structures, and incorporation of extensive data on the characteristics of the sediment bed. However, as is always the case with a model of this complexity describing a system of the scale of this reach of the Kalamazoo River, further refinement of both the hydrodynamic and sediment transport models is possible. Notably, the sediment transport model, while providing valuable insight into sediment transport behavior in the river under a range of conditions, was constrained by limited data determining total suspended sediment concentrations in the water column, sparse data on the responsiveness of total suspended solids to the range of flow events, and also limited data on the time evolution of bed elevation and other characteristics that could provide insight into the long-term behavior of the system. It is expected that further refinement of the model and incorporation of future datasets will enable the model to provide more quantitative estimates of the movement of solids and solids-associated contaminants like OPA.

The models were applied to a variety of different conditions representing a range of river flows, hydrodynamics and sediment transport conditions across the full 38 miles of the spill-affected reaches of the Kalamazoo River. Since it is not possible within this document to report on every condition at every location in the system, examples were provided to demonstrate model behavior in important areas and to highlight differences from the 2012 Enbridge model.

The models as currently developed represent high and low flow conditions with different model configurations, using a grid optimized to best represent the prevailing direction of flow for in-channel flows with the lower flow riverine model, and a different grid configuration to represent the less sinuous floodplain flows with the floodplain model. While this model configuration has certain disadvantages, including an inability to fully represent the transition from bank full to flooded conditions and vice versa, the models do allow for accurate representation of the hydrodynamics operative under a range of river stages, without the compromises that are inherent in models that attempt to represent a sinuous river geometry and a floodplain geometry with a single grid configuration. While there may be future advantages in exploring an unstructured mesh approach or hybrid grid configuration that could successfully represent the range of hydrodynamic conditions that occur in this system, we feel that the current models provide a good mix of representativeness, flexibility in application, and computational efficiency for the problems considered.

As shown in the presentation of results, the models provide valuable insight into the patterns of deposition and resuspension of solids under varying hydrodynamic conditions, providing site cleanup planners and long-term managers of the waterway with a tool for anticipating where and when solids may accumulate along the different reaches of the river.

As this report is being finalized, algorithms describing the related transport of OPA are in development, and will be refined with field data and further laboratory characterization of OPA particulate behavior. The sediment transport evaluations described here do provide evidence suggesting that OPA transport is regular and predictable. In portions of the river where it has been possible to refine and calibrate the models with current data, there are strong indications that OPA transport is similar to and linked with sediment transport behavior, significantly with the transport of silt-sized particles. Further development, application, and refinement of tools for prediction of OPA transport will be beneficial and helpful for management of other, similar oil spill sites in riverine environments.

6 References

Cheng, N. S. 1997. Simplified settling velocity formula for sediment particle. *Journal of Hydraulic Engineering*,123(2), 149-152.

Chow, V.T. 1959. *Open-Channel Hydraulics*. McGraw-Hill, New York.

Dietrich, W.E., and P.J. Whiting. 1989. Boundary shear stress and sediment transport in river meanders of sand and gravel: in River Meandering, Ikeda, S. and G. Parker, ed., pp. 1-50, American Geophysical Union Water Resources Monograph 12.

EPA website - Environmental Fluid Dynamics Code (EFDC). http://www.epa.gov/athens/wwqtsc/html/efdc.html

Galperin, B., L. H. Kantha, S. Hassid, and A. Rosati. 1988. A quasi-equilibrium turbulent energy model for geophysical flows. *J. Atmos. Sci.*, 45, 55-62.

Hamrick, J. M. 1992. A three-dimensional environmental fluid dynamics computer code: Theoretical and computational aspects. The College of William and Mary, Virginia Institute of Marine Science, Special Report 317, 63 pp.

Hayter, E.J., R. McCulloch, T. Redder, M. Boufadel, R. Johnson, and F. Fitzpatrick. 2015. Modeling the Transport of Oil Particle Aggregates and Mixed Sediment in Surface Waters. Letter Report. U.S. Army Engineering Research and Development Center, Environmental Laboratory. Vicksburg, MS. January 10. Draft, in review.

James, S.C., C. Jones, and J.D. Roberts. 2005. Consequence Management, Recovery & Restoration after a Contamination Event. Sandia National Laboratory report SAND2005-6797.

Johnson, R., Global Remediation Technologies, Inc. and Weston Solutions, Inc. 2014. Written Communication.

Jones, C. and W. Lick. 2001. SEDZLJ: A sediment transport model. University of California – Santa Barbara. Santa Barbara, CA.

Lick, W. J. 2009. *Sediment and Contaminant Transport in Surface Waters*. CRC Press.

Mellor, G. L., and T. Yamada. 1982. Development of a turbulence closure model for geophysical fluid problems. *Rev. Geophys. Space Phys.*, 20, 851-875.

Perkey, D.W., S.J. Smith, and T. Kirklin. 2014. Cohesive Sediment Erosion Field Study: Kalamazoo River, Kalamazoo, Michigan. Letter Report. U.S. Army Engineering Research and Development Center, Coastal and Hydraulics Laboratory. Vicksburg, MS. April 24.

Personal Communication, Faith Fitzpatrick, USGS, 8/21/2013.

Reneau, P.C., D. Soong, C. Hoard, and F. Fitzpatrick. 2014. Hydrodynamic Assessment Data Associated with the July 2010 Line 6B Spill into the Kalamazoo River, Michigan, 2012-14. USGS Open-File Report. December 13. Draft, in review.

Soong, D. T., C. Hoard, F. Fitzpatrick, R. Zelt. 2015. Preliminary Analysis of Suspended Sediment Rating Curves for the Kalamazoo River and its Tributaries from Marshall to Kalamazoo, Michigan. Proceedings Paper, SEDHYD Conference, Reno, NV.

Tetra Tech. 2012. Enbridge Line 6B MP 608 Marshall, MI Pipeline Release, Kalamazoo River Hydrodynamic and Sediment Transport Model, Prepared for United States Environmental Protection Agency, Enbridge Energy Partners.

Thanh, P.H.X., M.D. Grace, and S.C. James. 2008. Sandia National Laboratories Environmental Fluid Dynamics Code: Sediment Transport User Manual. Sandia National Laboratory report SAND2008- 5621.

USGS. 2008. Simulation of Flow, Sediment Transport, and Sediment Mobility of the Lower Coeur d'Alene River, Idaho. Scientific Investigations Report 2008-5093.

USGS. 2014. United States Geological Survey National Water Information System. Retrieved 9 29, 2014, from USGS 04105500 KALAMAZOO RIVER NEAR BATTLE CREEK, MI: http://waterdata.usgs.gov/nwis/inventory/?site_no=04105500&agency_cd=USGS&

Weston Solutions, Inc. 2014. Enbridge Oil Spill, Kalamazoo River Bathymetry and Floodplain Topography Updates used for 2014 Site Hydrodynamic and Sediment Transport Models. Weston Solutions Technical Memorandum. December 18. Draft, in review.

Appendix A
Model to Data Comparisons of Discharge at USGS Gages (Comstock and Battle Creek)

Blank page

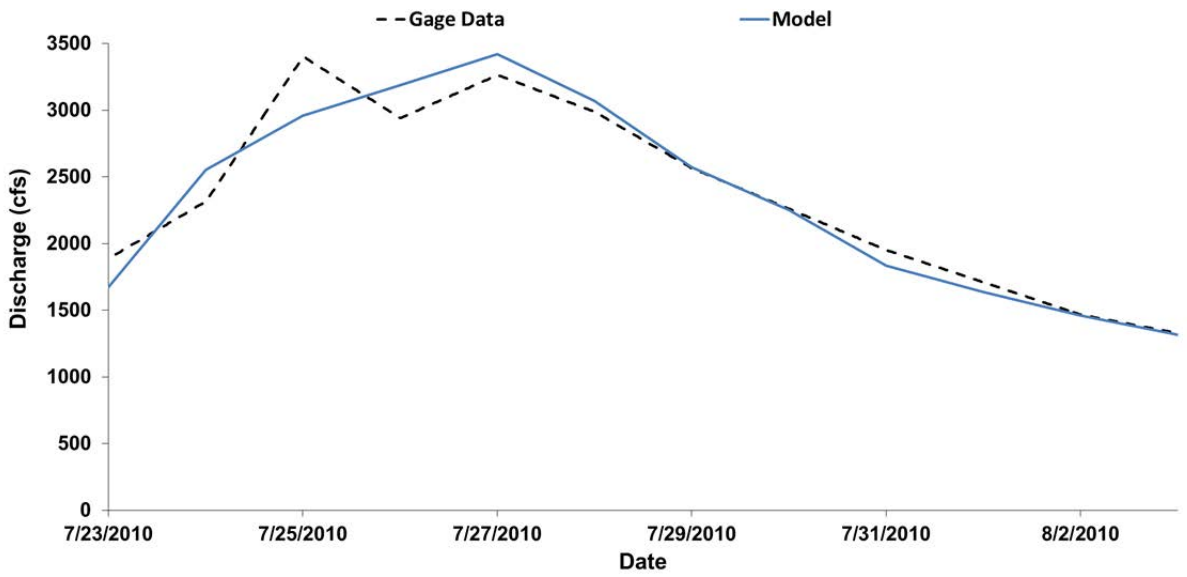

Figure A-1. Model to data comparison at Comstock gage (USGS 04106000), July 2010, daily average discharge.

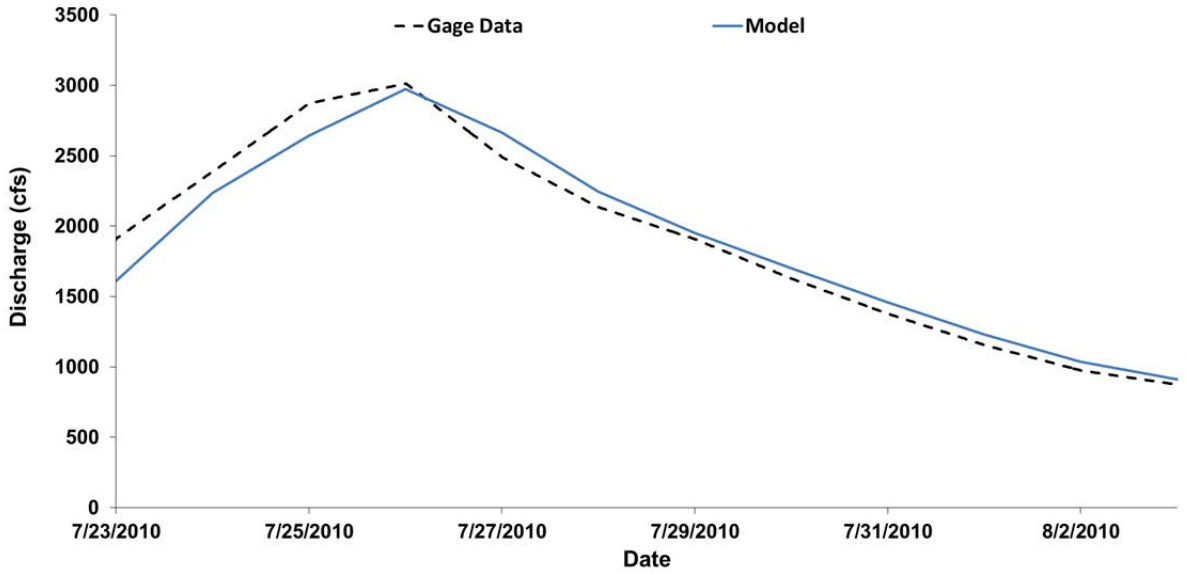

Figure A-2. Model to data comparison at Kalamazoo near Battle Creek gage (USGS 04105500), July 2010, daily average discharge.

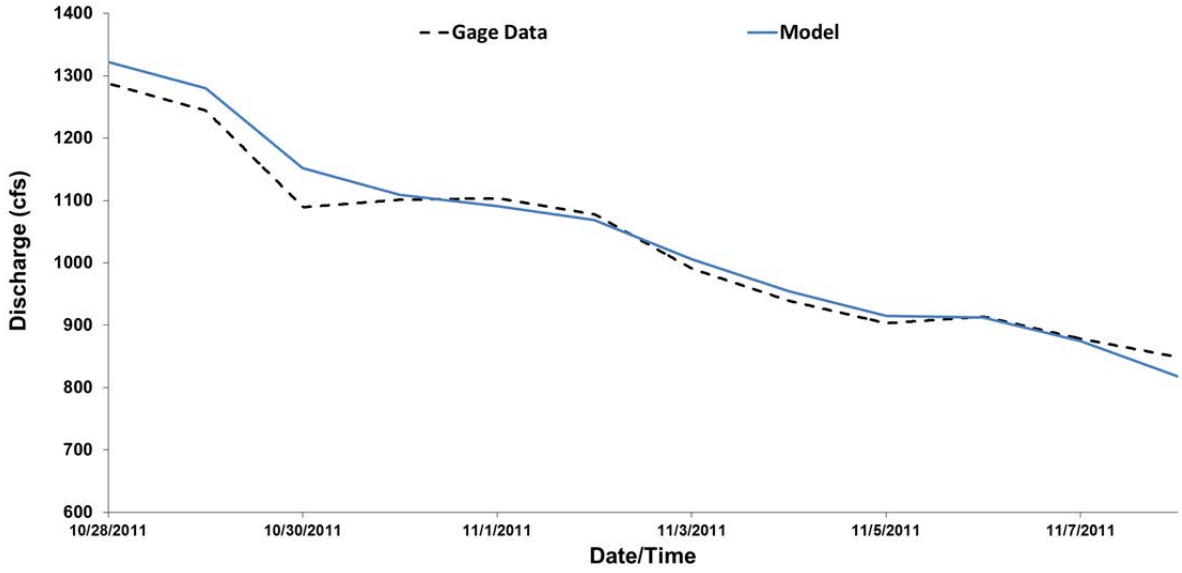

Figure A-3. Model to data comparison at Comstock gage (USGS 04106000), October to November 2011, daily average discharge.

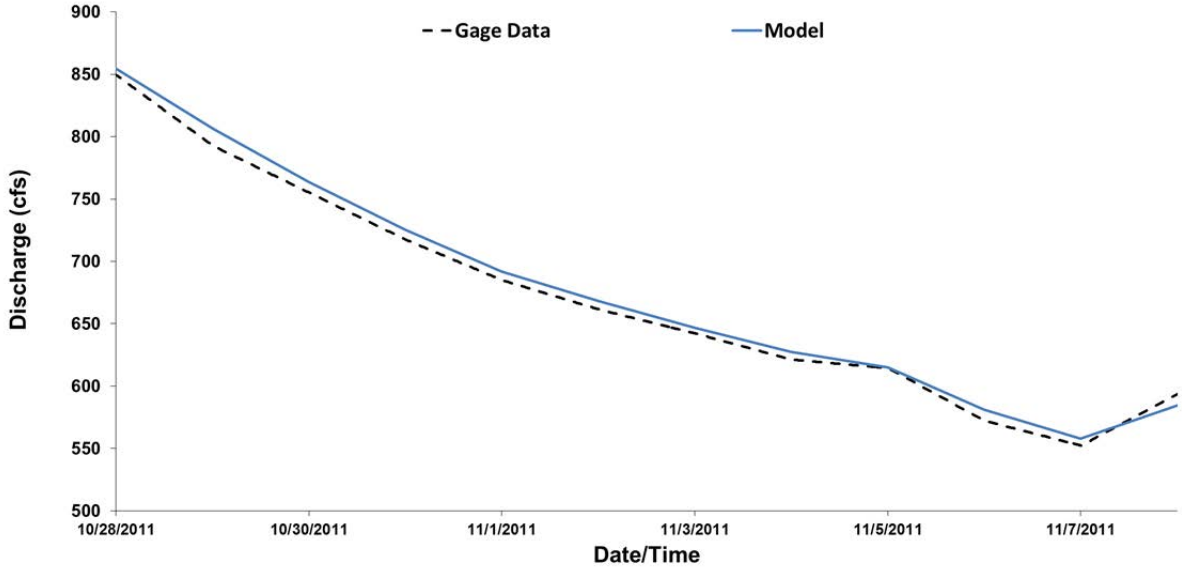

Figure A-4. Model to data comparison at Kalamazoo near Battle Creek gage (USGS 04105500), October to November 2011, daily average discharge.

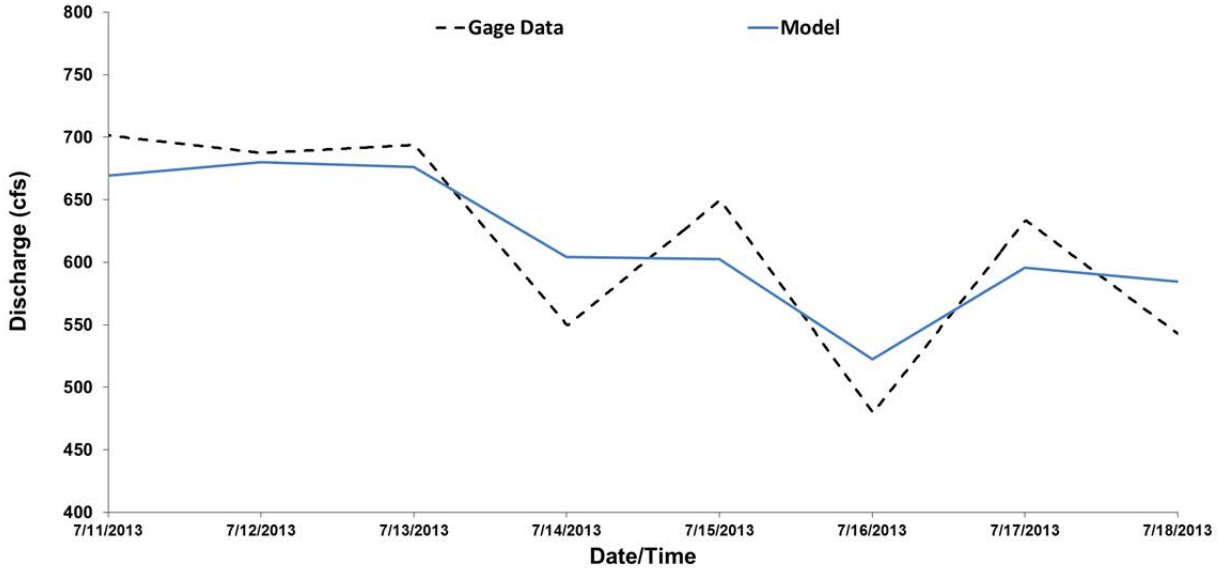

Figure A-5. Model to data comparison at Comstock gage (USGS 04106000), July 2013, daily average discharge.

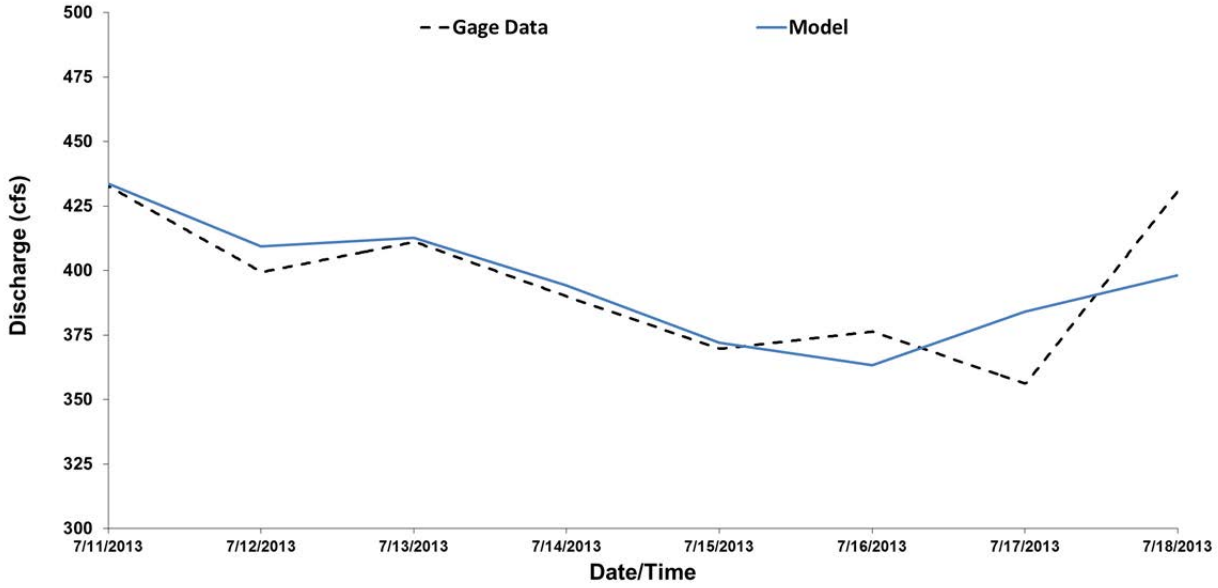

Figure A-6. Model to data comparison at Kalamazoo near Battle Creek gage (USGS 04105500), July 2013, daily average discharge.

Blank page

Appendix B
Model Comparisons to USGS April 2013 Velocity Data

Blank page

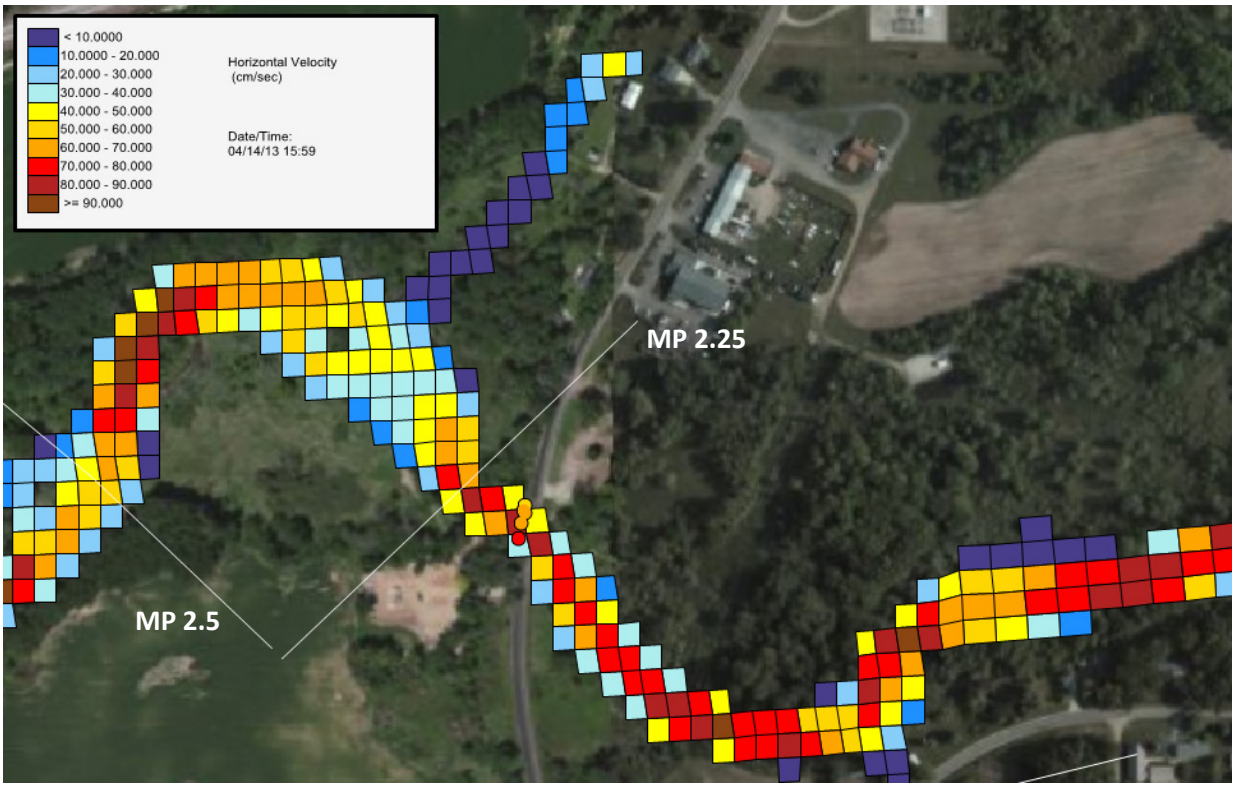

Figure B-1. Model comparison to velocity data at transect 2.22 on April 14, 2013. Circles represent velocity measurements, with transect data averaged by grid cell. Legend in 10 cm/sec increments.

Figure B-2. Model comparison to velocity data at transect 7.18 on April 16, 2013. Circles represent velocity measurements, with transect data averaged by grid cell. Legend in 15 cm/sec increments.

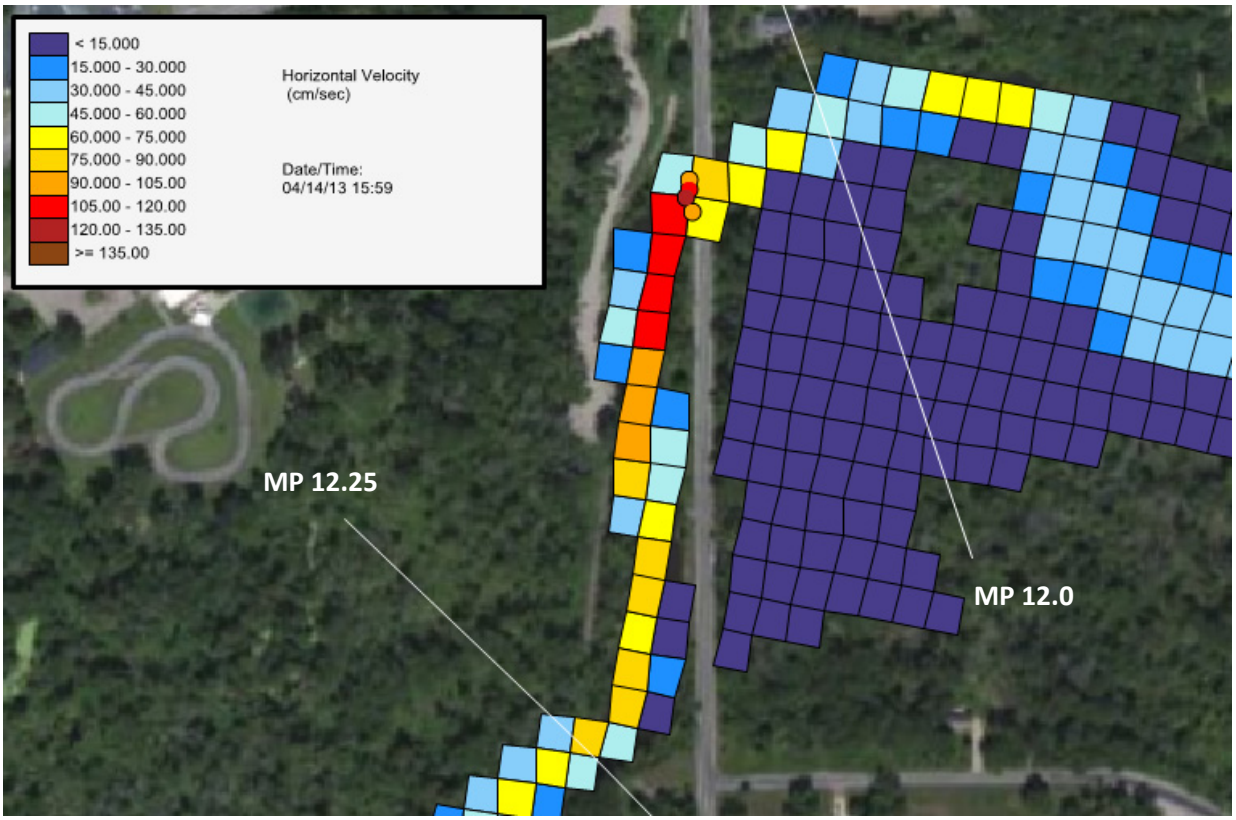

Figure B-3. Model comparison to velocity data at transect 12.05 on April 13, 2013. Circles represent velocity measurements, with transect data averaged by grid cell. Legend in 15 cm/sec increments.

Figure B-4. Model comparison to velocity data at transect 13.89 on April 13, 2013. Circles represent velocity measurements, with transect data averaged by grid cell. Legend in 15 cm/sec increments.

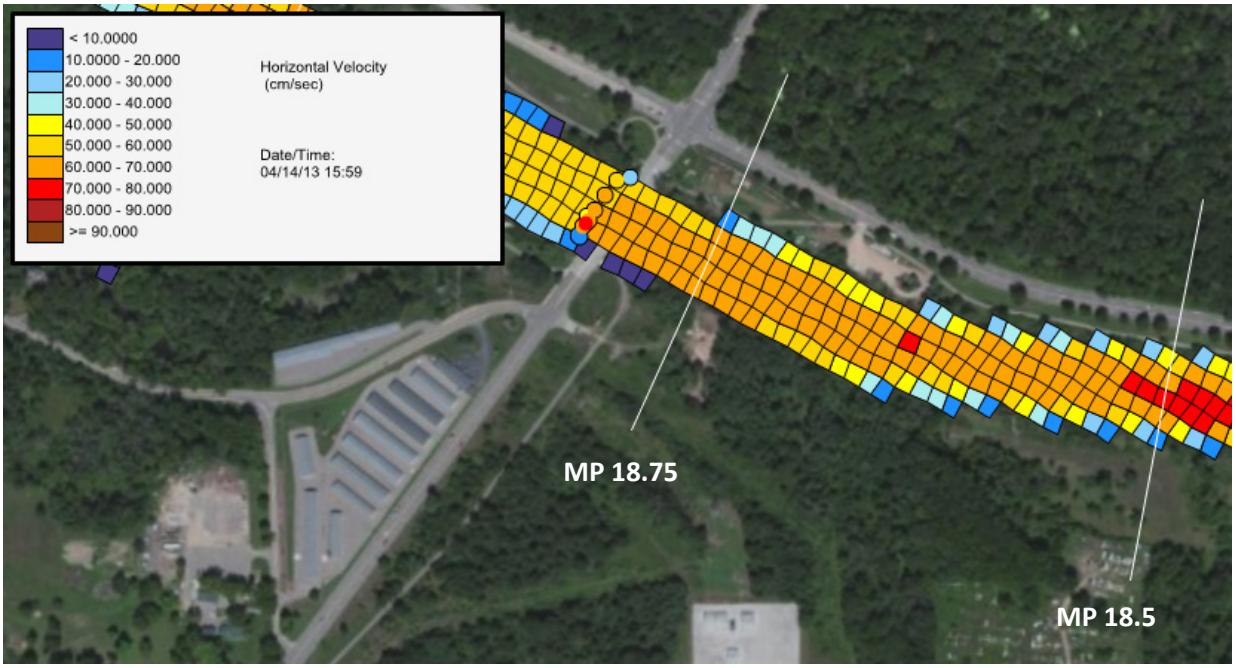

Figure B-5. Model comparison to velocity data at transect 18.83 on April 14, 2013. Circles represent velocity measurements, with transect data averaged by grid cell. Legend in 10 cm/sec increments.

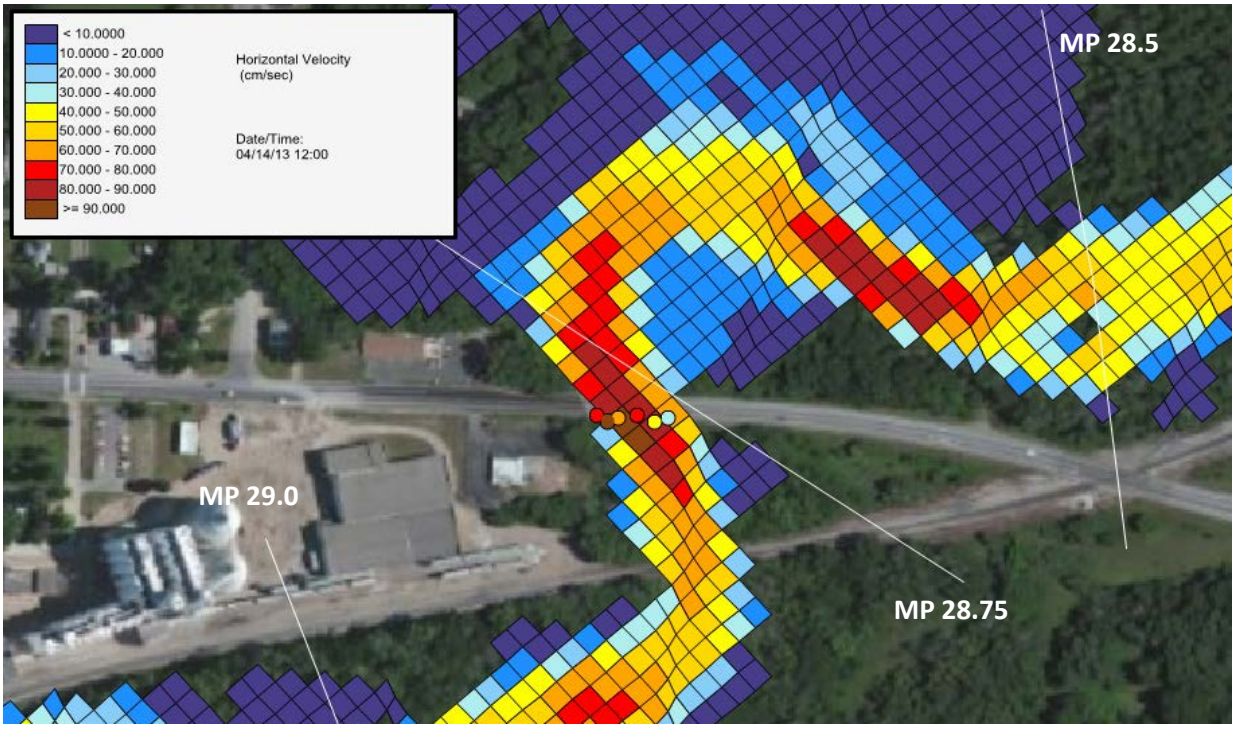

Figure B-6. Model comparison to velocity data at transect 28.8 on April 14, 2013. Circles represent velocity measurements, with transect data averaged by grid cell. Legend in 10 cm/sec increments.

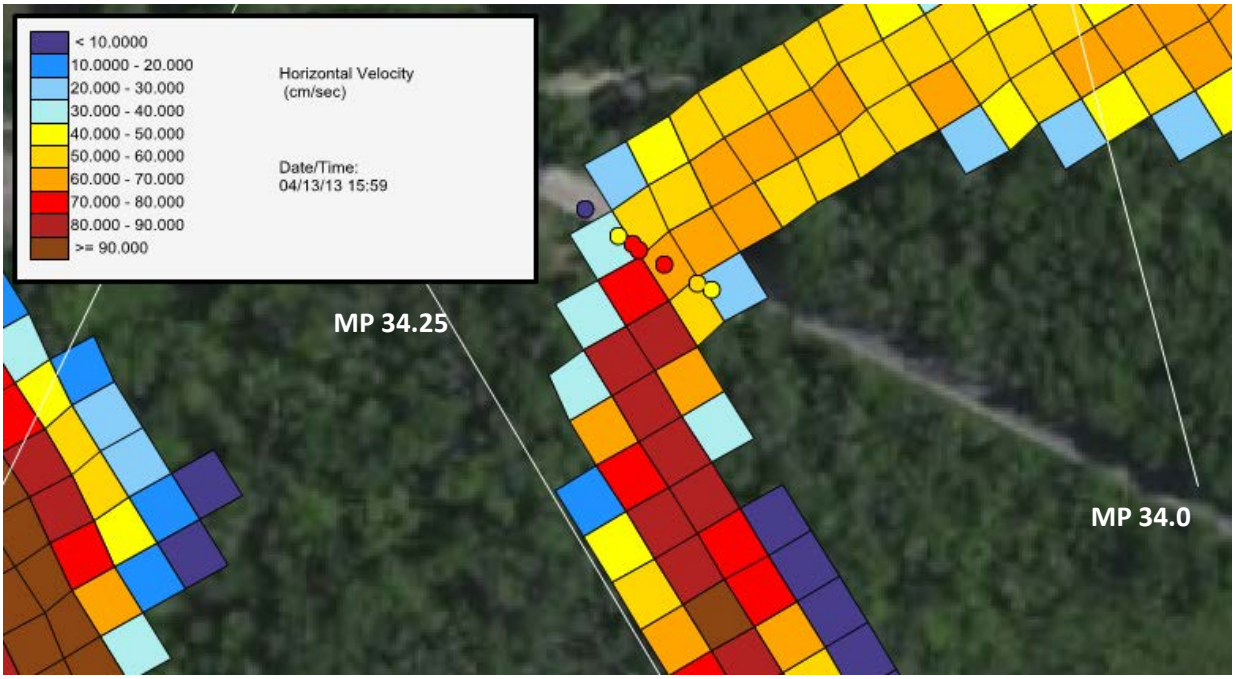

Figure B-7. Model comparison to velocity data at transect 34.12 on April 13, 2013. Circles represent velocity measurements, with transect data averaged by grid cell. Legend in 10 cm/sec increments.

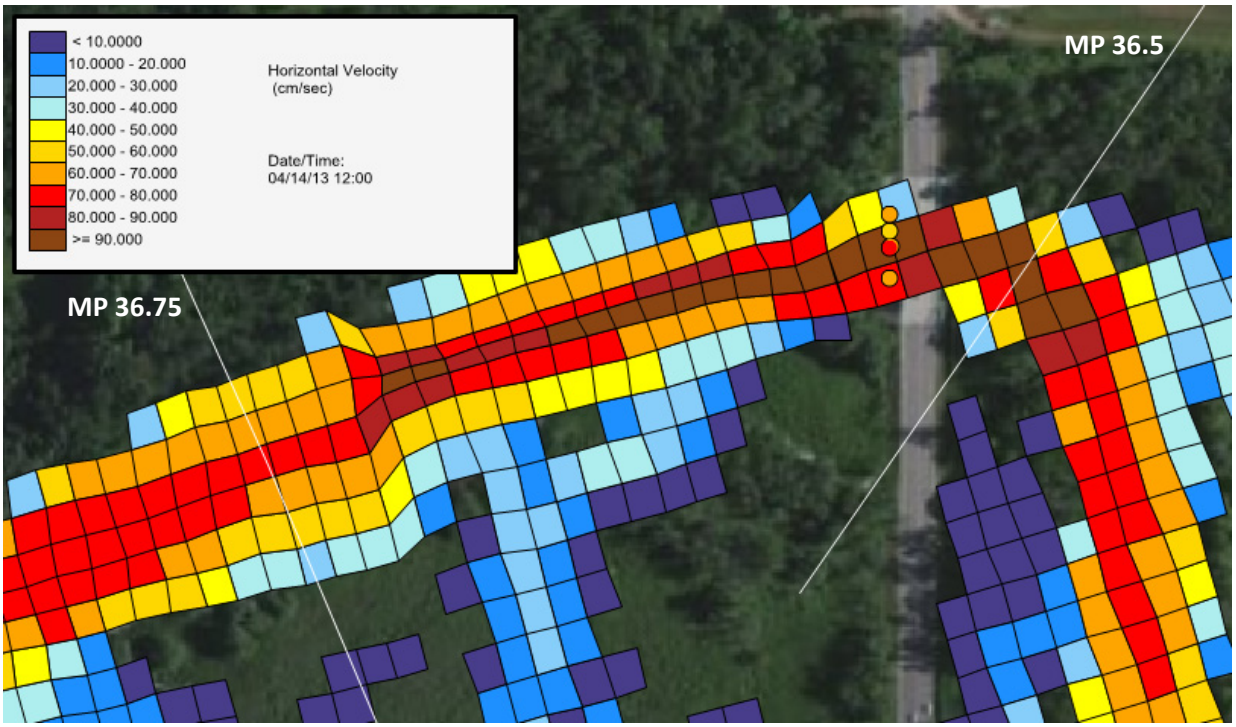

Figure B-8. Model comparison to velocity data at transect 36.55 on April 14, 2013. Circles represent velocity measurements, with transect data averaged by grid cell. Legend in 10 cm/sec increments.